Hillslope seepage erosion, spring sapping, and knickpoint migration: evidence of groundwater sapping Middle Trinity aquifer, Honey Creek basin, Comal County, Texas

by

Kristin Miller White, B.A.

Thesis

Presented to the Faculty of the Graduate School

of The University of Texas

in Partial Fulfillment

of the Requirements

for the Degree of

Master of Science in Geological Sciences

The University of Texas at Austin

May 2005

Hillslope seepage erosion, spring sapping, and knickpoint migration:
evidence of groundwater sapping
Middle Trinity aquifer, Honey Creek basin,
Comal County, Texas

Approved by
Supervising Committee:

John M. Sharp, Jr.

Paul F. Hudson,

Libby A. Stern.

Dedication

To my family, husband Kemble White, our son Kemble Thorn White, and daughter Carys Morgan White.

Acknowledgements

Thank you to thesis advisor John M. Sharp, Jr. for his guidance and for supervising the work. Thanks to Paul F. Hudson for helping to formulate ideas and for providing instructions to install the erosion pins. Thanks to Libby A. Stern for sharing her time and energy in the field and for her guidance. Thanks to the Texas Parks and Wildlife Department (TPWD) for providing permits to access Honey Creek State Natural Area and to George Kegley and David Riskind of TPWD for providing data collected by volunteers from central Texas speleological chapters of the National Speleological Society (NSS). The United States Geologic Survey (USGS, 2001) made provisional data at Honey Creek (water well levels, precipitation, and stream hydrograph data) possible. Honey Creek stream discharge measurements were measured by students during field methods classes (Geo 376L/328C), June 2001. Funding was made possible by the Geological Society of America, University of Texas Environment Science Institute Summer Research Fellowship (2001), Geological Society of America (2002), Ronald K. DeFord Field Scholarship Fund Award (2002), Arnold P. (Dutch) Wendler Professional Fund (2002 and 2003), and John A. and Katherine G. Jackson Fellowship in Geohydrology (2004).

Abstract

Hillslope seepage erosion, spring sapping, and knickpoint migration: evidence of groundwater sapping Middle Trinity aquifer, Honey Creek basin, Comal County, Texas

Kristin Miller White, degree sought M.S.

The University of Texas at Austin, 2004

Supervisor: John M. Sharp, Jr., Ph.D.

Geomorphic features within Honey Creek basin are consistent with formation by spring sapping which is the erosion of soil and rock by groundwater. Geomorphic evidence includes: swallow holes (stream swallets) that pirate spring discharge into the subsurface, groundwater piping and seepage along weathered marly slopes, headward erosion at knickpoints and spring orifices, fracture controls on incised streams, and generation of alluvium from scarp collapse. Erosion pins were used to measure erosion and sediment accumulation on marly slopes. Aerial photograph interpretation, Arcview GIS, 3D Analyst, and Geoorient techniques were used to evaluate the physical hydrogeologic features (potentiometric surface, karst springs, recharge features, knickpoints, and fractures) and their relationship to surface erosion patterns. Honey Creek basin is underlain by interbedded marl and limestone units of the Cretaceous Middle Trinity aquifer. Springs and caves provide a window into subsurface processes, including flow direction along preferential flowpaths and perched water tables. Precipitation affects spring discharge and water table levels in both stratigraphically perched aquifers and deeper aquifers. Upland karst features allow recharge of surface water to focus flow into spring conduits that rapidly discharge into streams following intense precipitation. Spring conduits and upland creeks feed into intermittent tributaries, then into perennial channels of Honey Creek and the Guadalupe River. Perched aquifers focus flow toward intermittent springs, while perennial springs are supported by a deeper regional system. Transmissivity is high within rock units that contain solutionally enlarged fractures and spring conduits. Elsewhere, the transmissivity of limestone and marl is generally low so that preferred flow pathways concentrate spring discharge where hillslope erosion has intersected bedding planes, conduits, and fractures. As springs discharge into local surface water bodies, erosion occurs at the spring orifices causing headward erosion along the pathways. Dominant fracture trends within the basin are generally aligned with the northeast-trending Balcones Fault Zone and a secondary fracture distribution to the northwest. These trends strongly influence spring location and sapping.

Table of Contents

List of Tables

List of Figures

List of Photographs

Hillslope seepage erosion, spring sapping, and knickpoint migration: evidence of groundwater sapping Middle Trinity aquifer, Honey Creek basin, Comal County, Texas

KRISTIN MILLER WHITE

Jackson School of Geological Sciences, The University of Texas at Austin, Texas

INTRODUCTION

The Honey Creek State Natural Area (State Natural Area) and its larger watershed basin are located in the central Texas Hill Country, about 45 miles north of San Antonio, Texas (Figure 1). Honey Creek Stream Cave is Texas longest navigable cave and is found within Honey Creek basin and the larger Guadalupe River watershed (Figure 2) (Elliott, 1991 and TSS, 1994). Stream caves, such as Honey Creek Stream Cave (Photo 1A) and Preserve Cave (Photo 1B) provide ample airspace where one is able to swim or wade and to observe karst processes, stream cave flow direction, and to measure conduit orientations from below ground. Paleosprings (Photo 1C) and perched aquifer springs also allow for observation of the patterns of dissolution and erosion near spring orifices (groundwater discharge points) above the fluvial-level groundwater table. Karst terrain is a type of landscape that develops as the result of the dissolution of soluble rocks to form a topographic expression of well-developed subsurface drainage, collapsed features such as sinkholes, dry valleys, vertical shafts, caves, and fluted rock surfaces (epikarst). Spring conduits intersect perched zones and water flows downward along the steepest available gradient toward the springs that flow within the entrenched canyon of Honey Creek (Figure 3).

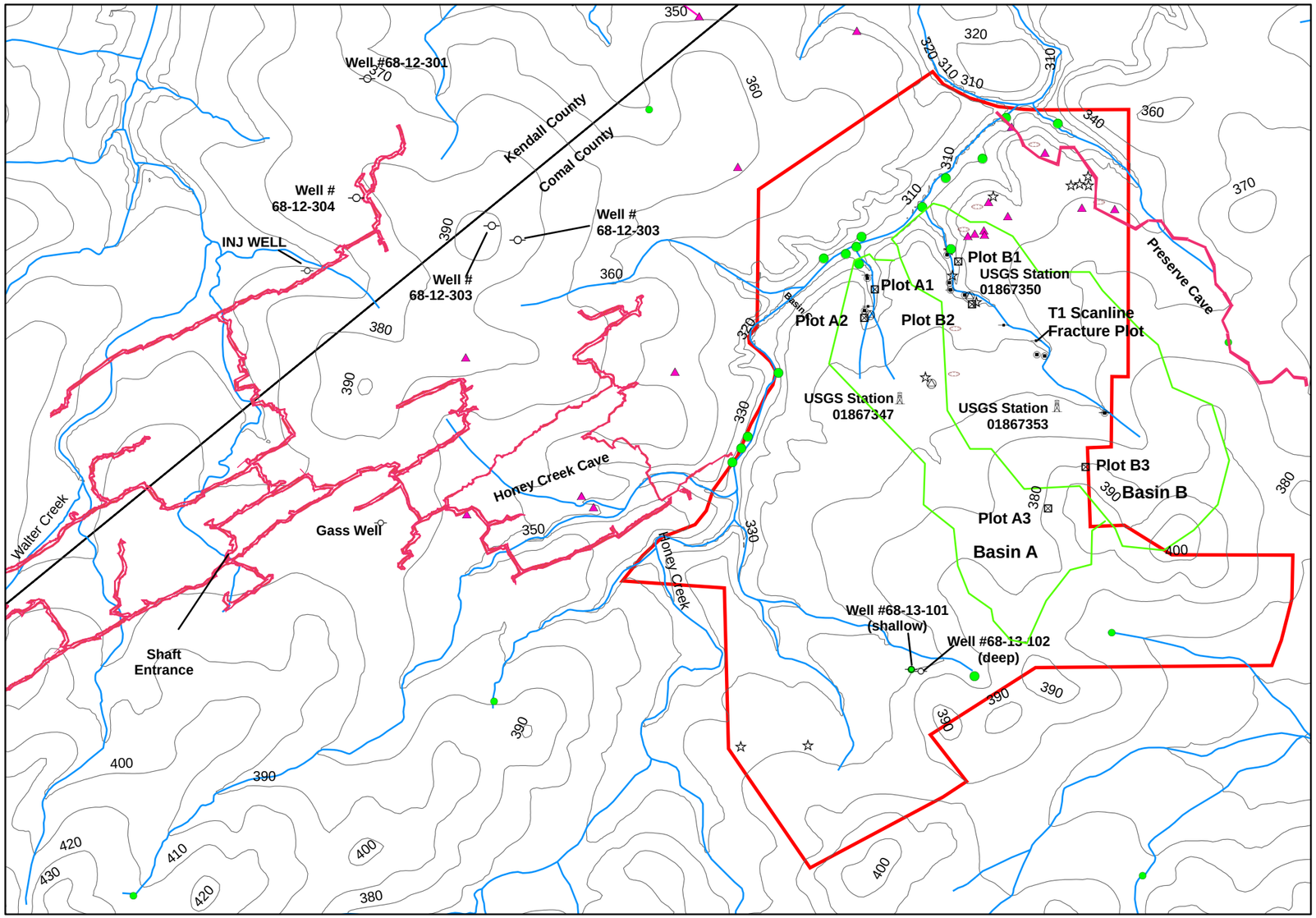

Legend

- Honey Creek State Natural Area
- Cave
- Erosion Plot
- Fracture
- Karst Feature
- Knickpoint
- Paleospring
- Sinkhole
- Spring
- Water Well
- Weather Station
- USGS Stream Gauges
- Elevation Contour (10-m interval)

0 1,000 2,000 3,000 4,000
Feet

0 320 640 960 1,280
Meters

N

Stream and River Data: National Hydrography Dataset, 2005.
Honey Creek Footprint: Texas Speleological Society, 1994. Map of Honey Creek Water Cave.
Preserve Cave Footprint: Sumbera, J. and Veni G, 1986, Trip report #2 and field reconnaissance, unpublished report to Texas Parks and Wildlife Department, 2 p.

FIGURE 2

MAP OF HONEY CREEK STATE NATURAL AREA AND SURROUNDING AREA COMAL AND KENDALL COUNTIES, TEXAS

Photo Group 1. **1A)** Honey Creek Stream Cave passage (June, 1999). The location of Honey Creek Stream Cave is shown on Figure 2. 1B) Kemble White enters Preserve Cave (May 2003). **1C)** Photo of John M. Sharp, Jr. in entrance to a paleospring/shelter cave (PS-3) found approximately 15 feet (4.6 m) above the ordinary water level of Honey Creek. Photo locations are shown on the Site Feature Map in Appendix A.

1A 

1B 

1C 

Figure 3. Conceptual cross section of stream caves and canyon sidewalls of entrenched valley of Honey Creek (based in part on Palmer, 1990).

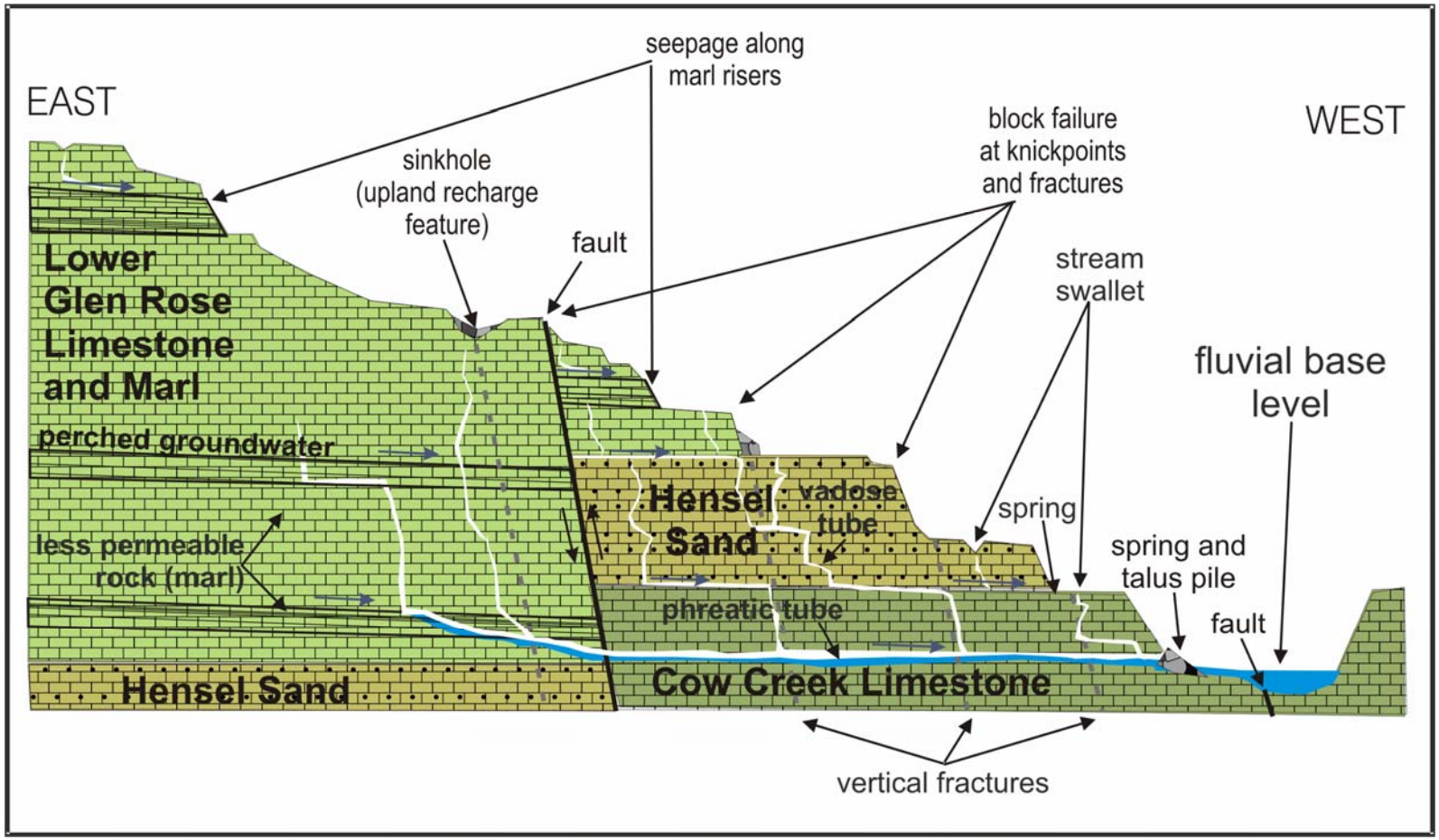

Statement of Problem

This study proposes that headward erosion of stream caves (spring sapping) played a role in current dimensions of Honey Creek basin and downcutting of its steep canyon walls (Figure 3 and Figure 4). Geomorphic features are consistent with groundwater sapping and stream piracy, including structural controls on incised streams (Photo 2A); headward erosion at springs; (Photo 2B), loss of runoff from springs into stream swallets (Photo 2C); groundwater piping, hillslope seepage erosion; headward erosion of knickpoints at fractures (Photo 3A and 3B); generation of alluvium from scarp collapse (Photo 3C); and stream caves that pirate water from basin to basin (Figure 2). As shown in Figure 4, spring sapping has been attributed to the sapping the rocks of the canyon walls, causing them to separate and retreat, resulting in widening and steepening of the canyon walls. Phreatic conduits are located above water table and may intermittently transmit fluids following precipitation events, which continues to support headward erosion at perched springs. Some return flow (runoff) from these springs enters sinkholes downstream where it recharges the next lower level of the aquifer via stream swallets downstream from springs. Surface water and groundwater are linked by an intricate network of karst features and springs, resurgent groundwater, downstream recharge features (such as stream swallets), and fractures.

Figure 4. Conceptual cross section of groundwater sapping in marl and limestone within canyon walls (based in part on Palmer, 1990).

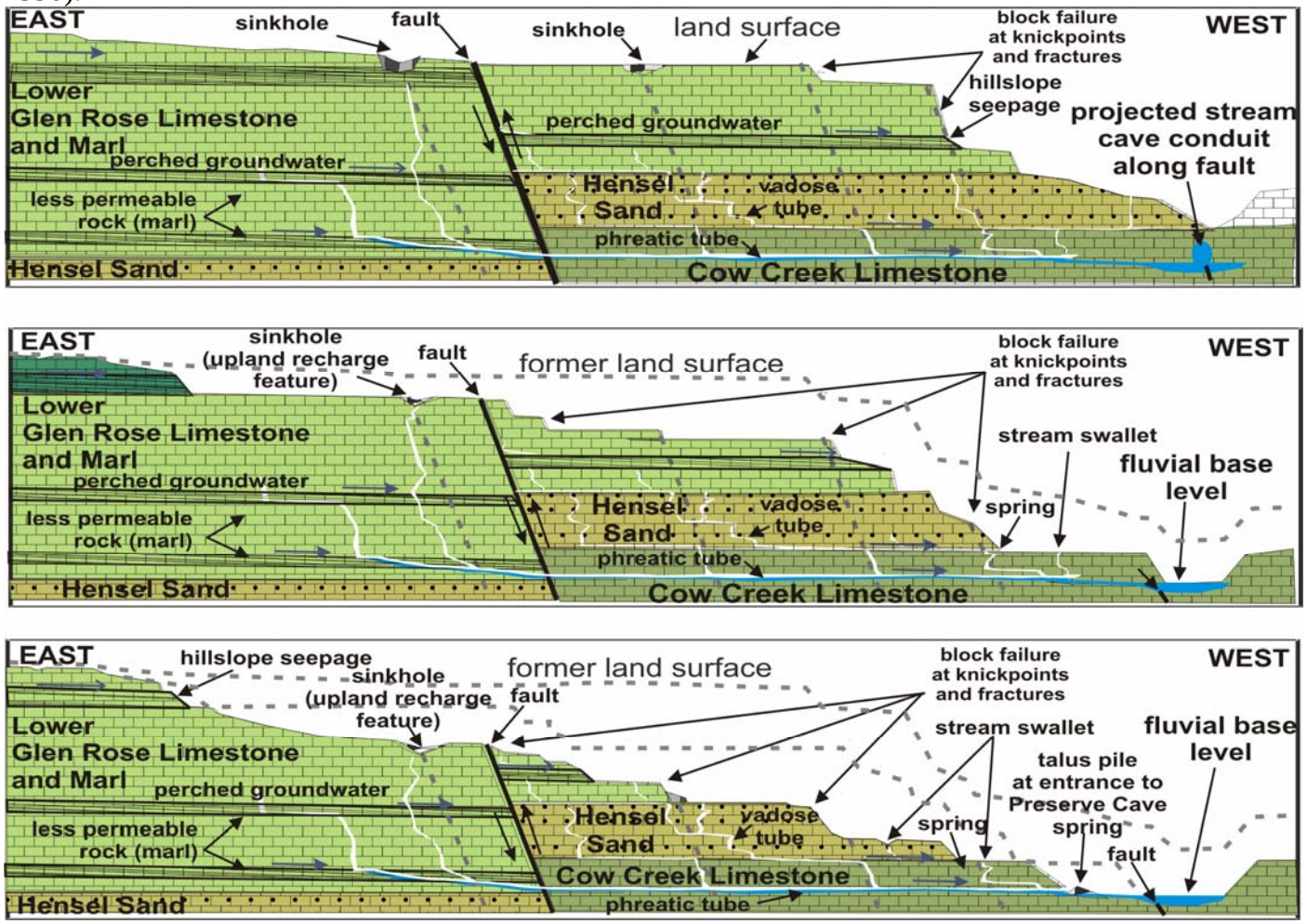

Photo Group 2. Photos of geomorphic features consistent with stream piracy and groundwater sapping (as defined by Pederson, 2001): **2A)** Photo of fracture segment of fractured rock outcrop FR-2 (facing upstream to the southeast). Some segments of surface stream patterns are parallel to faults and fractures, suggesting structural controls on drainage patterns. **2B)** Headward erosion occurs at a spring orifice (Preserve Cave entrance – March 2005) where the once buried conduit now forms a surface stream. **2C)** A stream swallet (KF-10) is situated downgradient from a perched spring orifice (SPR-8).

2A 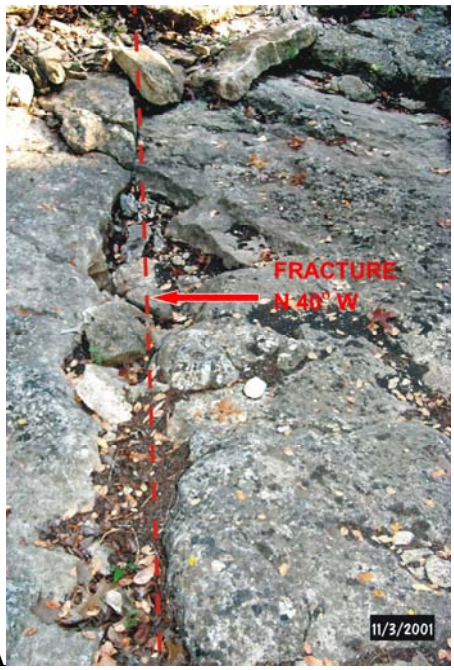

2B 

2C 

Photo Group 3 These photographs show additional geomorphic features that are consistent with stream piracy and groundwater sapping: **3A)** Conjugate fractures intersect the face of knickpoint KP-4B in Basin B (Lower Glen Rose Fm.) **3B)** Photo of knickpoint KP-1B in Basin B facing upstream to the southeast. **3C)** Photo shows fractures and travertine (from spring SPR-8). Photo of scarp collapse and alluvium, looking upstream to the southeast. The undercut scarp along the northern stream bank (Cow Creek Limestone) may be the preserved remains of a paleoconduit or may be formed by corrosion within the stream channel.

3A

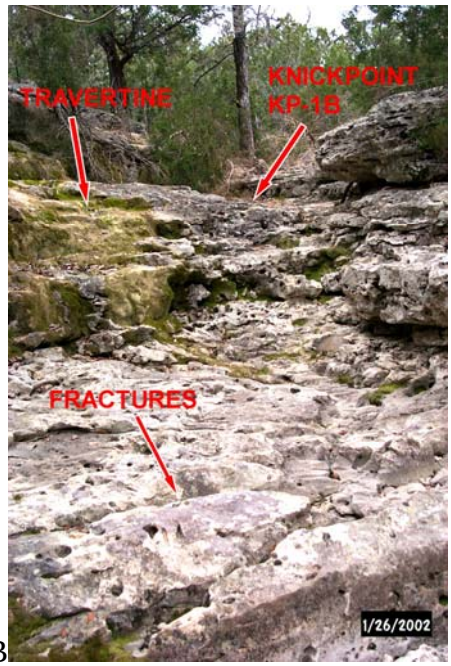

3B

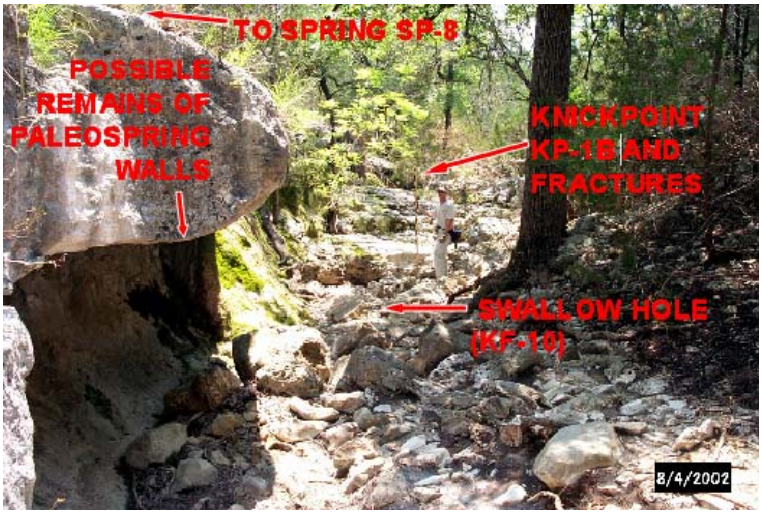

3C

Objectives

This study provides observations of the stratigraphic and structural controls on the stream cave dissolution patterns, hillslope erosion rates, differential weathering, slope stability, spring sapping, and knickpoint erosion. Alternating rock units of soft and hard limestone and dominant fracture trends play a role in the orientation of stream caves and subsequently surface erosion patterns.

Honey Creek basin provides an ideal setting in which to observe whether groundwater flowpaths and fractures leave an imprint on surface drainage patterns. Texas Parks and Wildlife Department management decisions and concurrent research projects may benefit from baseline data collected in this study (such as the hydrogeologic characterization, spatial karst feature database, and one year of erosion and deposition measurements).

This project may be useful in surface water and groundwater management decisions within this setting and the central Texas Hill Country by providing a better understanding of stratigraphically perched springs and fluvial base level springs that may respond differently to environmental changes at the surface. Stream piracy and groundwater sapping affects such things as migration patterns for aquatic animals, rates of erosion in upland areas, and stream chemistry changes, as well as landscape evolution.

Additionally, the baseline hillslope erosion and deposition measurements taken during this study may possibly be compared to data taken following Ashe juniper tree removal, which is being conducted by TPWD (Steffens and Wright, 1996; TPWD, 1999). Invasion of uplands by Ashe juniper is suspected to exacerbate periodic declines in groundwater yield by reducing infiltration. The results of the

Seco Creek Study by Steffens and Wright (1996) showed an 80% increase in spring flow when 80% of the Ashe juniper was cleared from an 8-acre site. Slaughter (1997) attempted to establish rates for "canopy interception, throughfall, stemflow, and infiltration for Ashe juniper." Slaughter found that throughfall (84% to 92%) and stemflow are higher for Ashe juniper than for plateau live oak (71%), as measured by Thurow (1987). This suggests that total interception losses for Ashe juniper are less than for plateau live oak. Slaughter found infiltration to be slightly lower beneath Ashe juniper trees (180mm/hour) than for plateau live oak (200 mm/hour) as calculated by Thurow et al., (1987). Dugas et al. (1998) conducted a soil water balance study to measure the effect of removing Ashe juniper on evapotranspiration and runoff in a paired basin study (treated and untreated basins) in Uvalde County, Texas. The results showed brush removal did not significantly affect evapotranspiration and did not consistently affect runoff rates. Ashe juniper clearing provided short-term potential for greater water yields by lowering evapotranspiration for two years following juniper removal (treatment) (Dugas et al., 1998). The increased water yield declined after 2 years as grasses became established where juniper had been cleared. The results of the Dugas et al. (1998) study suggest that juniper removal might temporarily increase infiltration and local spring flow. However, it is not known whether stratigraphically perched springs would respond to increased infiltration or whether it would provide significant recharge to the deeper aquifers.

Many studies (Harding and Ford, 1993; Leopold et al., 1964 and 1966; Rapp et al., 1972; Smith and Stamey, 1965) show that the removal of vegetation, particularly of shrubs and trees, is associated with accelerated rates of erosion because of increased runoff and a lack of ground cover to intercept precipitation

(Dunne and Leopold, 1978, p. 510-585). Little information is available that documents the effect of tree removal changes on erosion or surface and groundwater interactions in this setting. Due to the complexity of the hydrogeology, vegetation removal studies completed in different settings such as the northwest logging areas are not applicable to the central Texas Hill Country.

Surface water features in the study area (streams, lakes, rivers, wetlands, and discharge from spring orifices) interact with groundwater. A better understanding of surface and groundwater interactions is needed to evaluate their effects on groundwater availability, environment, and to provide baseline data to support watershed management decisions. This thesis contributes some baseline data that be used for future evaluation at Honey Creek.

Groundwater in karst zones and fractured-rock aquifers is particularly responsive to groundwater and surface water interactions. Groundwater response to precipitation or land use changes is particularly amplified in fractured-rock aquifers due to responses to pumping stress and drought conditions. Additionally, contamination can be more rapid than in aquifers where water flows through open conduits or fractures.

The Guadalupe River, of which Honey Creek is a tributary, is highly valued for its aesthetic qualities and is sensitive to a change in water quality because of accelerated soil erosion. Farther downstream, Canyon Lake is used as a drinking water source and recreational resource. Additionally, studies related to erosion, stream piracy, and groundwater sapping are relevant to Texas Hill Country aquatic ecology that supports many federally protected species. Studies in this area are also relevant to groundwater quality and quantity issues of the Edwards-Trinity aquifers (Mace et al., 2000).

Stream and spring ecology support unique aquatic species such as the spring-dependent Honey Creek Salamander (*Eurycea tridentifera*). Springs, streams, and rivers often fall within areas of prime habitat for the federally protected migratory songbird known as the golden-cheeked warbler (*Dendroica chrysoparia*) (Oberholser, 1974; Pulich, 1976; USFWS, 1992; Wahl et al., 1990). Therefore, it is important to understand the interaction of surface and groundwater to aid in ecological management decisions in similar settings.

The purpose of this study is to provide an interpretation of the surface water and groundwater interaction in this basin. This investigation of the controls on surface water and groundwater flow uses 5 primary steps: 1) comparison of orientations of fractures, streams, and stream caves; 2) identification of hydrostratigraphic controls; 3) comparison of regional vs. local groundwater gradients; 4) comparison of stream cave footprints vs. surface streams; 5) sediment sampling and erosion/deposition monitoring on marly slopes where seepage erosion is suspected; 6) measurement of longitudinal profile distribution of knickpoints, fractures, stream swallets, and lithology.

To accomplish these goals, field measurements of fractures, creeks, stream cave passages, and karst feature orientations were measured and plotted on rose diagrams using Geoorient computer software to compare their relationships statistically. USGS real-time data (USGS, 2001) at Honey Creek State Natural Area were used to compare seasonal rainfall and runoff events to groundwater depths in one deep water well (TWDB Well No. 6813102) and one shallow water well (Well #68-13-101) to better understand the potential response of environmental variables. Erosion and deposition along marly risers was measured using pins and washers for the period of one year (August 2001 to August 2002) to analyze the effect of seepage

erosion and seasonal variations on 3 pairs of test plots at 3 elevations within each of the paired Honey Creek State Natural Area basins. A high precision global positioning system (GPS) unit was used with carrier phase correction data to survey the locations and elevation data of knickpoints and stream segments within Basin B of Honey Creek State Natural Area. A tape measure and stadia rod were used to take measurements where tree cover was too thick to obtain the appropriate accuracy or to refine the GPS elevation data. ArcGIS software was used to plot karst features, fractures, geologic contacts, streams and rivers, knickpoints, and springs. Arc Map with Spatial Analyst was used to evaluate the Digital Elevation Model (DEM) to generate surface contours and to delineate watersheds.

PREVIOUS INVESTIGATIONS

Stream piracy occurs when water is captured by a stream found at a lower stream base level (elevation). Stream piracy is often associated with unconsolidated sedimentary deposits; however, Higgins (1984, p. 18-58) findings suggest that groundwater sapping is possible in rock and cemented sediments where streams channels become incised or entrenched into the water table and due to hillslope processes. Existing literature (Dunne, 1990; Howard, 1988) suggests that seepage erosion also occurs in consolidated rock. Howard (1988, p. 3) proposed that *"Groundwater sapping, as distinct from piping, is a generic term for weathering and erosion of soils and rock by emerging groundwater, at least partially involving intragranular flow (as opposed to the channelized through flow involved in piping)."*

Pederson (2001) defines groundwater sapping as the erosion and weathering of rock and soil by groundwater. Evidence of groundwater sapping includes seepage erosion along hillslopes, spring sapping, and headward erosion of stream channels (Fenneman, 1931; Fabel et al., 1998, Pederson, 2001). Spring sapping erodes a hillslope where a spring emerges and includes collapse of saturated hillslopes and chemical weathering (Baker, 1990). Spring sapping is known to occur in Northern Yorkshire, England at or above the contact between the Upper Oxford Clay and Lower Calcareous Grit within siltstones with little clay (Nash, 1996).

Pederson's (2001, p. 6) review of current literature and academic history of stream piracy concluded that it is likely that "*most hillslope erosion and channel extension patterns carry the imprint (pattern) of groundwater-flow systems"*. Pederson's assessment of the literature supports his opinion that under conditions of stream piracy, topography follows groundwater in some areas.

Existing literature from research conducted by Freeze (1987), Fyodorova and Sasowsky (1999), and Johnsson (1999) suggests that topography reflects groundwater flow in karstic and groundwater sapping settings. Freeze (1987) modeled of the potentiometric surface between parallel rivers, so that recharge and aquifer characteristics were coupled with the slope stability calculations to show the effects of infiltration from various precipitation events. The results suggested that hydrogeology, climatic variation, and storm-event precipitation events affected slope and surface topography. Freeze found that in some areas topography is a reflection of the groundwater table because pore water pressure and saturated hydraulic conductivity affect erosion and decrease slope stability. Saturated hydraulic conductivity controls whether the primary erosion agent will be surface runoff or subsurface pore pressure. Freeze's results suggest that surface topography may reflect the water table; this is the reverse of the popular idea that the water table is a subdued reflection of topography.

Groundwater sapping can be identified by erosional patterns that result from geologic conditions and groundwater flow patterns. Caves may develop along larger fractures within bedrock that continue to enlarge due to erosion and dissolution (Fyodorova and Sasowsky, 1999). In Swago Creek, West Virginia, Johnsson (1999) identified two sets of horizontal cave passages at two historic elevations of the groundwater table and groundwater flow directions to find that the fracture orientations and groundwater flow directions affected the groundwater sapping patterns.

Hack (1960 and 1965) proposed that the equilibrium landscape is one that is in balance with ongoing erosion or dissolution processes. The water table adjusts to changes in elevation of the incised creeks and to other controls on spring water (Palmer, 1990).

Springer, Wohl, Foster, and Boyer (2003) found evidence that bedrock streams maintain concave profiles while adjusting channel geometries and hydraulics at Buckeye Creek (a fluviokarst basin) and the Greenbrier River (underlain by limestone), in southeast West Virginia. This suggests that the adjustment of channel geometries and hydraulics in bedrock streams with stable concave profiles is analogous to alluvial rivers.

Woodruff and Abbott (1979) explained that the low relief, resistant, karstic uplands of central Texas are an equilibrium landscape punctuated by groundwater infiltration, attenuated erosion, and deposition by surface streams. They suggest that low-relief karstic plains and deeply incised streams represent historically slow rates of fluvial downcutting and high rates of groundwater recharge that helped to form a network of stream caves and springs. Woodruff and Abbott (1979) observed that upland karst plains and deeply incised stream channels are in disequilibrium with one another, indicating stream piracy within the Guadalupe River basin. Honey Creek basin is a sub-watershed of the Guadalupe River basin.

Veni (1994a) characterized the Lower Glen Rose Limestone with in the Guadalupe River basin as gravity-drained with discharge from springs along the river. Veni identified the long stream caves as dendritic with evidence of flow piracy and rapid responses to storm events. Within the Guadalupe River basin, Veni calculated the hydraulic conductivity as 5.81×10^{-4} m/s, the transmissivity as 3.48×10^{-3} m^2/s, and the specific yield as 8.1%. He explained that the specific yield was relatively high

due to the honeycombed texture of the Lower Glen Rose Limestone. Veni calculated the mean aquifer storage as 1.5 x 10^5 m^3/km^3 and 3.7% in conduits. He concluded that the rising limb of the hydrograph of flow from a spring orifice in this basin could be used to calculate the size of a spring's catchment area, volume, and transmissivity of the conduit. He found piracy to occur "within and between caves and surface streams." Veni hypothesized that Honey Creek Stream Cave was truncated by the downcutting of Honey Creek and created a series of maps showing a possible evolution scenario of Honey Creek Stream Cave that included a hypothetical projection of Honey Creek Stream Cave across the creek channel draining toward the Guadalupe River (Veni, 1994a, Figures 4.46a and b, p. 218-219) (Figure 5). Veni's maps suggest a relationship of the hypothetical conduit to the potentiometric surface and the down-cut Guadalupe River basin (instead of Honey Creek).

Observations and quantitative measurements in previous studies suggest that the layering of rock units of alternating resistance and permeability influences weathering and erosion (Johnsson, 1999, Palmer, 1990, Woodruff and Marsh, 1992, Wilson, 1986, and Veni, 1994a). The orientation, density, infilling and aperture of fractures, faults, recharge and discharge features serve as useful indicators of preferential erosion and groundwater flow (Rasco, 1998 and Wermund et al., 1978). Locally, sequences of interbedded limestone and weathered limestone described as calcareous marl (or locally as caliche) consist of layered rock units of alternating resistance and groundwater properties (Woodruff and Marsh, 1992). Near Honey Creek, sequences of dolomitic limestone contain solutionally enlarged fractures and spring conduits. Woodruff and Marsh (1992) suggest that alternating layers of calcareous marl (or caliche) form more ductile layers, which form an aquitard between, fractured limestone units (Figure 6).

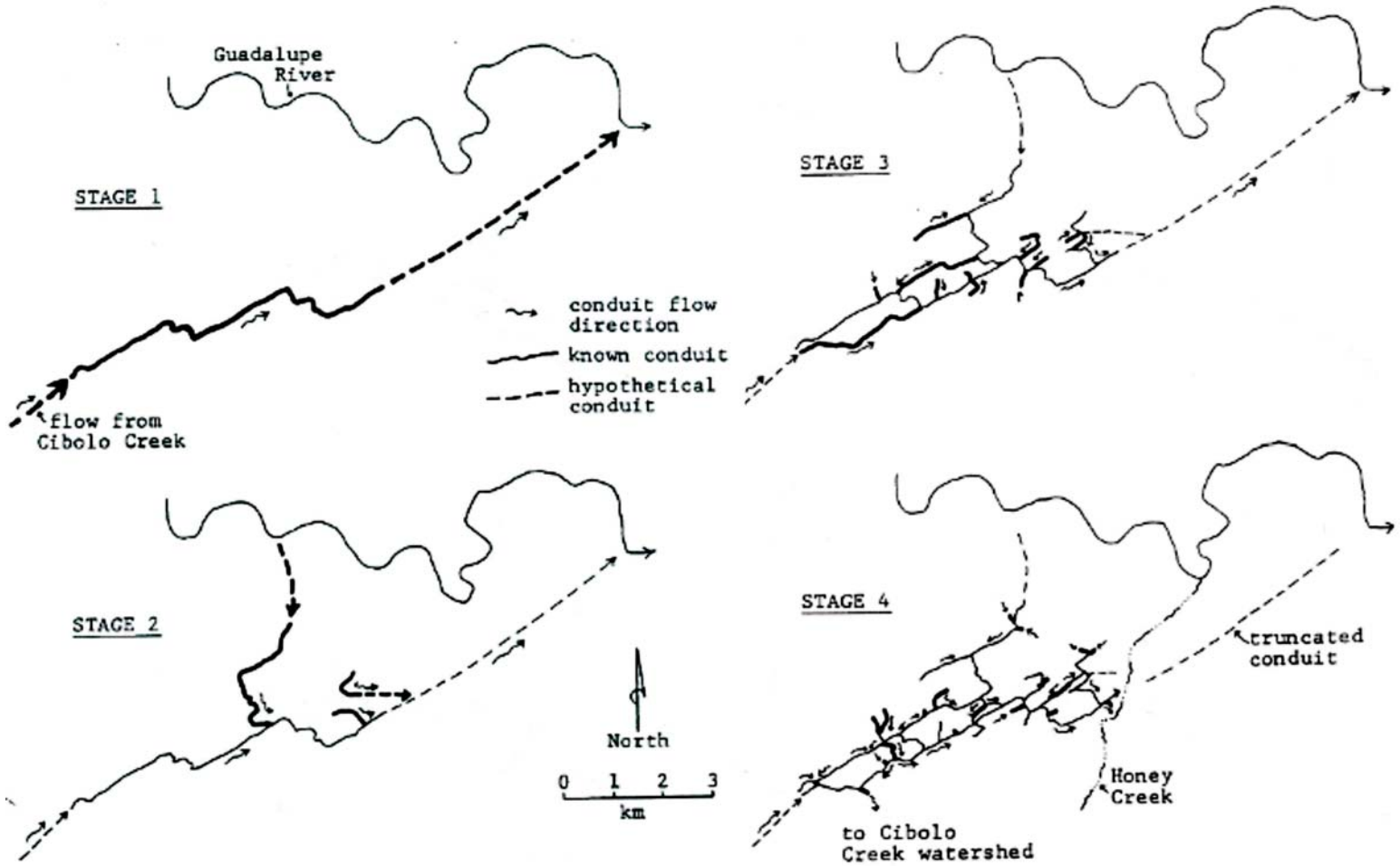

Figure 5. Model of evolution of Honey Creek (Veni, 1994a, Figures 4.46a and b, p. 218-219).

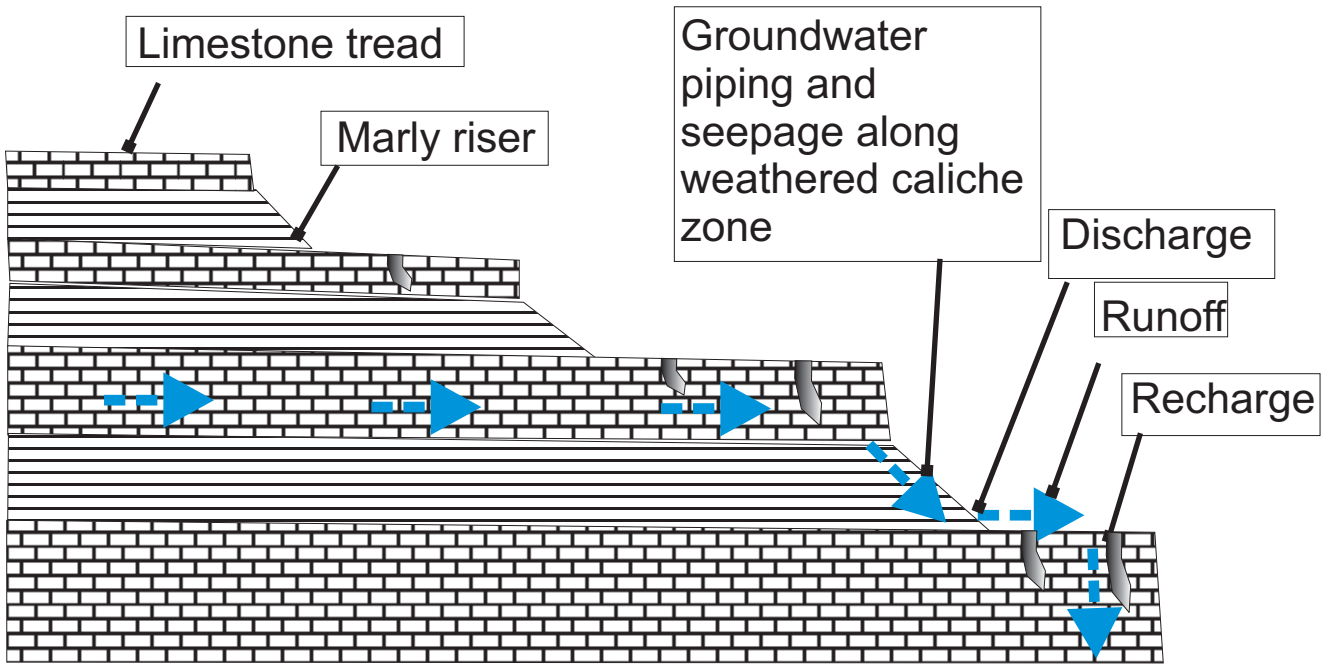

Figure 6. Treads and risers of lower member of the Glen Rose Formation.

ENVIRONMENTAL SETTING

Honey Creek State Natural Area contributes runoff and spring flow to the main channel of Honey Creek and to the Guadalupe River. The Middle Trinity aquifer is a primary aquifer in the Texas Hill Country (Barker et al., 1994, Figs. 3 and 4, p. 4-6). It includes the Lower Glen Rose Limestone, Hensel Sand, and Cow Creek Limestone and is typified by rolling rangeland and dissected by numerous intermittent drainages (Figure 1). Two paired tributary basins (Basins A and B) are located along the southeastern edge of Honey Creek basin, about 2000 feet (620 m) (to its confluence with the Guadalupe River) (Figure 2).

Land Use

The approximately 2294-acre (928-hectare) Honey Creek State Natural Area is located within Honey Creek basin (Figure 2). Both the natural area and basin are situated in an area that was historically rural within an unincorporated area of Comal County, Texas. Land use in the general area remains rural in nature and is primarily related to the livestock ranching industry and the adjacent Guadalupe River State Park. Nearby land uses in the area include recreation such as camping, canoeing, and rafting. The site consists of cleared upland lands (pasture) and mostly uncleared grazing rangelands, although most of the woodlands on the site were historically thinned. The state natural area is irregularly shaped, extending over an area approximately 12,000 feet (3658 m) in length (north to south) and 6000 feet wide (1829 m) (east to west). Along its western boundary, the Honey Creek State Natural Area has approximately 12,000 feet (3658 m) of frontage of the main channel of Honey Creek, which flows south to north. The natural area also has 1500 feet (457 m)

of Guadalupe River frontage to the north. Other improvements include solar and battery-powered USGS weather stations and weirs, one shallow and one deep water well, and electricity installed to serve the former residence that is now used to serve the USGS water wells (USGS, 2001).

The historic land use of Honey Creek State Natural Area was as a working cattle ranch. Cattle production primarily focused on cow-calf management and beef production. Small sheds, barns, and cattle pens are scattered along the uplands of Honey Creek State Natural Area. The areas with structures and much of the remaining acreage are accessed by a network of ranch roads, some of which are improved with caliche road-base material (excavated from the abundant calcareous marl layers of the Lower Glen Rose Limestone). Within the past 100 years, the land-use disturbance, agriculture, timber harvesting of mature forests in canyon areas, fire-suppression, and drought have affected the vegetation coverage and have contributed to the invasion of secondary growth Ashe juniper on the uplands and the reduction of plant diversity (Palmer, 1920, Palmer et al., 1984, and Seele, 1885).

Physiography

The study area is located between the Edwards Plateau region and Balcones Escarpment within an area commonly referred to as the central Texas Hill Country (Figure 1). The Texas Hill Country is typically underlain by the Glen Rose Limestone that forms stair-step topography (Figure 6). Thin soils are typically found on uplands. High velocity storm-flow events have dissected narrow canyons into the carbonate rock. The carbonate terrain is dissected by the headward erosion of streams and rivers, forming steep gradients, and canyon walls (Figure 3). Amphitheater-shaped canyon heads open to steep-walled canyons.

Climate

Mean annual precipitation was approximately 30 inches (76 cm) per year over the Texas Hill Country between 1951 and 1980 (Barker et al., 1994; Riggio et al., 1987). The highest rainfall amounts are typically in May and September (Carr, 1967). Additionally, an orographic affect causes the Edwards Plateau (and Honey Creek basin) to receive a significantly higher amount of rainfall than surrounding areas (Larkin and Bomar, 1983). This pattern is also evident in maps produced by Asquith and Roussel (2003).

Vegetation

Honey Creek basin is mapped as within the eastern edge of the Edwards Plateau vegetation region (Gould, 1975). Field investigation revealed a complex distribution of plant flora (McMahon et al., 1984). The following plants were identified on the uplands during the field investigation portion of this study: Ashe juniper and plateau live oak savannah with scattered brush and interspersed grasslands. Plateau live oak is the dominant overstory species and mottes of trees are scattered throughout the site. Secondary-growth Ashe juniper, Texas persimmon, agarita, and sumacs dominate the mid-story. Short and mid-grasses include buffalograss; hairy tridens, perennial and annual three-awn, little bluestem; silver bluestem, King Ranch and bluestem. Many forbs and wildflowers, as well as prickly pear, are abundant on the upland grasslands. Vegetation on the majority of the slope and drainage areas consists of Ashe juniper, Texas oak, plateau live oak, cedar elm, shin oak, and sugarberry. Ashe juniper, plateau live oak, agarita, and Texas persimmon dominate the dry, rocky hills (Photo 4A).

Photo Group 4. These photographs show typical vegetation at Honey Creek State Natural Area: **4A)** Photograph of mid-basin vegetation within an intermittent tributary to Honey creek, consisting of Ashe juniper with interspersed Texas oak and assorted grasses (Basin B) 4B) Photograph of vegetation within perennial Honey Creek, consisting of cypress trees, Texas palmetto, columbine, sedge, and maidenhair fern occur along the rocky banks. Lily pads and spatterdock float on the surface of Honey Creek.

4A 

4B 

Downslope within Honey Creek canyon, an abrupt change in plant fauna was observed, which includes more cedar elm and older Ashe junipers with the addition of Spanish oak, pecan, walnut, and Mexican buckeye (McMahon et al., 1984). The terrain levels out in the narrow floodplain of Honey Creek where the dominant species are sycamore and bald cypress, and a variety of riparian floodplain species (Ford and Van Aucken, 1982). Texas palmetto, columbine, sedge, and maidenhair fern occur along the rocky banks (Photo 4B). Lily pads and spatterdock float on the surface of Honey Creek (McMahon et al., 1984). Emergent plants are also present in the perennially flowing channel of Honey Creek.

Soils

According to the Soil Survey for Comal County (Batte, 1984), soils within Honey Creek basin are found within the Comfort-Rumple-Eckrant association, which consists of very shallow, to moderately deep, undulating, and steep to hilly soils over indurated limestone and calcareous marl, on uplands of Edwards Plateau). Primary soil types within Honey Creek State Natural Area can be distinguished from one another by changes in the dominant vegetation, topographic position, and steepness of slope. Fractured limestone interbedded with calcareous marl is overlain by soils that range in permeability from moderate to moderately slow when saturated and rapid when dry (Batte, 1984). Soils on calcareous marl slopes tends to be calcareous, while soils on dolomitic hilltops and sideslopes tends to be noncalcareous. The calcareous nature of the soils may be helpful to determine whether the parent material is calcareous marl or dolomitic limestone. A map of published soils is shown in Figure 7 and a table of soil units is provided in Table 1 (Batte, 1984).

Table 1. Table of soils (Batte, 1984).

Soil Name	**Soil Type**	**Soil Depth (inches)**	**Underlying Material**	**Perme-ability**	**Available Water Capacity**	**Surface Runoff**	**Erosion Hazard**	**Calcareous Nature**	**Location**
Bracket Rock Outcrop Comfort Complex, undulating (BtD)	Gravelly clay loam to stony clay	0 to 17	Limestone	Moderately slow	Very low	Medium	Severe	Brackett soils are moderately calcareous. Comfort soils are noncalcareous.	Uplands, escarpments, and high rounded hills. Slopes are benched in appearance because of horizontal rock outcrop.
Bolar clay loam, 1 to 3 % slopes (BrB)	Clay loam to cherty clay	28	Indurated limestone and marl	Moderate	Low	Medium	Moderate	Moderately calcareous.	Concave valley slopes and foot slopes of hills on uplands.
Denton Silty Clay, 1 to 5% slopes (DeC3)	Silty clay	31	Fractured limestone interbedded with calcareous marl.	Slow when wet, rapid when dry.	Low	Rapid	Moderate	Calcareous	Valley slopes on uplands.

Soil Name	Soil Type	Soil Depth (inches)	Underlying Material	Perme-ability	Available Water Capacity	Surface Runoff	Erosion Hazard	Calcareous Nature	Location
Real-Comfort-Doss complex, undulating (RcD)	clay loam to gravelly loam	7 to 12	Indurated limestone and marl	moderate to moderately slow	Very low	Low	Low	Noncalcareous throughout.	Low hills and ridges on uplands.
Anhalt clay 0 to 1 % slopes (AnA)	Clay	28	Fractured, hard limestone	Very slow when wet, rapid when dry	Low	Slow	Slight		
Comfort Rock outcrop complex, undulating (CrD)	Shallow extremely stony, clay soils and rock outcrop	0 to 13	Indurated, fractured limestone.	Slow	Low	Slow to medium,	Slight hazard.	Noncalcareous throughout	Side slopes, hilltops, ridgetops, and uplands on side slopes. Slopes are convex.
Eckrant-Rock Outcrop complex, steep (ErG)	Shallow, clayey soils and rock.	0 to 10	Indurated, fractured limestone	Moderately slow.	Very low.	Rapid. Well Drained.	Severe hazard.	Noncalcareous throughout.	Long narrow slopes on high hills, ridges, and along escarpments. Slopes are convex and range 0 to 30%.

Topography

Topography of the Honey Creek basin is characterized as a gently rolling landscape that is dissected by numerous steep, narrow drainages. At Honey Creek State Natural Area, land surface elevations range from approximately 1080 feet (329 m) above sea level in the northern portion of the site along the Guadalupe River to 396 m (1302 feet) above sea level on the highest hilltops. Topographic relief between the highest and lowest points within the Honey Creek State Natural Area is close to 68 m (222 feet).

Lithology

Honey Creek basin is underlain by the Upper and Lower Glen Rose Limestone (with occasional dikes of Upper Cretaceous basalt), Hensel Sand, and Cow Creek Limestone (Figure 8) (Barker et al., 1994; Collins, 2000, Lonsdale, 1927). The Cretaceous strata of the Middle Trinity aquifer are nearly flat lying and dip slightly toward the southeast above Paleozoic and Triassic rock units that dip westward.

Cow Creek Limestone

The Lower Cretaceous Cow Creek Limestone consists of fossiliferous dolomitic limestone with interbedded sand and shale layers with silicious geodes (Barnes, 1983). The thickness of the Cow Creek Limestone is approximately 75 feet thick (22.9 m) near the study area (George, 1952). About 50 feet (15.2 m) of the formation crops out within the Guadalupe River and some of its tributaries such as Honey Creek (Cooper, 1964). Fossils include *Exogyra* sp. and pelecypods. Upper Cow Creek Limestone commonly forms a distinct ledge along the Guadalupe River and its tributaries (Collins, 2000).

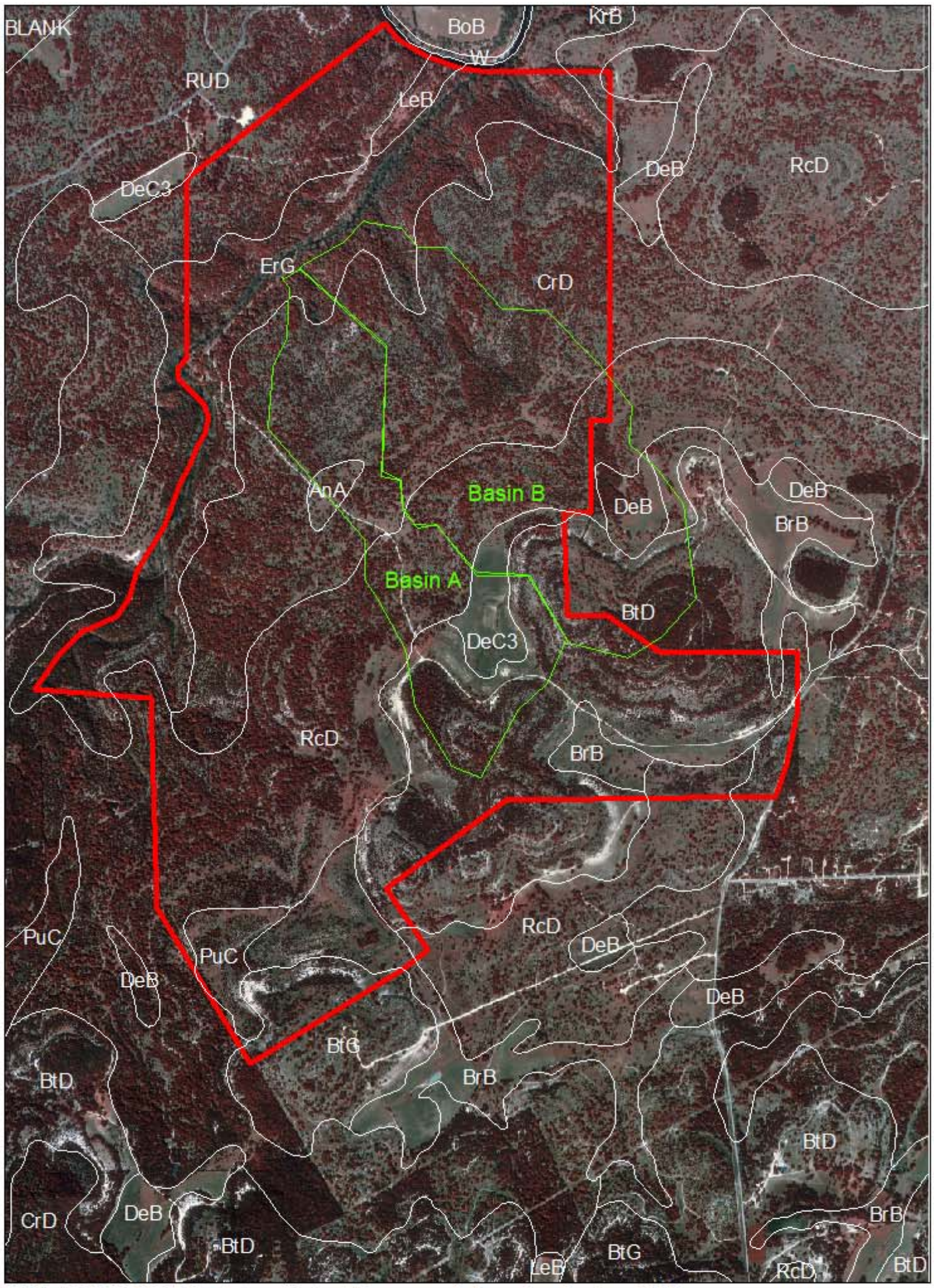

AERIAL PHOTO SOURCE: Texas Natural Resources Information System, 2002.
SOILS DATA: Batte, C.D., 1984, Soil survey of Comal and Hays Counties, Texas.
US Department of Agriculture, Soil Conservation Service, in cooperation
ith the Texas Agricultural Experiment Station

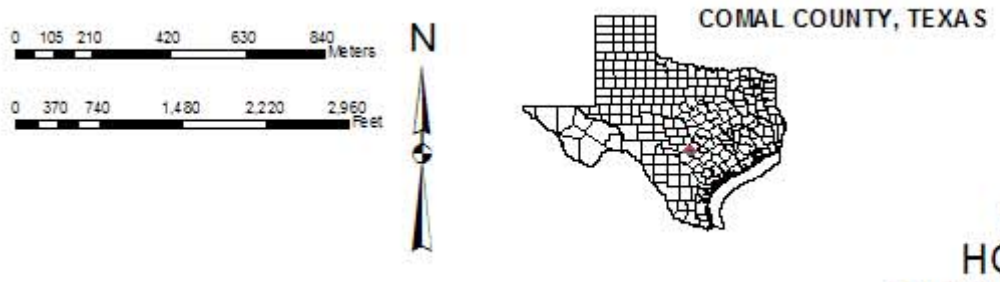

FIGURE 7

SOILS MAP
HONEY CREEK
STATE NATURAL AREA
COMAL COUNTY, TEXAS

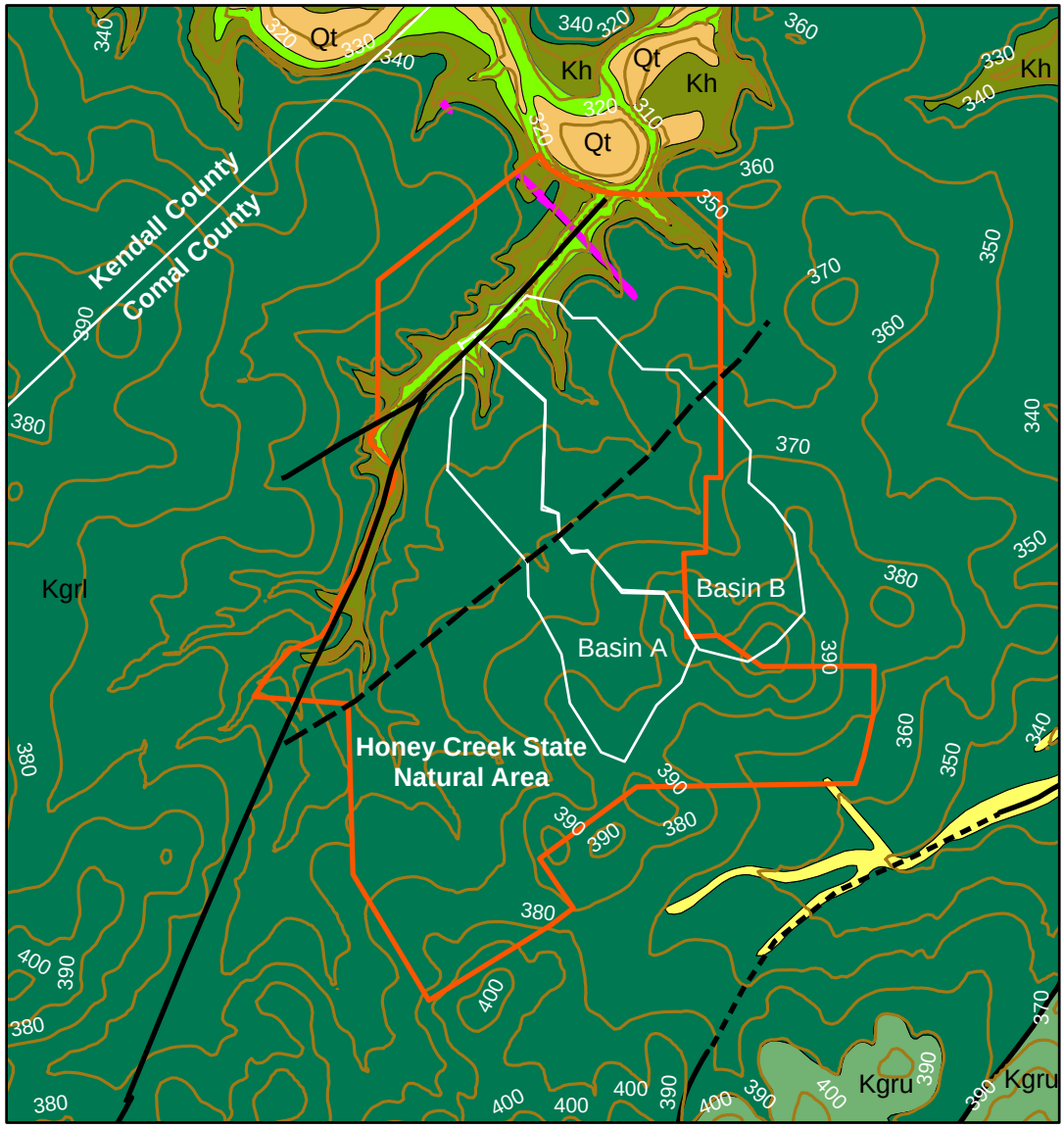

Geologic Map Modified From:
Collins, E.D., 2000, Geologic Map of the New Braunfels, Texas 30 x 60 Minute Quadrangle, University of Texas Bureau of Economic Geology.

0 162.5 325 650 975 1,300 Meters

0 600 1,200 2,400 3,600 4,800 Feet

N

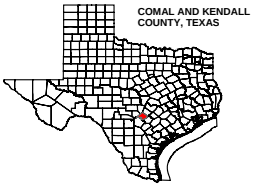

Legend

- Honey Creek State Natural Area
- Contour (10-m interval)
- Normal Faults
- Qal - Alluvium; gravel
- Qt - Terrace alluvium
- Kb - Basalt, minor occurrences
- Kgru - Upper Glen Rose Formation
- Kgrl - Lower Glen Rose Formation
- Kh - Hensel Formation
- Kcc - Cow Creek Formation

FIGURE 8
SITE GEOLOGIC MAP
HONEY CREEK
STATE NATURAL AREA
COMAL COUNTY, TEXAS

Hensel Sand

Hensel Sand is composed of sandy limestone and sandy dolomitic limestone. Approximately 45 feet of the Hensel Sand outcrop along the Guadalupe River and its tributaries (Cooper, 1964). The upper unit that is exposed in the Honey Creek tributaries is a glauconitic sandy limestone. The lower Hensel is less weather resistant and weather to loose yellowish-brown soil (Collins, 2000).

The Lower Cretaceous Hensel Sand consists primarily of alluvial and near-shore marine sands, which are equivalent to the Glen Rose Formation (Stricklen et al., 1971). The Hensel Sand and Glen Rose Limestone form a wedge that thins toward the northwest (Llano uplift). The relationship between the Hensel Sand clastic sediment and the Glen Rose Limestone carbonates is gradational (Stricklen et al., 1971). The depositional dip is to the southeast and reflects facies changes and on-lap over pre-Cretaceous rocks near Llano to the northwest.

The Hensel Sand consists of nearshore marine deposits, which are about 9 m (30 feet) thick at Honey Creek State Natural Area and consist of sandy dolomite beds. These sandy dolomite beds progressively replace younger terrestrial deposits up-dip toward the northwest. Typically, the Hensel Sand comprises a mixture of limey sand, silt, chert, and dolomite pebbles in a basal conglomerate. However, near Spring Branch, Texas and within Honey Creek basin, these beds form the southernmost down-dip beds of the Hensel Sand Formation and contain abundant clay, siliceous concretions, and large bivalves (Ashworth, 1983; Stricklen et al., 1971). The name “Hensel” is commonly spelled with 2 letter “l’s”, but only one “l” is used herein because the original spelling of the family name associated with the formation contains only one letter “l” (Stricklen et al., 1971).

Glen Rose Limestone

The Lower Cretaceous Glen Rose Limestone is divided in to two stratigraphic units, based on lithology and index fossils. The widespread Corbula species fossil bed marks the boundary between the Upper and Lower Glen Rose Limestone (Whitney, 1952). The lower portion of the lower member of the Glen Rose Limestone consists of thick dolomitic layers, which form aquifers characterized by local cave development and fracture permeability. Alternating beds of limestone, dolomitic limestone, argillicious limestone, and some marl are typical of the upper part of the lower member of the Glen Rose Formation, forming stratigraphically perched aquifers and springs. The upper member of the Glen Rose Formation consists of alternating beds which are resistant beds of dolomite, mudstone, and limestone and non-resistant beds of calcareous clay. Stair-step topography is characteristic of the Glen Rose Formation and is formed by the alternating resistant and recessive beds. Foraminifera tests (*Orbitilina texana)* that indicate the top of the lower member of the Glen Rose Limestone.

Basalt

One dike of igneous intrusive rocks (basalt) is present near the mouth of Honey Creek where it flows into the Guadalupe River. This dike is formed along a northwest-trending fracture (~300° to 330°) (Londsale, 1927).

Quaternary Terrace Deposits

The Quaternary-age alluvial deposits consist of gravel, sand, silt, and mud. The deposits are found on uplands near alluvial channels. Terrace deposits are considered indicators of stream piracy and a relict potentiometric surface (Woodruff, 1974).

Photo Group 5. Rock unit identification photographs: **5A)** Photo (in mm) of foraminifera tests (*Orbitilina texana)* that indicate the top of the Lower Member of the Glen Rose Limestone (photograph by James Sprinkle, University of Texas at Austin, 2001). This sample was taken at the base of Plot-3B. **5B)** View of exposed Hensel Formation (yellowish-tan) at the contact with overlying Lower Glen Rose FM. (gray) exposed within incised channel of Basin B.

5A

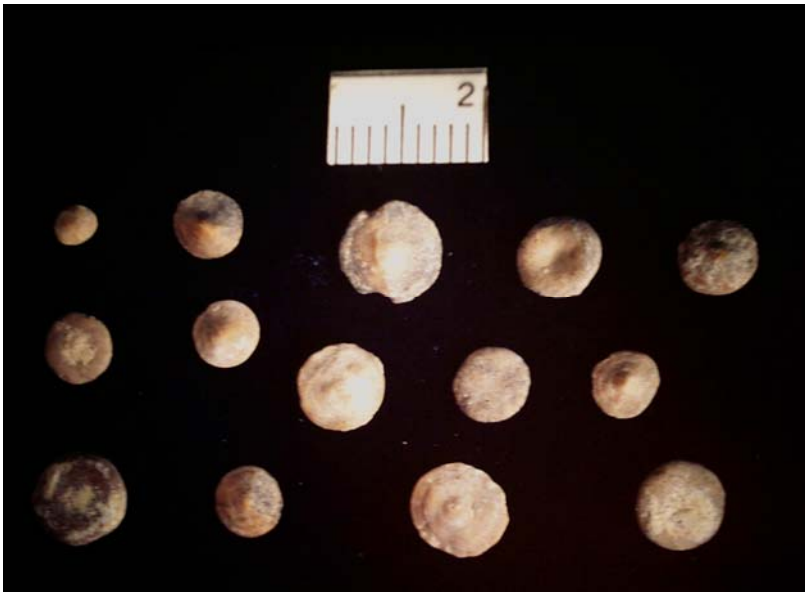

5B

Hydrogeologic Setting

The Middle Trinity aquifer occurs parallel to regional faulting associated with the western edge of Balcones Fault Zone and spans many surface drainage basins (Abbott, 1975; Collins and Hovorka, 1997; Rose, 1972; and Stricklin et al., 1971). The Middle Trinity aquifer is the principal aquifer in Honey Creek basin. The Middle Trinity aquifer yields very small to moderate quantities of fresh to moderately saline water (Reeves, 1967).

Hydrostratigraphy

Honey Creek basin is underlain by the Cow Creek Limestone, Hensel Sand, Lower Member of the Glen Rose Limestone, Upper Member of the Glen Rose Limestone, and Quaternary terrace deposits (Collins, 2000). Hensel Sand consists primarily of permeable sands (Barker et al., 1994). However, here the Hensel Sand contains abundant clay that may reduce permeability (Ashworth, 1983; Stricklen et al., 1971). The Cow Creek Limestone is relatively more permeable at the surface than it is in the subsurface because of calcite cement precipitation (Barker et al., 1994). The subsurface portion of the Lower Glen Rose Limestone may have lower permeability than at the surface (Barker et al., 1994). Large, fracture-controlled caves are formed within the Lower Glen Rose Formation in Bexar, Comal, and Kendall Counties (Kastning, 1983; Mace et al., 2000, Veni, 1994a and b). Although many of these caves are accessible and laterally persistent, groundwater flowpaths are often difficult to trace.

Table 2. Hydrostratigraphic units and water-bearing properties (from Ashworth, 1983).

System	Series	Group		Stratigraphic Unit	Hydrologic Unit	Approx. Maximum Thickness	Identification	Water-Bearing Properties
Cretaceous	Comanche	Trinity	Glen Rose Limestone	Upper member	Upper Trinity aquifer	500 ft.	Alternating resistant and nonresistant beds of blue shale, nodular marl, and fossiliferous limestone. Also contains two distinct evaporite zones.	Yields very small to small quantities of relatively highly mineralized water. Highly mineralized water has greater than 500 milligrams per liter (mg/l) of dissolved solids.
				Lower member	Middle Trinity aquifer	320 ft.	Massive fossiliferous limestone, grading upward into thin beds of limestone, dolomite, marl, and shale. Numerous caves and reefs occur in the lower portion of the member.	Yields small to moderate quantities of fresh to slightly saline water*. Cow Creek Limestone is locally water-bearing
			Travis Peak Formation	Hensel Sand		300 ft.	Red to gray clay, silt, sand, conglomerate, and thin limestone beds grading downdip to silty dolomite, calcareous shale, and shaley limestone.	
				Cow Creek Limestone		90 ft.	Massive, fossiliferous, argillaceous to dolomitic limestone with local thinly interbedded limestone and sand layers.	
				Hammett Shale Member		80 ft.	Fossiliferous, argillaceous to dolomitic limestone with thinly bedded sand, shale, and lignite.	Not known to yield water.
				Sligo Limestone	Lower Trinity aquifer	120 ft	Sandy dolomitic limestone.	Yields small to large quantities of fresh to slightly saline water*.
				Hosston Sand Member		350 ft.	Red and white conglomerate, sandstone, claystone, shale, dolomite, and limestone	
pre-Cretaceous rocks							Folded shale, hard massive dolomite, limestone, sandstone, and slate.	Yields moderate quantities of fresh water* in northern Hill Country.

* Fresh water is less than 1,000 ppm. Slightly saline water ranges from 1,000 to 3,000 ppm

Structural Controls

The structural geology of Honey Creek basin is characterized by a southeast regional dip, regional faulting, and hydrostratigraphic controls due to wedges of sediments of alternating permeability and resistance. Middle Trinity rock units consist of stacked layers of Lower Cretaceous sediments that pinch out toward the Llano Uplift and become thicker down-dip toward the southeast. The Trinity Group sediments were deposited on an unconformable surface of uplifted and folded Paleozoic rocks (Barker and Ardis, 1992). The Llano Uplift forms a structural high that provided eroded sediments that were deposited as terrigenous and near-shore depositional facies of the Trinity Group (Ashworth, 1983; Barker et al., 1994). The Balcones Fault Zone follows a northeast-to-southwest alignment. It consists of normal faults and down-thrown fault blocks that place Trinity Group sediments side by side with the stratigraphically higher Edwards Group Limestone.

Stratigraphic Controls

The Upper and Lower Glen Rose Formations consist of alternating resistant and non-resistant beds of limestone, shale, and calcareous marl. Nodular marl and blue shale form impermeable intervals (Ashworth, 1983) of resistant strata. The differential weathering of the rock layers within the Upper Glen Rose Formation contributes to the formation of stratigraphically perched aquifers and springs, differential erodability, and preferred stream erosion. Perched aquifer springs contribute runoff to intermittent creeks that provide runoff to recharge features such as stream swallets and solutionally enlarged fractures (Photos 2a, 2b, and 2c). Perched aquifer spring orifices correspond with hydrostratigraphic controls such as lithologic contacts between rock units with different permeabilities and structural

controls such as fractures and faulting. Fluvial-level springs discharge year-round (although with seasonally variable flow rates) at the base of tributaries from the banks and channel of the perennial Honey Creek (Photo 6A). Figure 4 is a conceptual cross-section of the canyon walls of Honey Creek. Spring sapping and seepage erosion has been attributed to the sapping the rocks of the canyon walls, causing them to separate and retreat, resulting in widening and steepening of the canyon walls (Fenneman, 1931; Barker et al., 1994). Photo 6B shows a view looking upstream from knickpoint KP-4B toward knickpoint KP-3B with retreating canyon walls on either side of the tributary (Basin B -Treatment).

Calcareous marl beds form aquitard layers and sloped risers. Alternating beds of different lithology provide an uneven resistance to erosion and solutioning, resulting in the stair-step topography (Figure 6 and 13). Calcareous marl risers form below the more resistant limestone ledges. The calcareous marl consists of marine shell fragments and calcium carbonates with clay and organic matter that result in a high moisture content that facilitates erosion. Wilding and Woodruff (1994) describe these risers as functioning as local water retention and storage devices. A series of locally perched aquifers and underlying aquitards are comprised of stacked sequences of weathered strata with alternating permeability (Barker et al., 1994, Woodruff and Abbott, 1979). Stair-step topography forms along the interbedded resistant and nonresistant beds (Figure 6). Wilson (1986) proposed that swelling at the edge of hillslopes caused upland limestone treads to warp and become bowl-shaped, causing concentrated karstification on the uplands.

Photo Group 6. 6A) This photo shows spring SPR-2 at the mouth of Basin A (treatment). Spring water flows out through alluvial gravel and Hensel Sand where Basin B (treatment basin) drains into Honey Creek (facing southwest and looking upstream toward Basin B). 6B) Photo looking upstream toward knickpoint KP-3B, with retreating canyon walls on either side of the tributary (Basin B -Treatment).

6A

6B

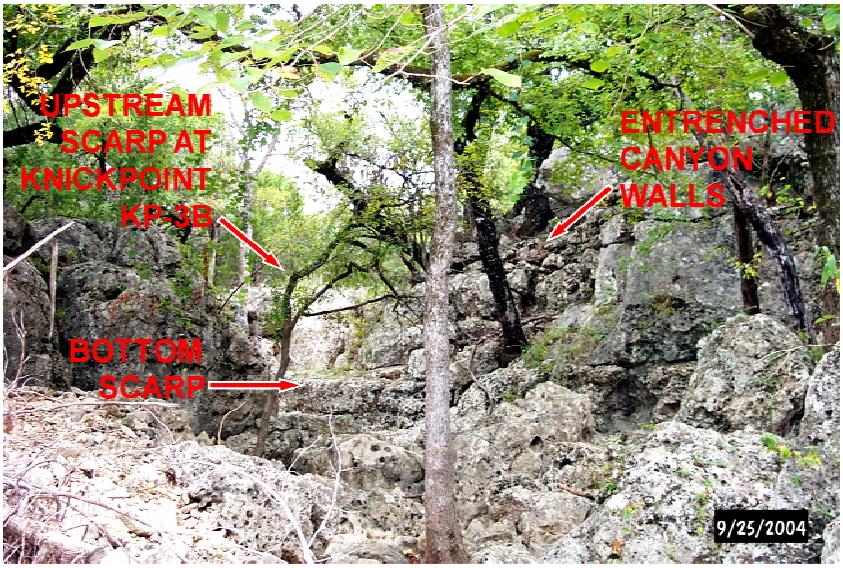

Regional Potentiometric Surface

Within the Honey Creek basin, most water wells obtain water from the Middle Trinity aquifer (Lower Member of the Glen Rose Limestone, Hensel Sand, and Cow Creek Limestone), as well as from the deeper Lower Trinity aquifer (Hosston Formation), as shown in a stratigraphic column provided in Table 2. At elevations of 1200 feet (365.76 m) above mean sea level (msl), the static groundwater levels of the Middle Trinity aquifer are about 200 feet (61 m) below the surface (Figure 9) (TWDB, 2005). The potentiometric surface in Honey Creek basin correlates with the presence of fluvial-level springs at about 1000 feet (305 m) above msl (Figure 10 and Figure 11). Some water levels seasonally fluctuate up to 50 feet (15.2 m) (Barker and Ardis, 1996), especially in shallow wells that are less than 100 feet deep (< 30 m) that rapidly respond precipitation events.

As shown in Figure 10 and Figure 11, the potentiometric surface shows that hydraulic gradient is influenced by the location of springs and rivers (Barker and Ardis, 1996; Mace et al., 2000). The potentiometric surface forms a v-shape along the Guadalupe River where the perched aquifer is intersected by headward erosion and river valley entrenchment (Figure 10 and Figure 11). The potentiometric surface is described as a subdued reflection of surface topography because of upland recharge and fluvial level discharge (Kuniansky and Holligan, 1994).

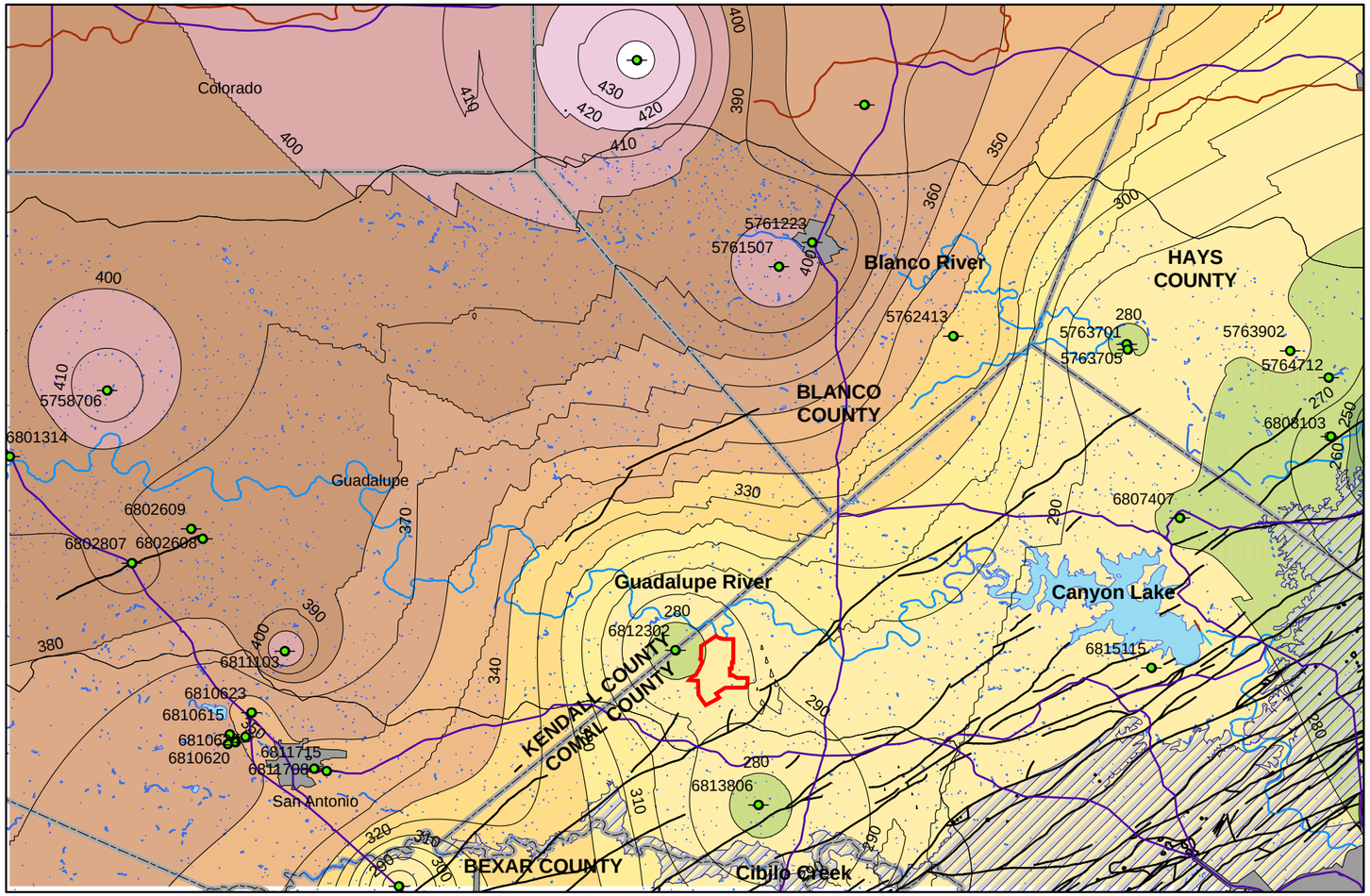

Legend

- Honey Creek State Natural Area
- Normal Faults
- Selected Water Wells
- Unconfined Zone of Edwards Aquifer
- Potentiometric Surface (m above msl)

0 4.5 9 18
Kilometers

0 3 6 12
Miles

N

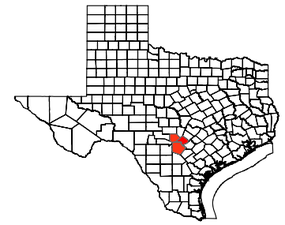

FIGURE 9

REGIONAL POTENTIOMETRIC SURFACE MAP
MIDDLE TRINITY AQUIFER (2004)
HONEY CREEK
STATE NATURAL AREA
AND SURROUNDING AREA
BEXAR, COMAL AND
KENDALL COUNTIES, TEXAS

REFERENCES: TWDB (Texas Water Development Board), 2005, Water Well Data.
National Hydrography Dataset, 2005, Rivers and Lakes.
TCEQ (Texas Commission on Environmental Quality), Edwards Aquifer Zone Boundaries, 1999.

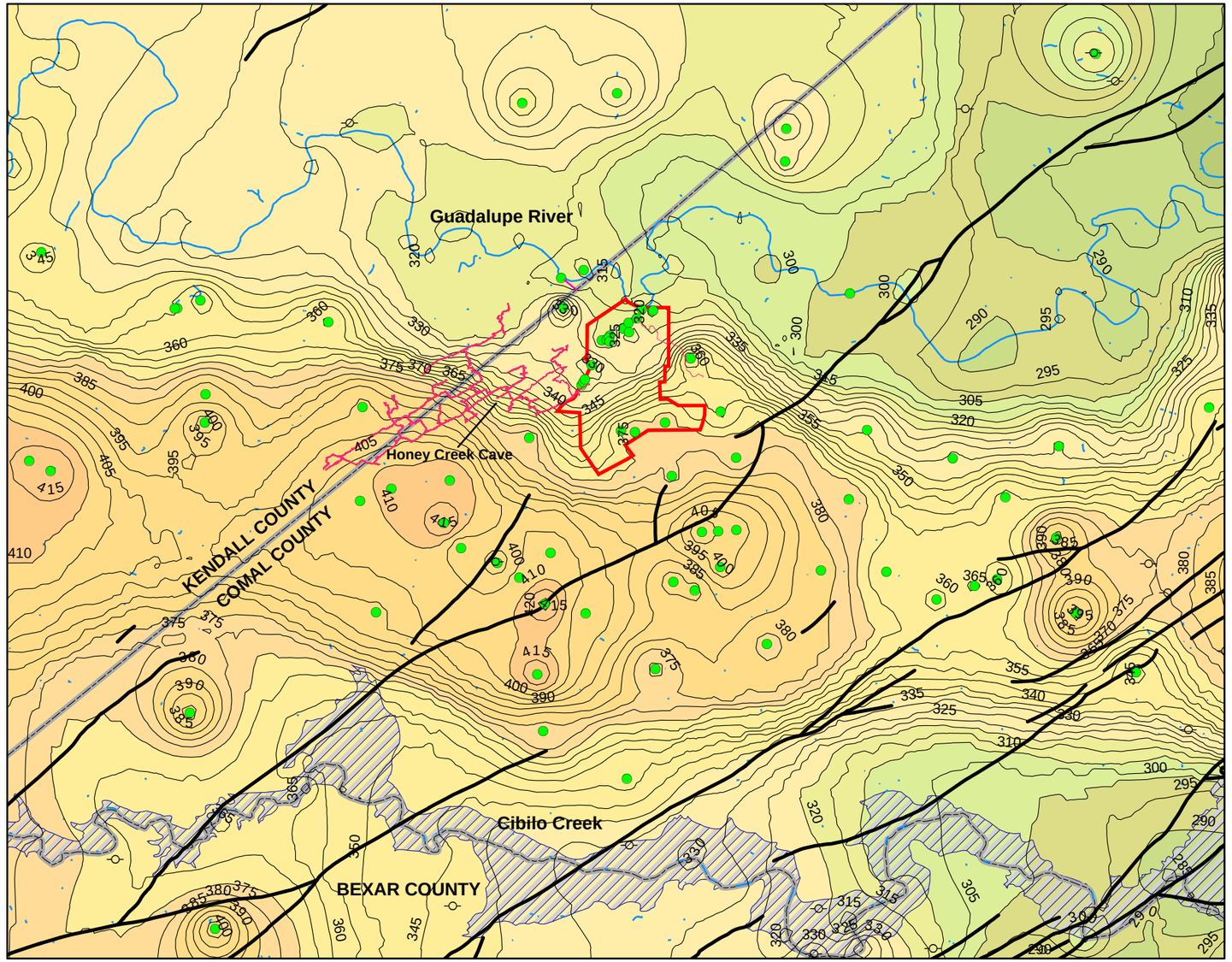

Legend

- Honey Creek State Natural Area
- Springs and Seeps
- Unconfined Zone of Edwards Aquifer
- Normal Faults
- Stream Cave Conduits

0 1,550 3,100 6,200
Meters

0 5,000 10,000 20,000
Feet

N

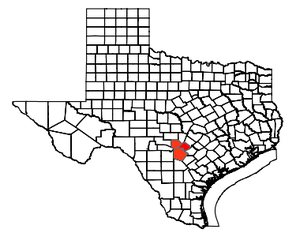

FIGURE 10

PERCHED POTENTIOMETRIC SURFACE MAP
MIDDLE TRINITY AQUIFER (2004)
HONEY CREEK
STATE NATURAL AREA
AND SURROUNDING AREA
BEXAR, COMAL AND
KENDALL COUNTIES, TEXAS

REFERENCES: TWDB (Texas Water Development Board), 2005, Water Well Data.
National Hydrography Dataset, 2005, Streams and Waterbodies
TCEQ (Texas Commission on Environmental Quality), Edwards Aquifer Zone Boundaries, 1999.

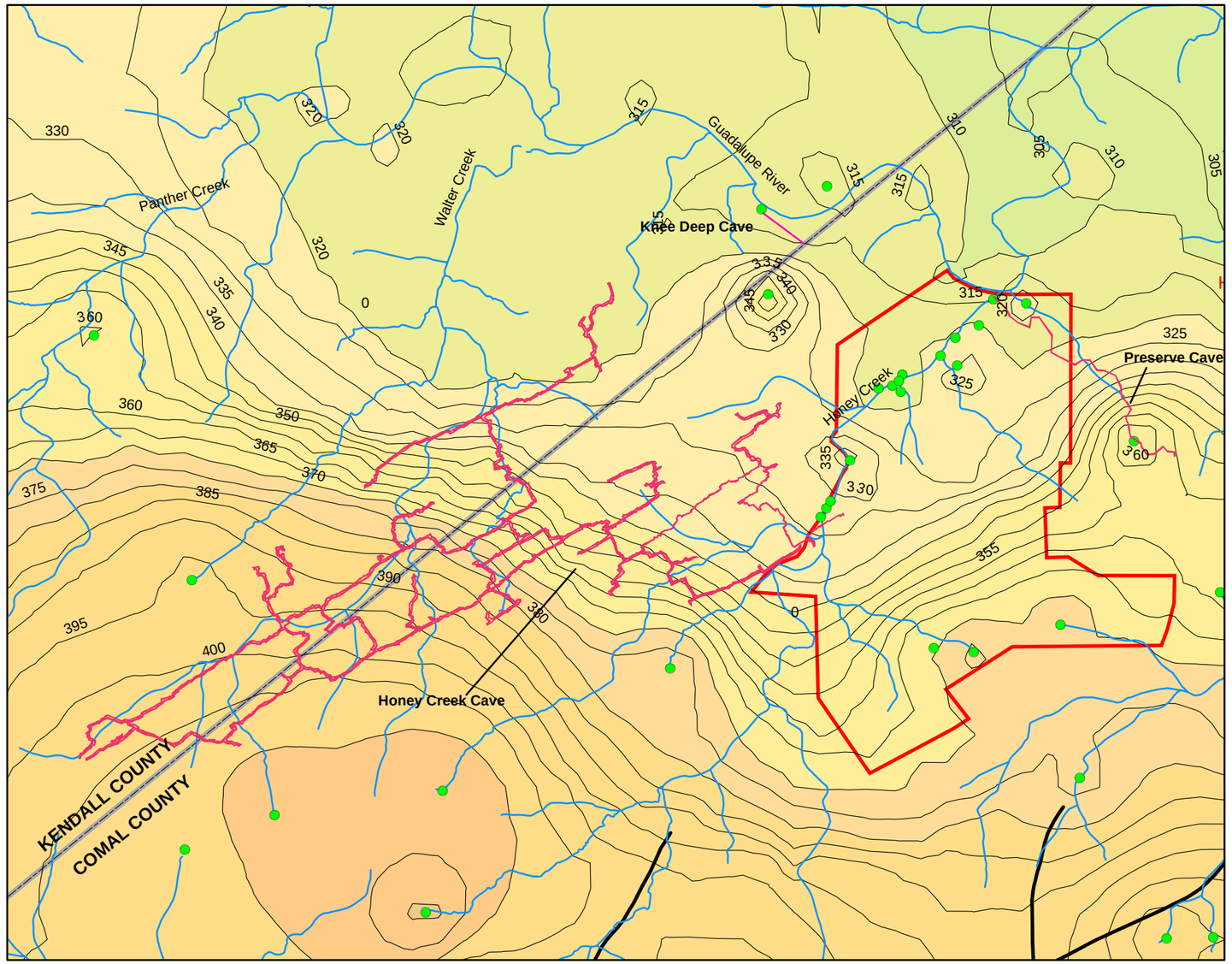

Legend

- Honey Creek State Natural Area
- Potentiometric Surface (in meters)
- Springs and Seeps
- Normal Faults
- Stream Cave Conduits

0 550 1,100 2,200
Meters

0 1,800 3,600 7,200
Feet

N

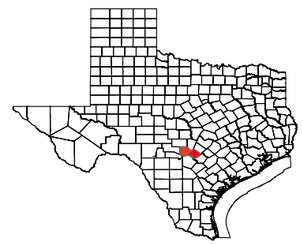

REFERENCES: Texas Water Development Board, 2005, Water Well Data.
National Hydrography Dataset, 2005, Rivers and Streams.

FIGURE 11

PERCHED POTENTIOMETRIC SURFACE MAP
MIDDLE TRINITY AQUIFER (2004)
HONEY CREEK
STATE NATURAL AREA
AND HONEY CREEK CAVE
COMAL AND
KENDALL COUNTIES, TEXAS

Potential Recharge

Recharge occurs primarily in the uplands and discharge in the fluvial valleys and along eroded hillslopes (Figure 6). Precipitation and runoff on rock outcrops, seepage, and ponding are primary sources of recharge. Upland karst features provide recharge to stratigraphically perched aquifers (Photo 7A and 7B). Upper Glen Rose Limestone, Lower Glen Rose Limestone, Hensel Sand, and Cow Creek Limestone are exposed in outcrop within Honey Creek basin. Low permeability calcareous marl and shale units of the Upper and Lower Glen Rose Formation may slow downward percolation of recharge before it is discharged from perched aquifer springs, fluvial-level springs, or gaining streams (Barker and Ardis, 1996; Ashworth, 1983).

Springs

Both Honey Creek and the Guadalupe River receive spring water from the Trinity aquifer (Ashworth, 1983) and both are hydraulically linked to the regional groundwater flow patterns (Kuniansky and Holligan, 1994). Fluvial-level and stratigraphically perched aquifer springs flow into creeks (Barker and Ardis, 1996). Entrenched perennial rivers and creeks receive water from shallow portions of the Trinity aquifer and do not reach deep into the aquifer (Ashworth, 1983, p. 47).

Many springs occur in Honey Creek basin at fluvial base level along perennial streams (Photo 6A). Other perched aquifer springs are associated with low permeability beds that focus spring discharge from eroded hillslopes of incised intermittent tributaries (Photo 8B). Vadose-level spring orifices may flow following a significant rainfall event and act as epikarst features that transmit groundwater to incised surface streams.

7A 

7B 

Photo Group 7. Photographs of upland karst features. 7A) Photograph of Kemble White in sinkhole (an upland recharge feature) formed at the contact between Hensel Sand and the overlying Lower Glen Rose limestone where a stratigraphically perched aquifer is formed. This feature is mapped as Big Hole Cave (C5). 7B) Entrance to Bone Head Cave formed in Upper Glen Rose Limestone (C9).

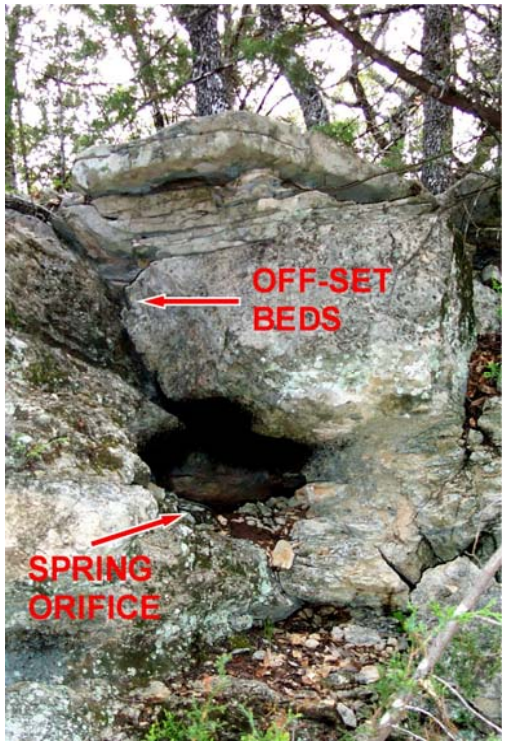

8A 8B 8C

Photo Group 8. Photographs of spring orifices observed on hillsides of Basin B (tributary to Honey Creek). **8A**) This paleospring orifice (PS-1) is exposed in the vertical wall of a creek bed and is formed along a dilational normal fault in the Lower Glen Rose Fm. **8B)** The source of the spring discharge is from a semi-confined, stratigraphically perched aquifer. This spring occurs at the contact between a calcareous marl layer of the Lower Glen Rose limestone and Hensel Sand. **8C)** View of dilational fracture, facing southwest from knickpoint KP-4B.

Water-loving plants such as sedges, cattails, ferns, and cypress trees within Honey Creek indicate a year-round water supply to Honey Creek (Brune, 1981). Other springs (such as PS-2) may flow intermittently following storm events (Photo 8A). Evidence that PS-2 is eroded spring orifice includes the fine, red, silt deposits in the base of the feature suggesting a long soil residence time. Spring SPR-2 is formed along a dilated fault that may provide an avenue for groundwater to move into the feature and enhance its dissolution. Stratigraphy influences the dip of normal faults with less competent layers failing in shear mode and more competent layers failing in hybrid mode at different angles (Ferrill and Morris, 2003). Displacement along the fault causes steeper segments to dilate (Photo 8A and 8C). Here, the dilatational faults are enlarged by groundwater flow, affecting permeability, infiltration, and spring conduit alignment.

Hydraulic Properties

Transmissivity of the Middle Trinity aquifer in the Hill Country varies from 464.5 to 4645 m^2/sec (5,000 to 50,000 ft^2/day) near Honey Creek basin (Barker and Ardis, 1996). Transmissivity is defined as the discharge through a unit width of the entire saturated thickness of an aquifer for a unit hydraulic gradient normal to the unit width sometimes termed the coefficient of transmissibility. The hydraulic conductivity of the Lower Glen Rose Formation was measured at 0.01 to 10 feet per day (0.03 to 3.05 m per day) (Hammond, 1984). The vertical hydraulic conductivity of the Upper Glen Rose Formation marl units were measured at 0.0001 to 0.003 feet per day (0.000031 to 0.000914 m per day) (Guyton and Associates, 1993). The Trinity aquifer has been described as having higher hydraulic conductivity perpendicular to regional fault trends (Kuniansky and Holligan, 1994).

METHODOLOGY

This study uses five primary methodologies: 1) field observations; 2) evaluation of hillslope properties (erosion pin measurements and soil sampling); 3) identification of hydrogeologic properties (e.g., stream discharge measurements, streamflow data, precipitation vs. water-table levels in shallow an deep water wells, and development of a longitudinal profile), 4) statistical analysis of structural controls on drainage, spring orifices, and recharge features, and 5) evaluation of hydrogeologic data using Arcview GIS.

Field Observations

Field observations were used to develop an understanding of the overall site geology and geomorphology. Inspections of creek bottoms were used to estimate the orientation and spacing of fractures and knickpoints. Caves, karst features, and springs were identified according to length, orientation, and depth of the conduit system. Surface evidence, TPWD data (2001), and field measurements were used to identify trends or structural controls. Surface geology was surveyed using standard geologic field mapping techniques (Compton, 1985). Fossil evidence such as *Orbitilina* sp. at the base of the Upper Glen Rose Formation (Photo 5A) and large pelecypods in the Hensel Sand Formation were used to verify the accuracy of published geologic maps of the area (Figure 8).

Evaluation of Hillslope Properties

Hillslope properties are evaluated using 2 primary methods: 1) erosion pin measurements (to study land surface changes, erosion, and deposition) and 2) soil sampling (particle size distribution, presence of carbonates; total carbon, carbon and organic matter, calcite, dolomite, and calcium carbonate equivalent and bulk density). These data were used to compare variations along the hillslope test plots and along the long profile of each tributary at Honey Creek State Natural Area. These data are provided in Appendices C, D, E, and F.

Hillslope Erosion Pin Measurements

Morphological changes such as erosion and deposition along hillslopes were measured using a paired basin approach in 3 pairs of test plots at matching elevations and slope conditions. Six test plots (3 within each basin) were selected based on similar stratigraphic position, slope, and vegetation. Hillslope surface changes were measured using erosion pins and deposition washers (Dunne, 1977; Leopold et al., 1966; Sirvent et al., 1997). From September 2001 to September 2002, erosion pins were monitored following significant rain events during one wet and dry season. Employing standard procedures (Sirvent et al., 1997), erosion pins (at 5-meter intervals) were installed June 2001 to monitor soil erosion and deposition along calcareous marl limestone slopes through one year (1 August 2001 – 2 August 2002) (Photos 9A and 9B).

Objectives of the monitoring plan were to: 1) estimate the present rates of hillslope erosion and deposition; 2) identify erosion controls (such as slope angle; rainfall intensity, vegetation composition, fossil aggregate size distribution); and 3) characterize particle size distribution and mineralogy of sediments along hillslopes. Results provide baseline for watershed management within this setting and information about the soil-rock interface and its relationship to land surface changes. Measurement from erosion pins accounted for spatial variation of slope surface changers within each monitored test plot and assessed changes to the hillslope profile. Plot locations are shown on the Site Feature Map provided in Appendix A.

Within each basin, 6 test plots (10 m x 12.5 m) were paired using similarities in elevation, lithologic units, slope, and vegetation (Boix-Fayos et al., 2001, Imeson et al., 1998; Lavee et al., 1991; and Sirvent et al., 1997). Erosion pins were installed to a depth of 5.9 inches (15 cm) along five rows spaced 6.6 feet (2 m) apart (perpendicular to the slope) (Photos 9A and 9B). Employing standard procedures (Dunne and Leopold, 1978, pa 519; Gustavson and Simpkins, 1989; and Sirvent et al., 1997), erosion pins were installed during summer 2001 to monitor soil erosion and deposition from August 2001 through August 2002. All measurements were taken following rainfall events significant enough to produce runoff or seasonally. Measurements were taken during dry conditions, at least 2 to 5 days following significant rainfall events to prevent unnecessary disturbance to the test plots and minimize error from swelling of clays.

9A 

9B 

Photo Group 9. Soil test plot photographs: **9A)** View of test Plot-A1 on calcareous marl riser. **9B)** Photo of erosion pin, deposition washer, and combination square used to take measurements.

Soil Measurements at Field Test Plots

Spatial interpolation of soil characteristics along hillslopes through sampling were used to estimate soil characteristics on upland, mid slope, and toe slope of each of 2 paired basins. Three pairs of test plots were identified by walking 3 transects across 2 paired tributary basins (Plot A1, Basin A and Plot B1, Basin B) at Honey Creek State Natural Area (Figure 2). Each transect was separated into three regions along the long profile of each tributary based on visible lithology, elevations, and topographic changes: upper, middle, and lower basin. Soil samples were collected from each of the 3 paired hillslope plots at 3 levels along the long profile of each slope and analyzed for particle size distribution (PSD) and bulk density. Down-slope variations were measured at each test plot such as particle size distribution (using pipette method and Stoke's Law) (Kilmer and Alexander, 1949, Steele and Bradfield, 1934); presence of carbonates; total carbon (Soil Survey Staff, 1972; Nelson and Sommers, 1982); organic carbon and organic matter (Nelson and Sommers, 1982); calcite, dolomite, and calcium carbonate equivalent (Dremanis, 1962), and bulk density.

Six samples (total of 36) were taken along the long profile of at the bottom middle and top of each of the 6 test plots. Samples were taken parallel to the gradient of the slope. Soil from each paired test plot and karst feature is characterized according to customarily accepted practices outlined by the Natural Resources Conservation Service, (Schoenenberger et al., 1998). Soil sampling chemistry data and particle size distribution (PSD) measurements from Honey Creek State Natural Area are provided in Appendix E.

Evaluation of Hydrogeologic Properties

Hydrogeologic properties were evaluated during this study using 3 primary methods 1) stream discharge measurements (Honey Creek and 2 tributaries in Honey Creek State Natural Area); 2) comparison of precipitation, runoff, and the potentiometric surface 3) representative longitudinal profile of Basin A at Honey Creek State Natural Area, showing caves, springs, lithology, fractures, and knickpoints.

Stream Discharge Measurements

Four cross-sections were measured along Honey Creek, upstream of its confluence with the Guadalupe River. Two cross-sections were measured approximately 500 feet (152 m) downstream from the mouth of Basin A (Figure 12). On 16 May 2001, stream gauging measurements were taken along 5 cross-sections of Honey Creek (sampling locations 1 through 5) and one each at the mouth of both of Basin A and Basin B (downstream from each spring at sampling locations A and B). Current meters (Section III) were used to measure stream discharge. The use of pygmy meters was confined to water of depths less than 1.5 feet. The AA current meter was used in water deeper than 1.5 feet (Station 3). Current metering measures discharge by dividing the cross-section of the channel into sections (of known dimensions), measuring velocity within each section, and multiplying each velocity measurement by its area (width * depth) to obtain the total discharge throughout the cross section. On 16 May 2001, discharge measurements were taken within Basins A and B, below flowing springs (Samples A and B - Figure 12).

Figure 12. Map of stream discharge measurement sampling locations.

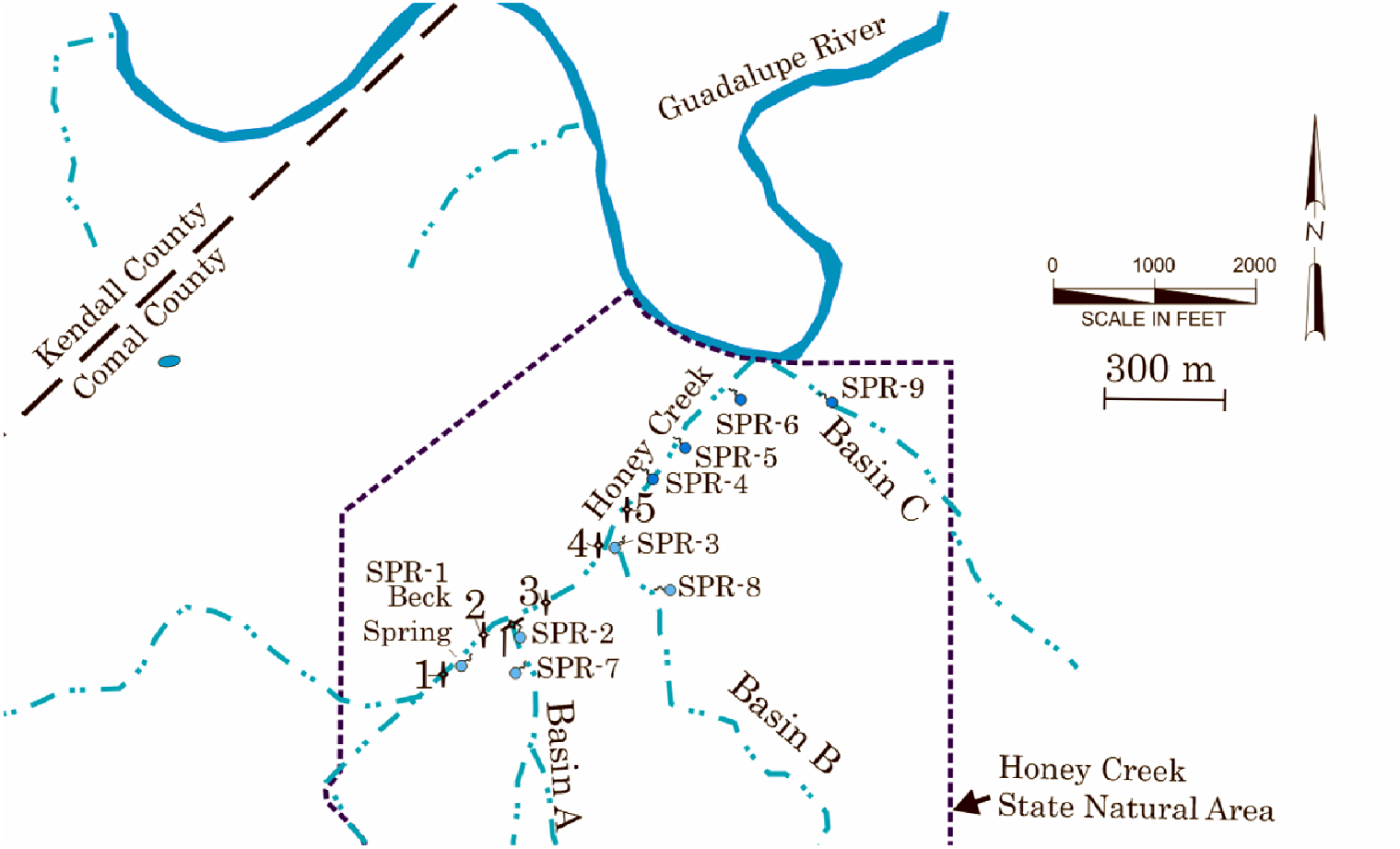

Streamflow data from 15 August to 30 September 2001 were based on real-time discharge measurements at Honey Creek State Natural Area (provisional data, USGS, 2001). A description of the USGS Real-Time Stations is provided in Appendix B. USGS weather station locations are shown on Figure 2.

Comparison of Precipitation, Runoff, and Potentiometric Surface

USGS real-time weather station and a v-shaped weir with a pressure transducer provided provisional precipitation and runoff data, respectively (USGS, 2001). One month of data (August – September 2001) were plotted using Microsoft Excel to compare the water levels of one deep and one shallow water well to precipitation. Additionally precipitation was compared to runoff to illustrate high infiltration rates and the flash flow in intermittent tributaries. Water levels (Well # 68-01-314), precipitation data (NOAA Cooperative Weather Station rainfall at Spring Branch) and runoff (USGS Guadalupe River at Spring Branch, Station # 01867500) were also plotted to show seasonal fluctuations (January 2001 - December 2001).

Longitudinal Profile Development

A high precision global positioning system (GPS) unit was used with carrier phase correction data to survey the locations and elevation data of knickpoints and stream segments within Basin B of Honey Creek State Natural Area. Carrier phase data is a processing technique that gathers data via a carrier phase receiver, using a radio signal (carrier signal) to calculate location and elevation, resulting in submeter accuracy after differential correction. Carrier phase data was obtained from The Schultz Group, Inc, New Braunfels, Texas (SG11). Survey tape, a level, and a stadia rod were used to accurately measure knickpoint dimensions and stream segments that were covered by thick vegetation that limited the accuracy of the GPS unit.

Table 3 shows a list of each longitudinal profile measurement sections. These data were used to plot the longitudinal profile of bedrock stream segments of Basin B, Honey Creek State Natural Area (Figure 13 and Figure 14). The longitudinal profiles were correlated with springs, lithology, potentiometric surface, sinkholes, fractured rock outcrop, and stream swallets to represent the hydrogeologic characteristics of this fluviokarst drainage network. A longitudinal profile is a cross section of a stream from its mouth to its head, showing elevation versus distance to the mouth. GPS location data were plotted using ArcGIS 9.0. The distance between each longitudinal data point and each feature was measured either in the field or by using the ruler tool in ArcGIS to obtain the linear distance between each point. Excel software was used to calculate the linear distance along the longitudinal profile (Table 3) and plotted on a graph or cross section and correlated with other landscape features (Figure 13).

Basins A and B were defined by delineating the sub-watersheds and stream network within the Honey Creek basin using ArcMap with Spatial Analyst to analyze a digital elevation model (DEM –a representation of height data). The DEM of the Anhalt quadrangle was added using the ADD DATA selection. A contour map was created by selecting SPATIAL ANALYST, SURFACE ANALYSIS, and CONTOUR. Contour data is shown Figure 2 The flow direction GRID was created by selecting SPATIAL ANALYST, HYDROLOGY, and FLOW DIRCTION. A flow accumulation Grid was created using SPATIAL ANALYST, HYDROLOGY, and FLOW ACCUMULATION. The Snap Pour Point was created using SPATIAL ANALAYST, SNAP POUR POINT, by inputting the raster flow direction and flow accumulation raster. Next, SPATIAL ANALYST, HYDROLOGY, WATERSHED, DEFINE BASIN. Topographic data Figure 2 and Appendix A topographic data represent height (in meters) above sea level.

Table 3. Longitudinal profile data points, Basin B, Honey Creek State Natural Area.

Data Point	Distance (M)	Latitude DD	Longitude DD	Elevation (meters)
U09	0	29.84387	-98.47209	394.11
U08	55	29.8443	-98.47181	391.06
U07	210	29.84567	-98.4712	384.66
U06	275	29.84616	-98.47086	381.00
U05	330	29.8467	-98.47075	377.04
U04	442	29.84772	-98.47075	372.17
U03	529	29.84855	-98.47069	370.95
U02	652	29.84943	-98.47148	368.51
U01	731	29.84982	-98.47215	366.37
T01	802	N29.85024	W98.47269	364.55
T02	817	N29.85026	W98.47273	363.33
T03	1784	N29.85173	W98.47521	348.14
T04	2434	N29.85314	W98.47575	357.53
T05	2471	N29.85324	W98.47576	355.10
T06	2497	N29.85329	W98.47572	352.66
T07	2547	N29.85381	W98.47613	352.05
T08	2860	N29.85445	W98.47678	350.22
T09	3032	N29.85455	W98.47730	347.17
T10	3142	N29.85477	W98.47785	345.95
T11	3532	N29.85569	W98.47846	345.04
T12	3983	N29.85625	W98.47969	341.99
T13	4035	N29.85628	W98.47985	337.72
T14	4274	N29.85648	W98.48054	337.72
T14B	4335	N29.85665	W98.48056	334.67
T15	4370	N29.85674	W98.48057	336.50
T15B	4441	N29.85694	W98.48058	332.24
T16	4971	N29.85831	W98.48094	327.66
T16B	5024	N29.85843	W98.48098	327.05
T16C	5077	N29.85856	W98.48106	326.44
T17	5272	N29.85908	W98.48099	327.97
T18	5600	N29.85981	W98.48148	325.23
T19	5829	N29.86030	W98.48190	322.79
T20	6049	N29.86082	W98.48215	320.04

Figure 13
Longitudinal Profile (Basin B)

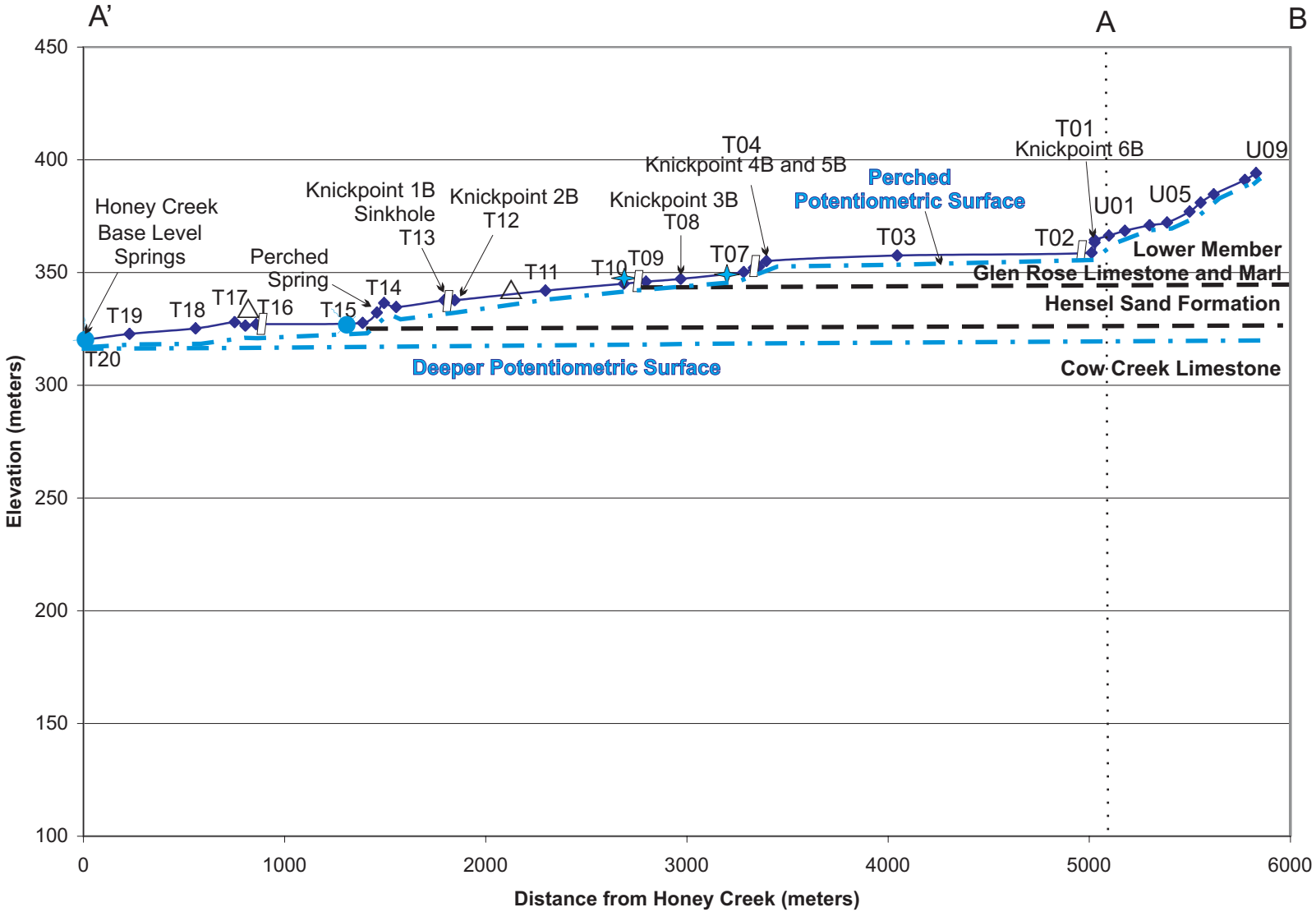

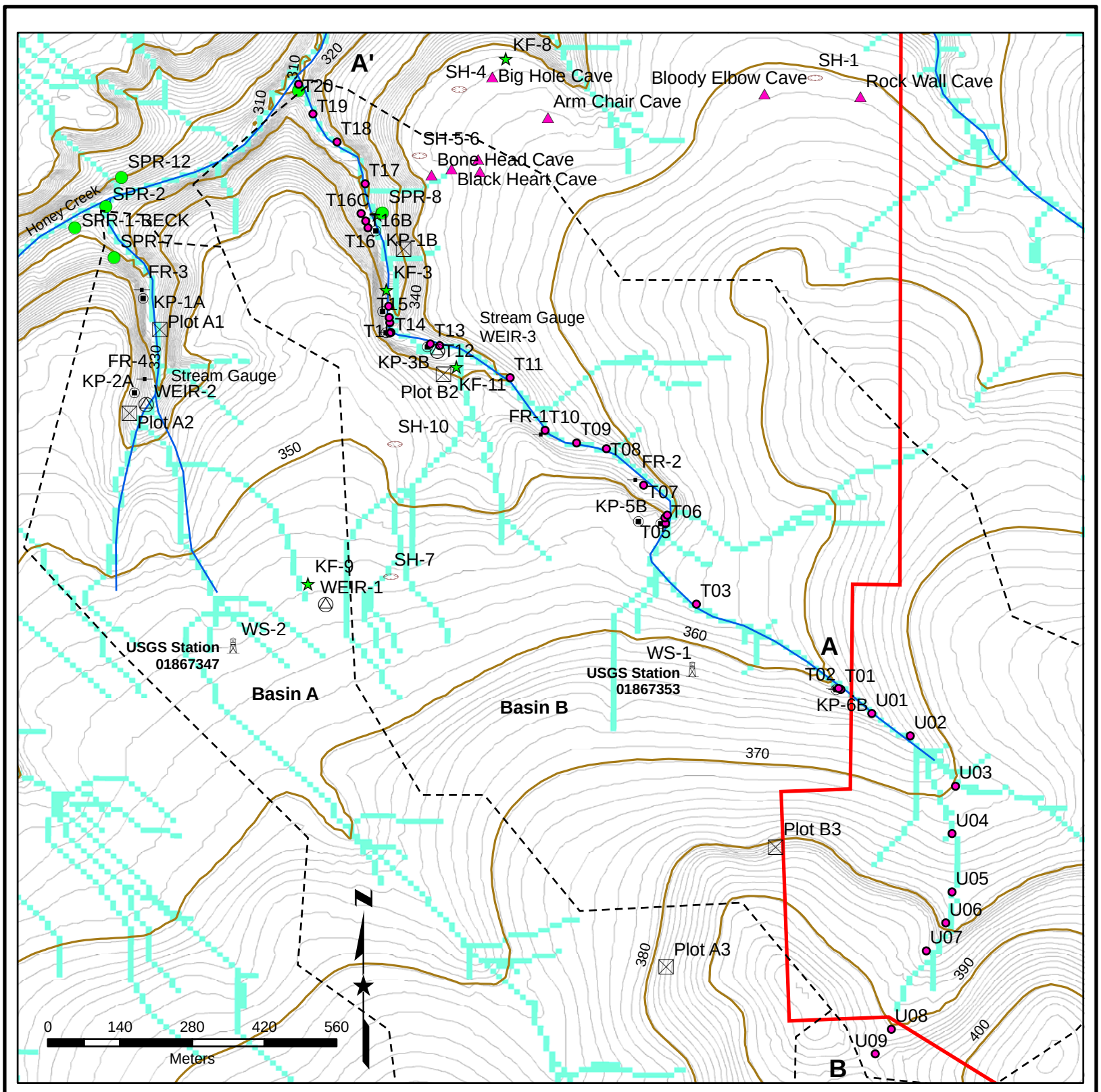

National Hydrography Dataset, 2005, Streams and Rivers.

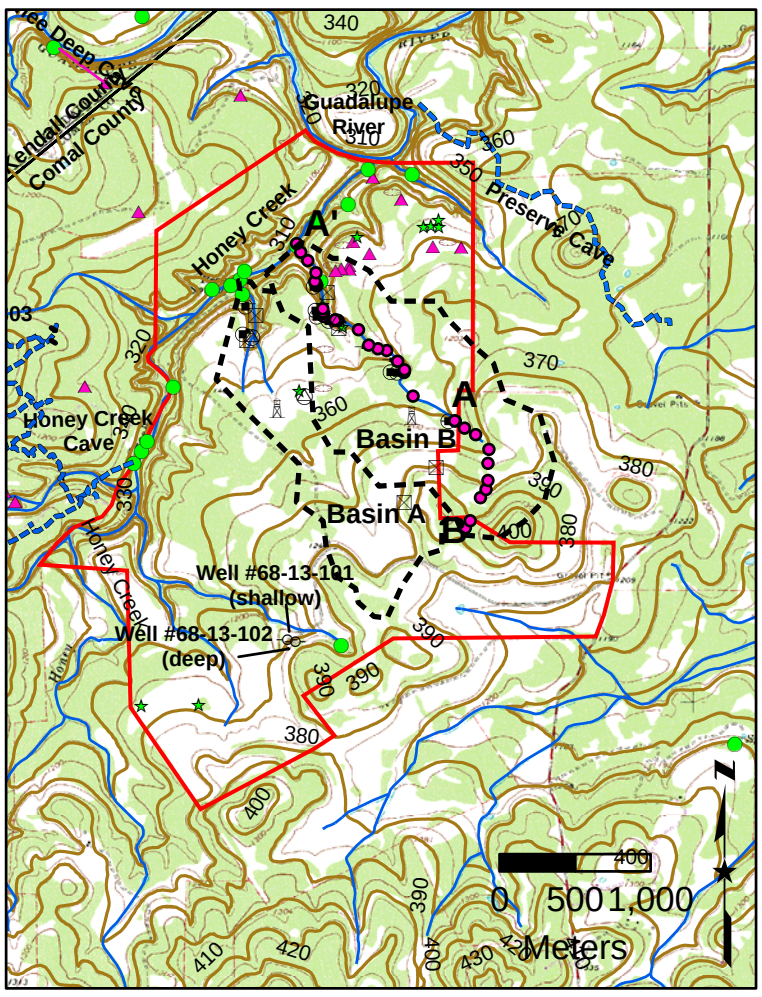

Base map: USGS, Ahalt 7.5' Quadrangle, Texas, 1954.

Legend

- Honey Creek State Natural Area
- Cave
- Elevation Data Point
- Erosion Plot
- Fracture
- Karst Feature
- Knickpoint
- Paleospring
- Sinkhole
- Spring
- USGS Stream Gauge
- Water Well
- Weather Station
- Stream Network

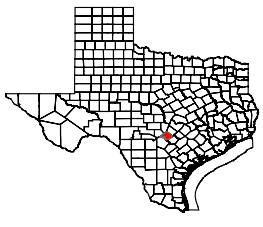

FIGURE 14
MAP OF LONGITUDINAL PROFILE POINTS
HONEY CREEK
STATE NATURAL AREA
AND SURROUNDING AREA
COMAL AND KENDALL
COUNTIES, TEXAS

Statistical Analysis of Structural Controls

Locating fractures and cavities within soil and rock and mapping their extent is commonly required for hydrogeologic and engineering considerations. Fractures, conduits, cave entrance orientations, and stream segments were measured within Honey Creek basin and compiled into a database (Appendix G) that was used to compare their relationship to one another in order to identify trends that will help improve our understanding groundwater and surface water interaction.

Stream Orientations

Stream segment orientations and lengths were identified in the field using a Brunton and tape measure. A protractor and ruler were used to measure stream segment using aerial photography (Figure 8) and a USGS topographic quadrangle map.

Karst Features

Quantitative assessment characterized each karst feature encountered (e.g., sinkholes, caves, solution cavities, faults, fractures, or partially filled voids that may be related to caves in the subsurface). Quantitative methods include numbering and recording each karst feature using a Global Positioning System (GPS), marking the locations, and describing morphological features such as length, width, depth, and azimuth. Cave and karst feature orientations and lengths were identified by measuring cave maps provided by Texas Parks and Wildlife (TPWD, 2001) and a map of Honey Creek Stream Cave, (TSS, 1994). Volunteers who mapped these stream caves (and other karst features) took measurements and azimuth readings using Suunto

clinometers and compasses and metric tapes. This information was used to construct a database of conduit of each segment of the cave passage.

Scanline Fracture Data

Fractures where characterized within the exposed bedrock in a tributary to Honey Creek. The location is mapped as FR-2 on Figure 2. Fracture orientations were measured in azimuth using a Brunton compass and lengths were measured with a tape measure. Most rock or engineering data sets typically consider 1-dimensional (1-D) rock exposures. Thus, statistical methods are designed for a single scan line. Single scan line surveys introduce bias to orientation data (Terzaghi, 1965; La Pointe and Hudson, 1985). Statistical methods may use a geometrical correction for sampling bias called the Terzaghi correction. This correction is based on the assumption that fractures are equally distributed in all orientations in the rock unit. La Pointe and Hudson (1985) conclude that this correction may work well in shattered areas, but may not work in many natural data sets (e.g., clustered fractures in fault zones). The Terzaghi bias correction was considered for use on scanline fractured rock measurement (FR-2) to account for any bias in the collection of data from other sources. Ultimately, a mean length-weighted distribution was selected for rose diagrams (Appendix G).

Rose Diagrams

Rose diagrams and statistical data were generated from the fracture, stream segments, and stream cave orientations databases using a software program Geoorient. Rose diagrams identify regional fracture, stream segment, and stream cave conduit trends to find the distribution of passage orientation. Length-weighted rose diagrams were created for linear classification.

Evaluation of Hydrogeologic Data Using ArcView GIS

Lithologic units, potentiometric surface, spring orifices, fractures, and recharge features were identified by field surveys and record reviews (TPWD, 2001, and TWDB, 2005). Features were mapped using Arcview GIS. Conduit dimensions and orientation; spring location; fracture orientation, spacing and aperture; karst feature locations; and knickpoints were also compiled into a database. These features were plotted using ArcGIS 9.0 to compare hydrogeologic and geomorphologic characteristics of the Lower Glen Rose Limestone and Hensel Sand. These data were used to verify existing stream cave orientation and lengths from the files of Texas Parks and Wildlife and to evaluate field observations. Field measurements, satellite imagery, and digital orthophoto quadrangle quadrant maps (DOQQ), and geological maps were integrated with subsurface information such as stream cave flowpaths, water elevation in wells, and elevations of spring orifices (Appendix A).

Potentiometric Surface Map

Water level measurements from the TWDB and real-time USGS water table measurements from local water wells were interpreted to create a generalized potentiometric surface map (Figure 9) (TWDB, 2005 and USGS, 2001). A potentiometric surface map is a two-dimensional representation of a three-dimensional water table elevation surface. It is defined by a set of coordinates that correspond to longitude and latitude respectively and the ‘z’ coordinate corresponds to the water table elevation above mean sea level. Typically, these data are provided in standard international (SI) or units. However, the TWDB water well depths to groundwater are given in feet on the potentiometric surface map to prevent rounding errors. Potentiometric surface maps were converted to SI (Figure 8 and Figure 9).

TWDB and USGS data were saved as a text file and opened as a table in Arcview. TWDB files named “aquifer.txt,” “welldta.txt” and “wlevels.txt” for Bexar, Blanco, Comal, Hays, and Kendall Counties, Texas. The “aquifer.txt” file contains codes and names for the aquifers in Texas. “Welldta.txt” contains water well data such as latitude and longitude, name of water-bearing geologic unit, aquifer code, and elevation of the wellhead. “Wlevel.txt” contains the date of measurement and depth to groundwater. These files were delimited with an “|” and all counties were combined and saved as 2 separate worksheets (“welldta” and “wlevels” in the one Excel file saved as “well_data.” Next, a column was inserted to the right of the water level data in the “wlevel” worksheet (table array). This column was titled “ALTITUDEFT” for potentiometric elevation. Next, the following function was entered into the first row of this column: +AD1-C1, then copied to the remainder of the columns. This temporarily reproduces the water level data, until the next procedure looks up the well elevation data and copies it to column AD.

Next, 4 columns were inserted after the first column of the “welldta” worksheet. Then, the worksheets were combined in Microsoft Excel by using the VLOOKUP function to search for the “WellID” value in the first column of the “welldta” table array, returning a value in the same row from each column in the table array to the last empty columns of the “wlevel” worksheet. The VLOOKUP syntax was typed into cells L2 through BB2, and then copied to each row below. The syntax for this function is VLOOKUP (lookup_value, table_array, col_index_num, range_lookup). More specifically, the syntax for the function used is VLOOKUP (lookup value, weldta!$A$1:$BA$3656, col index number, FALSE). The lookup_value is the value to search in the first column of the table array. The values

in the first column of the “weldta” table_array are the values searched by lookup_value. The column index number is the column in the “welldta” table_array from which the matching value must be returned. The range lookup is a value that specifies whether you want VLOOKUP to find an exact match or an approximate match: If FALSE, an exact match is returned. If an exact match is not found, the error value #N/A is returned for that cell. The results produce a combination of the “welldta” and “wlevels” worksheets. Before adding the text file to Arcview, the titles needed to be revised by removing all spaces, underscored, and symbols. Finally, the file is saved as an Excel file and text file called “Well-Data.”

The text file “Well-Data” was added to Arcview using <Tools, Add XY Data>, selecting the longitude data as the X coordinate, and the latitude data as the Y coordinate. Next, EDIT was selected and then SELECT to define the projection of the dataset as NAD83 match the basemap. An event layer called “Well-Data” was created. ArcView queried the database to find all water elevations for 2004. This was achieve by right-clicking on the event layer, clicking on SELECTION on the main toolbar, and the choosing SELECTION BY ATTRIBUTE and YEAR=2004. In the attribute table, OPTIONS and EXPORT were selected to create an even layer called “Wells-2004.” The potentiometric surface changes through time, depending on the season or annual inputs or outputs from the aquifer. Ideally, selected well data represent a short time interval. Therefore, data was preferentially selected for the months of January and February of 2004 (Figure 8).

Using a GPS unit and USGS topographic quadrangle maps, perched aquifer conditions were mapped using the elevation data of base-level rivers and springs, as well as perched seeps and springs that provide a general representation of perched aquifer conditions. The database of these data were compiled into a file called

“Springs.txt” and added to Arcview. The Spatial Analyst extension was used to create a potentiometric surface map using inverse distance weighting (IDW) method. The topographic position of the springs and base-level surface water in perennial rivers were used to complete water elevation field used to generate the potentiometric surface map (Figure 9).

RESULTS AND DISCUSSIONS

The results of this study include field observations, evaluation of hillslope properties, identification of hydrogeologic properties, statistical analysis of structural controls, and evaluation of hydrogeologic data using Arcview GIS. These data provide baseline data for future research and suggest that subsurface drainage patterns leave an imprint surface erosion patterns. Here, the potentiometric surface is a subdued reflection of topography. Conversely, erosional features and topography are a reflection of fluviokarst drainage patterns.

This fluviokarst drainage system consists of a network of conduits controlled by fractures and a repetitive stratigraphic sequence of rock units that provide a blueprint for erosional features in the landscape at Honey Creek State Natural Area and other areas underlain by similar rock units. Groundwater crosses surface water catchment areas and pirating groundwater toward a lower gradient, where springs emerge in creekbeds nearby or continue to migrate into deeper portions of the aquifer. The alignment of Honey Creek Stream Cave with the downcut channel of Honey Creek, suggests that headward erosion has occurred along the hypothetical continuation of Honey Creek Stream Cave, causing topography to reflect the former alignment the cave. The incised channel of Honey Creek has truncated tributary surface streams and stream caves that may once have been hydrologically connected to a continuation of Honey Creek Stream Cave. The longitudinal profile of modern streams and the position of springs, lithology, and stream swallets represent a hydrologic network that was once part of an aquifer (prior to headward erosion of stream caves and spring conduits).

Field Observations

Recharge and discharge features are associated with the karstification process. Drainage patterns reflect the headward erosion of springs. Evidence of groundwater sapping characteristics, including karst features, spring orifices, fractures, and knickpoints were identified and mapped using field observations and remote sensing techniques. Geologic units were identified using index fossils and stratigraphic correlation. The top of the Lower Glen Rose Limestone is characterized by interbedded limestone and clay units with various sizes of orbital-shaped foraminifera *Orbitilina texana* (Photo 5A) (Whitney, 1952, p 66). *Orbitilina texana* fossils were observed near the 374-meter contour interval at Honey Creek State Natural Area. The presence of these index fossils provides a topographic benchmark that helped identify the contact between the Upper and Lower Members of the Glen Rose Limestone (Figure 8). The underlying Hensel Sand was identified by the presence of large bivalves (pelecypods), abundant clay, and siliceous concretions (Ashworth, 1983; Stricklen et al., 1971). The Hensel Sand (exposed within an incised stream channel at Honey Creek State Natural Area (Photo 5B).

Evaluation of Hillslope Properties

Sediment transport on hillslopes occurs when water flow is initiated by raindrop impact, overland flow, erosion, and solution transport. Runoff occurs when precipitation exceeds the infiltration capacity of the soil (Schumm, 1965, p. 783-94; Dunne and Leopold, 1978, p. 259). High intensity erosion is expected to occur lower in the basin because here runoff is concentrated. These data are provided in Appendices C, D, E, and F.

Hillslope Erosion Pin Measurements

Land surface changes were measured on 3 pairs of test plots (Plots A1, A2, A3, B1, B2, and B3) on calcareous marl risers over a period of one year and compared to particle size distribution, slope, and proximity to a groundwater table. These data are provided in Appendix C and the location of the plots is provided in Figure 2. Analyses of these data suggest a great deal of mass movement at the bottom of the basin near the top of the Hensel sand, where slopes are greater (32%). This is evidenced by the widest range of slope erosion (-9.3) and deposition (6 cm) rates (Figure 15). These findings are in line with previous studies that demonstrate that sediment yield is directly proportional to increasing slope found lower in the basin (Wischmeier and Smith, 1978). Lithology (erodability) also affects erosion rates. For example, the second widest range of slope movement (between -3.8 and 3.5 cm) is found at the top of the basin (with a marl unit near the bottom of the Lower Glen Rose Limestone) where slopes are second steepest (20%). Mid-basin (along a limestone bench) slopes are the most gradual (11%) and land surface changes range the least (-1.8 to 1.6 cm)...

Figure 15. Land surface changes vs percent slope (May-01 to August -02).

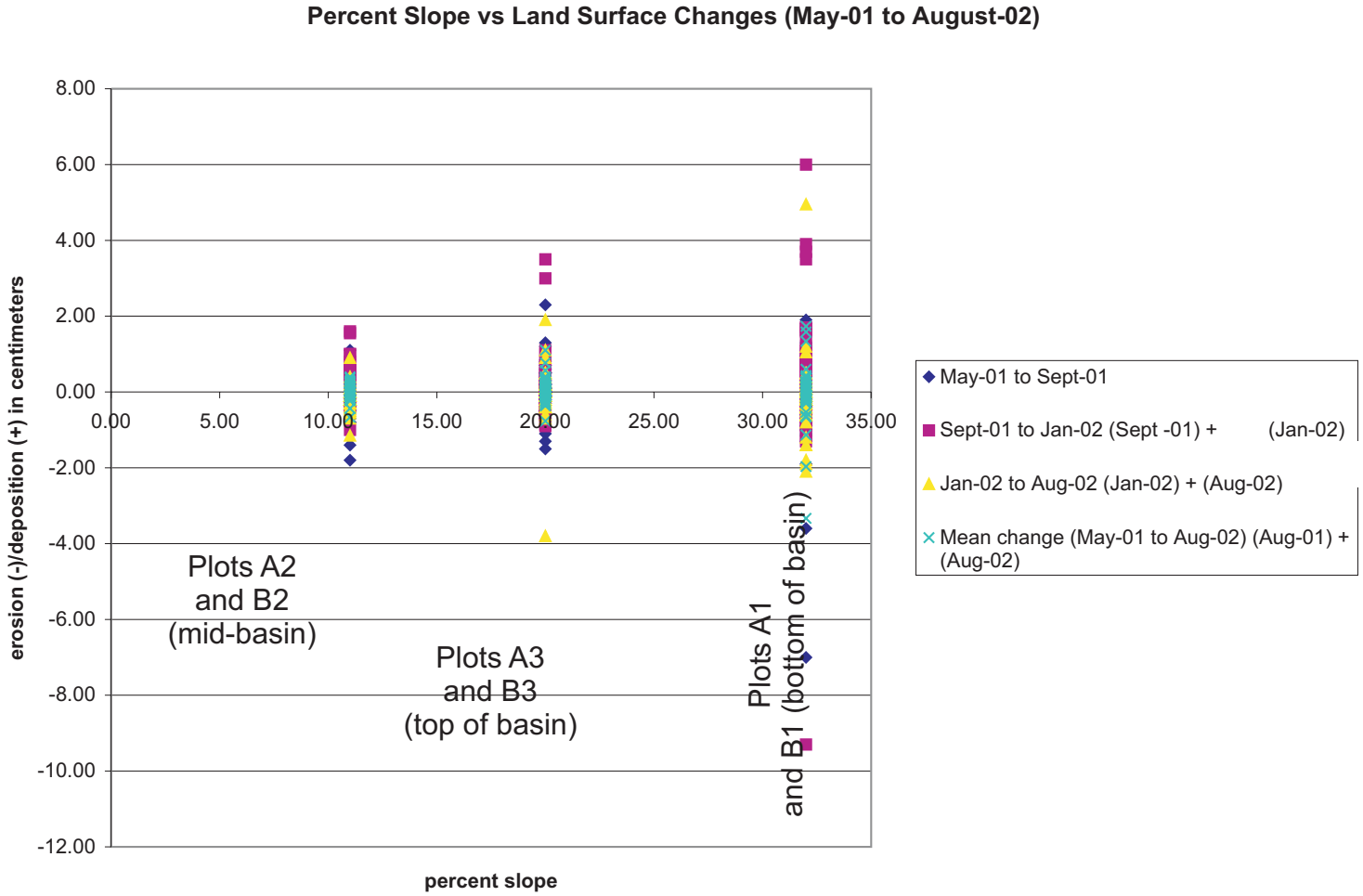

Photo Group 10. Photographs of seepage erosion. 10A) Seepage erosion along scarp face at a lithologic contact between a massive sandy dolomitic limestone (Cow Creek Limestone) and an overlying shaly layer (Hensel Fm.). 10B) Seepage erosion along scarp face of tributary within Basin A.

10A 

10B 

Seepage erosion (Photo 10A and Photo 10B) may also enhance slope erosion along hillslopes (Higgins, 1984, p 18-58). Seeps and springs are found near test plots at the bottom of the basins where erosion is highest (Figure 2 and Photo 6A).

Limestone of variably layered, resistant strata results in differential erodability and weathering of the landscape. Erosion on the test plots varied with position on the slope and with time. Silt and clay are easily transported by sheetflow, which formed minor rills or channels in soils (Gustavson and Simpkins, 1989).

Debris is deposited on the limestone treads and risers following storm events, suggesting high rates of sheetflow, especially on the flat-lying surfaces. Sheetflow is often recognizable by deposition of debris lines that can be measured with the erosion pins (Photos 8B and 9A) (Gustavson and Simpkins, 1989). Erosion was accelerated in micro-erosion channels on the risers (Photo 9A and 9B), where some pins were more affected by erosion than neighboring pins outside these channels and showed little relation to predictor variables discussed by Gustavson and Simpkins (1989): Precipitation intensity, slope angle, or percent vegetation coverage affect the rates of erosion.

Soil moisture is linked to runoff on hillslopes (Horton, 1945) with infiltration rates often being lower in moist soils than in dry soils, especially in soils with high clay content. Soil moisture results are provided in Appendix D. Runoff is produced faster in moist soils. Shrink-swell of clay minerals may contribute to soil creep (net downslope transport of soil). Soil expansion is perpendicular to the slope because during contraction the soil settles downslope.

Photo Group 11. Photos of test plots: **11A)** View of micro-erosion channels on test Plot B1. **11B)** View of Plot A1, Lower Glen Rose Limestone (Kgrl) ridge at the top of the test Plot A1. This riser is underlain by a sandy limestone and colluvium.

11A

11B

On Test Plot A1, at the bottom of Basin A, a natural act of a fallen tree at the top of a slope (Photo 11B) caused increased erosion on the subsequently disturbed western part of slope where there was no longer a protective canopy. Drainage density of microerosion channels increases as slope increases (Photo 11A). These observations are similar to measurements reported by Schumm et al. (1984).

The limestone ridges at the top of each slope are resistant to erosion. A zone of no erosion (Horton, 1945) is found at the resistant limestone ledges at the top of the test plots in the lower and upper basin (Photo 11B). Slopes contain silty sediment with abundant angular rock fragments (Photo 8B).

Colluvium deposits are found primarily on steeper slopes of the test plots. Colluvium consists of weathered calcareous marl and regolith, loose rock fragments deposited by gravity and enhanced by seepage near stratigraphically perched groundwater tables. Alluvium deposits are formed when eroded hillslope sediments and carbonate scarp faces are transported by flowing water during storm events. Mass movement is limited to steeper slops where transport of large rock or soil occurs due to gravity (Figure 15). In open areas that are not protected by canopy cover, rock fragments and washers on erosion pins often rest on pedestals where the regolith is protected from raindrop impact. The surrounding regolith is deflated by diffusive rain-splash erosion

Transport-limited slopes, such as on calcareous marl risers at the top (Plots 3A and 3B and at the bottom of the basins Plots A1 and B1) are found where rates of weathering exceed rates of transport of material from the hillslope. The mid-slope test plots A1 and B1 have weathered parent material (such as soil or regolith) that obscures the view of the bedrock. However, on weathering-limited and rock slopes

the sediment and regolith transport rates exceed weathering rates (e.g., mid-slope plots A2 and B2).

Soil Sampling on Hillslope Field Test Plots

Soil sampling chemistry data and particle size distribution (PSD) measurements from Honey Creek State Natural Area are provided in Appendix E. Regolith on the hillslope test plots consisted of calcareous marl risers and carbonate treads (flat-lying limestone benches) with a range of 35 to 76% calcium carbonate equivalent ($CaCO_3$ EQ) from top to bottom of the basin (Appendix D). Samples from plots at the lowest elevations with the steepest slopes (Plots A1 and B1) showed moderate levels of $CaCO_3$ EQ near 25% and moderate rock fragments from the underlying Hensel sand and float from upslope (Lower Glen Rose Limestone). Samples from the rocky mid-basin plots (Plots A2 and B2) contained about 5% $CaCO_3$ EQ and relatively few parent material clasts (massive, dolomitic, Lower Glen Rose Limestone). Soil samples from the highest elevations at the top of both basins (Plots A3 and B3) had the highest $CaCO_3$ EQ at 60% and an abundance of parent material clasts (calcareous marl). Soil on calcareous marl slopes tends to be calcareous, while soil on dolomitic hilltops and sideslopes tends to be noncalcareous. The calcareous nature of the soil reflects the whether the parent material is calcareous marl or dolomitic limestone.

Processes Affecting Measurements of Land Surface Changes

Soil infiltration and runoff capabilities, vegetation composition and thickness, and erodability of the substrate affect land surface changes. Following is a description of these processes.

Soil Infiltration and Runoff Capabilities

In areas of high infiltration, where rainfall intensity rarely exceeds infiltration capacity, Horton overland flow does not occur on much of the land surface (Dunne and Leopold, 1978, p. 263). Water percolates through the soil matrix. This concept is also possible in permeable consolidated sediments or karst terrain. Within Honey Creek basin, water percolates through soil and rock with relatively high infiltration rates. Tributary streams with high infiltration capacities rarely flow in Honey Creek basin. Following intense precipitation, surface runoff within intermittent tributaries peaks and subsides rapidly, largely due to steep, fractured terrain.

Studies regarded these Hill Country soils as thin and stony with soil horizons only a few inches thick (Batte, 1984). Hill Country soils are traditionally thought of as having a minor infiltration capacity with runoff as the dominant hydrologic process (Wilding and Woodruff, 1994). This assumption suggests that these soils cycle a minimal amount of water and associated organic and inorganic constituents.

Batte (1984) prepared a county soil survey that is not intended for site-specific applications (Figure 7 and Table 1). Therefore, these maps do not show spatial diversity or the true thickness of soil bodies, especially as they relate to the treads and risers. Wilding and Woodruff (1994), spent 18 months making observations based on digging trenches and cross sections with a backhoe to study soils over the Glen Rose

Formation. Brackett soils previously described as loamy soils were shown have a greater depth, spatial diversity, subsoil development, and biological activity than was previously published. According to Wilding and Woodruff (1994), the steep risers have the highest physical and chemical sorptive capacity based on their thickness and silt content, highest loading rate potential. The ledges or treads function as natural, vegetative filter strips that may control soil erosion and filter pollutants (Wilding and Woodruff, 1994). Natural buffers in the central Texas Hill Country may lessen the adverse impacts of land use changes. These buffers include locally thick hydrologically active soils and riser and ledge landforms. Woodruff (1994) describes the soil-moisture relationships along the treads and risers of the Glen Rose Formation, as follows:

> *Infiltration, storage and recharge of soils and bedrock strata in the Glen Rose Formation are highly variable. Hydrology is highly responsive to rainfall events, indicating rapid infiltration is occurring along roots and cracks in stony soil materials…The treads and risers function as independent hydrological units…Locally perched groundwater tables are divided into compartments among the hard and soft limestone layers with limited interconnection…Seasonal saturation of marly limestone zones occurs in winter and early spring, but moderate to severe water depletion occurs during summer months. These marly zones usually have adequate moisture for plant growth even in the summer.*

Vegetation Thickness

Vegetation was evaluated during this study using the author's personal knowledge of plant identification and TPWD classifications. Vegetation is described in the Environmental Setting section of this thesis. Vegetation on each test plot was evaluated and is described on the soil characterization sheets provided in Appendix F.

Runoff and Erosion

High intensity runoff occurs lower in the basin where slopes are steeper (Figure 15). Aggregates on slopes (cobbles, and rock fragments) have a higher threshold of sediment transport (velocity required to entrain sediment), requiring larger magnitude events to transport aggregates (Boix-Fayos et al, 2001). Schumm (1965) suggests that sediment yield should be highest in a semiarid setting. However, erosion rates and sediment yield may be higher in areas of intense precipitation creating higher rates of erosion. Likewise, areas with less rainfall may have less mean annual runoff and less erosion. The spatial variability of rainfall in this region means that certain areas may contribute more to stream runoff than others (Lane et al., 1978).

Statistical Analysis of Structural Controls on Drainage

Rose diagrams show a strong correlation of fracture orientations with groundwater and surface water flow in the area. Conduit and fracture orientation suggest a complex matrix of rectilinear fluviokarst drainages that feed stream caves, springs and stream baseflow. Fluviokarst is defined as a region with mixed karstic and fluvial characteristics (White, 1988). In central Texas, an uplifted karstic plateau is incised by fracture-controlled rectilinear to dendritic stream courses with steeply sloping terrain. Some catchment basins are connected by fault-controlled fractures that allow communication of groundwater between surface drainage basins. Tributary valleys are steeply graded and are parallel to the orientation of many conduits and fractures. Additionally, springs within Honey Creek basin often coincide with local fracture and cave conduit orientations. Caves (such as Preserve Cave) are roughly parallel to tributary valleys until they reach the dissected bed of Honey Creek where

the conduits have been intersected by erosion (Figure 16 and Figure 17) (Photo 1B and Photo 2C).

Length-weighted orientations of Honey Creek Stream Cave (Figure 2) are predominantly oriented at N40° to 60°E. This agrees with similar findings that recharge occurs on karstic uplands and cave development is concentrated along faults and fractures that follow regional northeast trends in the area (Woodruff and Abbott, 1979). At least two stream caves, Preserve Cave and Knee-Deep Cave, follow a linear trend of 310° to 330º (N 30° to 50°W) that is perpendicular to Honey Creek Stream Cave and regional faulting (Figure 2). Kuniansky and Holligan (1994) found that the Trinity aquifer has a higher hydraulic conductivity perpendicular to regional fault trends, which may explain the preferred northwest trend of cave conduits that feed into Honey Creek.

Knickpoints are often found near the intersection of fracture sets (Photo 3a) in the fossiliferous limestone in the Lower Glen Rose Limestone. This observation agrees with Weissell and Seidl's (1997) findings that fractures affect hillslope processes that in turn control knickpoint migration. Factors other than surface water are at work in knickpoint migration because of the presence of groundwater sapping and seepage erosion (LaFleur, 1999, Pederson, 2001). The main channel of Honey Creek parallels Honey Creek Stream Cave (Figure 2). Surface tributaries parallel a northwest-trending fault scarp that is an extension of a fault shown on published maps (Collins, 2002). This fault is shown on the geologic map (Figure 8) and in the profile of Preserve Cave (Figure 16). A secondary set of fractures have a trend to the northwest (Figure 2). Many upland spring conduits are dissolution features that feed into downcut streams and rivers (Figure 3, Figure 4, and Figure 16) (Gillieson, 1996; Veni, 1994a, Woodruff, 1974, and Woodruff and Abbott, 1979).

Figure 16. Conceptual model of Preserve Cave (from Sumbera and Veni, 1986).

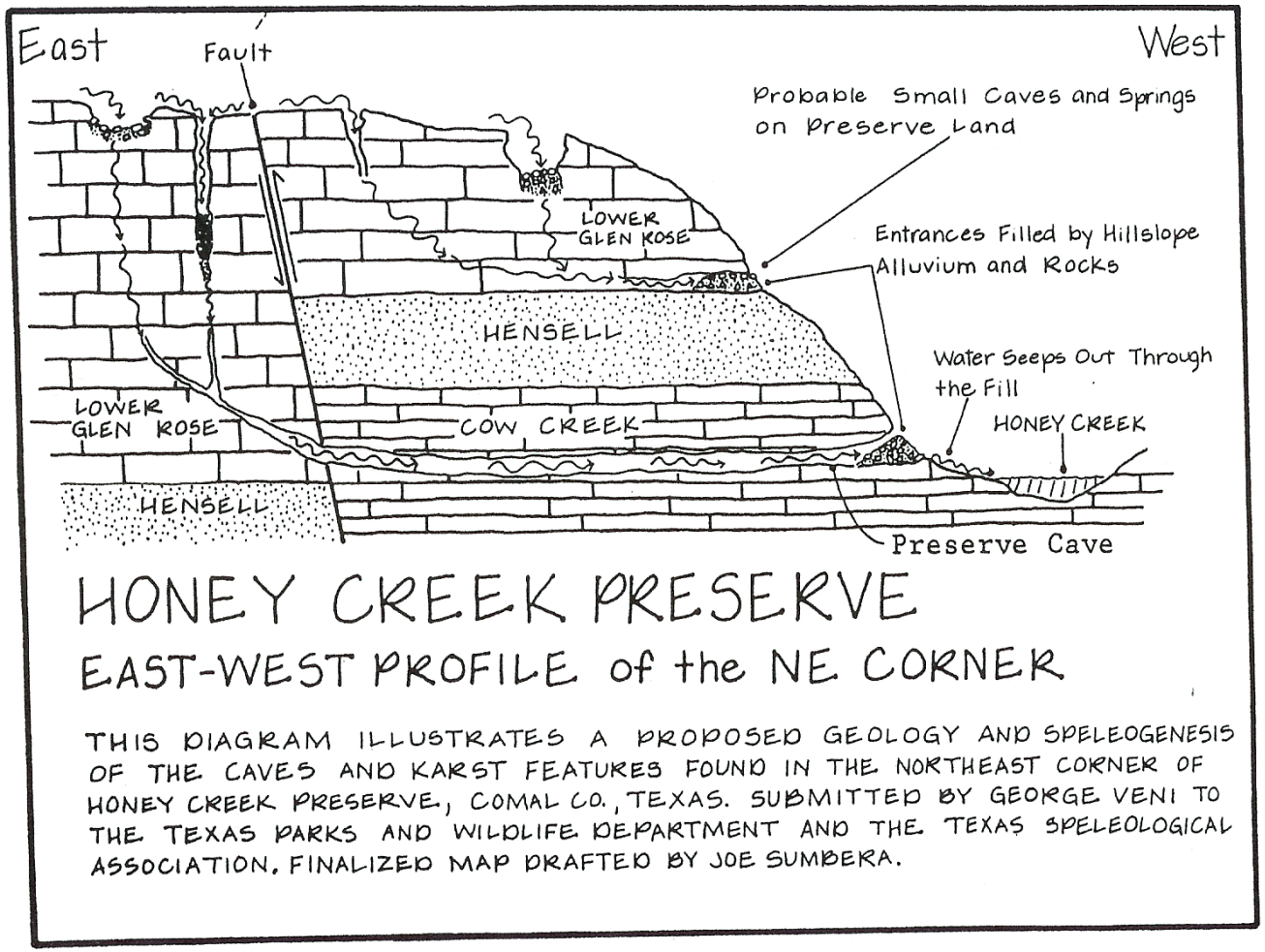

Fractures

Fractures affect cave development and hillslope erosion. Uplands are dissected by rectilinear to dendritic streams and subsurface conduits. Knickpoints and abrupt 90-degree bends in stream courses are often located at the intersection of perpendicular fractures. Streams may also follow a sub-parallel fracture set until reaching the next knickpoint formed at the next perpendicular fracture. Fractures follow a regional northeast trend with a secondary orientation trending to the northwest. Streams dissect uplands and solutionally enlarged fractures and follow similar trends. Bedrock fractures control geologic structure of Honey Creek basin, where fractures, streams, and spring conduits are parallel to one another. Some knickpoints are intersected by vertical fractures that intersect at an acute angle of between 20° and 40° (Photo 3A) and trend northwest and northeast. Navigable stream cave conduits in Honey Creek basin include Preserve Cave, Knee Deep Cave, and Honey Creek Stream Cave, which run parallel fracture-controlled creeks (Figure 2). These findings suggest that surface erosion and conduit dissolution are controlled by similar fracture orientations. Spring sapping processes subsequently follow conduit orientations and knickpoint migration occurs where fractures intersect streams at perpendicular angles.

Karst Features

Karst terrain has surface and subsurface features formed by dissolution of soluble rocks with mechanical enlargement by erosion and strain. Caves, sinkholes, losing streams, springs, and rapidly flowing groundwater are typical of karst regions. Subsurface conduits range from less than 3 to 33 feet (1 m to greater than 10 m) in diameter (TPWD, 2001). Variable conduit depths are controlled by the rock unit

thickness, fractures, bedding plane partings, and the aerial extent of a particular limestone (Veni, 1994a). The position and length of karst features may extend over an area of considerable extent. They may be filled with air, water, recemented minerals (such as calcite or silica), or sediment. Water-filled passages occur at or just below the water table within bedded and fractured limestone (Veni, 1994a). Phreatic conduits are located above water table and may intermittently transmit fluids following precipitation events (Figure 3, Figure 4, and Figure 16). Springs discharge water into the upland tributaries where conduits feed into downcut creeks. Some return flow (runoff) from these springs enters sinkholes downstream where it recharges the next lower level of the aquifer, based on the presence of recharge features downstream from perched aquifer springs. Some spring water that is discharged from stratigraphically perched water tables may eventually reach the regional groundwater table via recharge to solutionally enlarged fracture zones (Photo 2A) or stream swallets (Photo 2C).

Surface water and groundwater are linked by an intricate network of karst features and springs, resurgent groundwater, downstream recharge features (such as stream swallets), and fractures. Streams with beds above the water table are ephemeral streams; those with beds below the water table are perennial streams. Perennial streams flow year-round and are supported primarily by groundwater discharge with some seasonal or storm-event surface runoff. Perennial streams (such as Honey Creek and the Guadalupe River) flow year round and support aquatic organisms that require a continuous supply of water throughout the year. Ephemeral streams (such as the tributaries to Honey Creek) flow only following storm runoff events.

At Honey Creek, perched springs lose their discharge to runoff (Photos 8B) and downstream recharge in stream swallets (Photos 2C) and fractured rock outcrops (Figure 2). Ultimately, spring discharge to Honey Creek flows into the Guadalupe River and some runoff is ultimately lost to recharge via fractures and stream swallets that recharge the Middle Trinity aquifer. The remainder runs off and flows toward the unconfined zone of the Edwards aquifer (Figure 1) (TCEQ, 1996). Honey Creek basin is not only within an area that is believed to provide recharge to the Middle Trinity aquifer, but is within an area that provides runoff into the creeks and rivers that flow toward the Edwards aquifer recharge zone (unconfined zone).

This fluviokarst drainage system consists of a network of conduits and fractures that provide a blueprint for erosional features in the landscape. Solutionally enlarged fractures provide pathways for conduit development. Caves like Preserve Cave follow fracture trends and drain parallel to surface runoff toward Honey Creek. The entrance to Preserve Cave shows evidence of spring sapping, such as a talus pile and evidence of collapse. The spring orifice of Preserve Cave is found at the head of amphitheater-shaped valley. The orientation of the Preserve Cave passages is parallel to a stream that flows from the spring orifice where spring sapping may have caused the canyon to erode headward. A branch of the mapped footprint of Preserve Cave is also aligned with a surface tributary to the north where another spring is found (Appendix A).

Honey Creek Stream Cave may have once followed a continuation of a northeast-trending fault along Honey Creek (Figure 3), downstream from the spring orifice entrance to Honey Creek Stream Cave. Tributaries, including those at Honey Creek State Natural Area, drain toward Honey Creek and follow a conjugate fracture

trend to the northwest. This differs from Veni's projection of a hypothetical extension of Honey Creek Stream Cave (Figure 5).

Rose Diagrams

A total of 123 orientation measurements of conduit, karst feature, and fracture segments were plotted from the Honey Creek basin (Appendix G and Figure 17). The primary fracture orientation is toward the northeast at ~50° to 60º azimuth (N50° to 60°E). The secondary fracture orientation is toward the northwest at ~310° to 330º azimuth (N30° to 50°W), which correlates with the orientations of both tributaries A and B (Figure16C) and stream caves (Figure 17B). The caves and fracture data obtained from cave maps and aerial photography have similar mean fracture orientations (Figure 17E), which parallel surface tributaries (Table 4). However, the measured fractured rock outcrop (FR-2) within the streambed of Basin B has a calculated mean that is approximately 90º from the other measurements (toward the northeast). These results represent a separate fracture event and the fact that the stream is eroded along the trend of the other measurements (to the northwest) so that other fracture orientations may not be preserved or visible in the stream channel (Table 4). The location of FR-2 is shown on Figure 2. Rose Plots for passages of 2 fracture-controlled caves and 4 out of 34 scanline measurements at a fractured rock outcrop (FR-2) resulted in northwest orientations that match the orientations of tributaries of Basin A and B (Figure 17). At least 16 other measurements were taken from surrounding karst features and caves shown on Figure 2 that are also parallel with the dominant orientation of these tributaries (to the northwest).

Figure 17. Rose Diagrams representing the length-weighted distribution of orientations of features within Honey Creek basin: A) Honey Creek Stream Cave conduit orientation, B) all other karst features and caves, C) stream orientations (Honey Creek and its tributaries), D) Honey Creek Stream Cave and all other karst features, E) Fractures associated with karst features (not including Honey Creek Stream Cave), and F) scanline fracture data (FR-2).

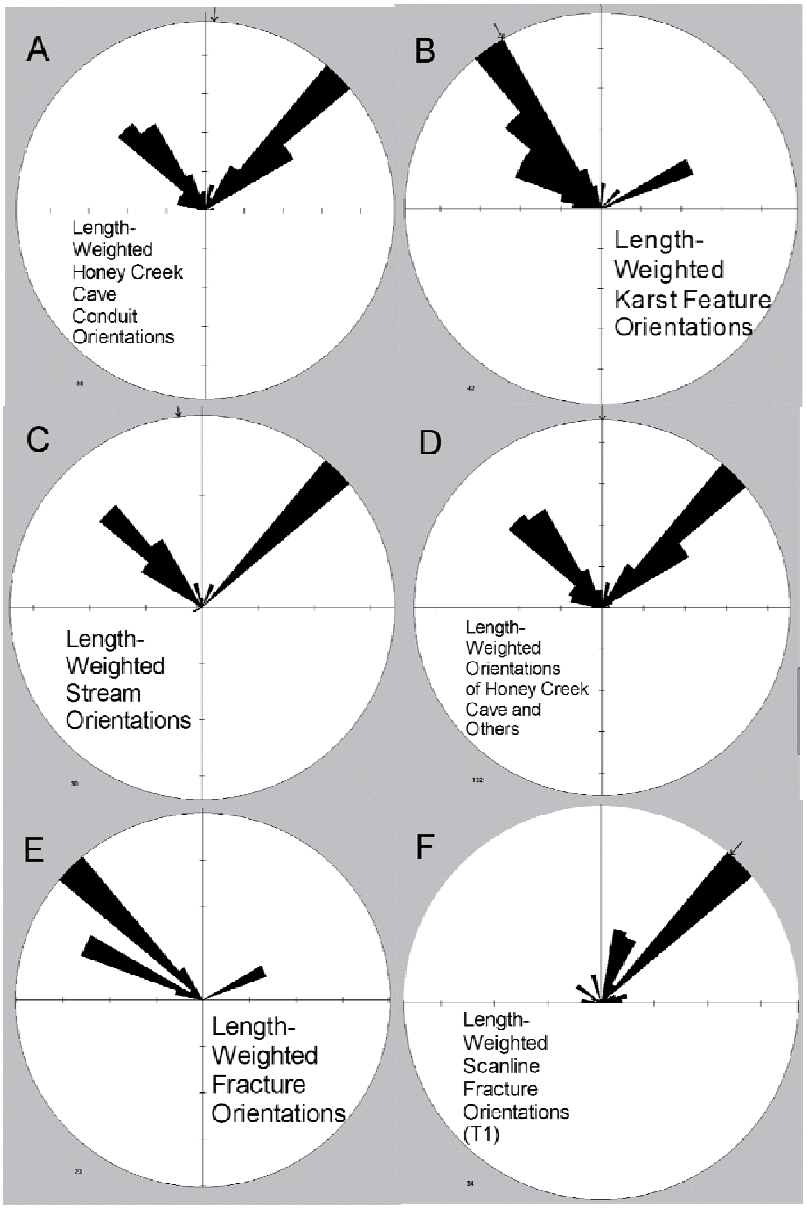

Table 4. Descriptive statistical information for orientation data shown on rose plots for fractures, caves, karst features, and streams.

	Scanline Fracture Orientation (FR-2)	**Honey Creek Stream Cave Conduit Orientation**	**Karst feature orientations**	**Fractures associated with karst features**	**Stream Orientation**
Mean	88.71	228.26	237.55	251.17	227.70
Standard Error	17.18	13.81	18.97	22.16	24.62
Median	48.50	303	302.50	295.00	310.00
Mode	73.50	323	330.00	285.00	320.00
Standard Deviation	100.15	131.05	122.94	106.27	134.86
Sample Variance	10029.62	17174.80	15114.01	11293.15	18185.94
Kurtosis	2.10	-1.36	-0.99	0.16	-1.49
Skewness	1.88	-0.74	-0.96	-1.38	-0.73
Range	340	358	341.00	313.00	349.00
Minimum	8.50	0	9.00	32.00	6.00
Maximum	348.50	358	350.00	345.00	355.00
Sum	3016	20543	9977.00	5777.00	6831.00
Count	34	90	42.00	23.00	30.00
Largest(1)	348.50	358	350.00	345.00	355.00
Smallest(1)	8.50	0	9.00	32.00	6.00
Confidence Level (95.0%)	34.940	27.45	38.31	45.95	50.36

Evaluation of Hydrogeologic Properties

Stream discharge measurements, stream longitudinal profiles, locations of springs, the potentiometric surface, and direction of groundwater flow in cave conduits were used to evaluate the hydrogeologic properties of Honey Creek basin. These data provide evidence of stream piracy and the potential for groundwater sapping and characterize the groundwater and surface water interaction.

Stream Discharge Measurements

Honey Creek is a gaining stream (Table 5 and Figure 18), based on stream discharge measurements taken by students during field methods classes (Geo 376L/328C), June 2001. A map of the sampling locations is shown on Figure 12. The discharge rates of the tributaries (downstream from fluvial-level springs) are significantly lower than in the main channel. Additionally, the station farthest downstream (SG-3) has the highest velocity of 10.00 cubic feet per second (cfs) or 283.17 liters per second (lps). The stream discharge for the station farthest upstream is 5.66 cfs (160.27 lps), so 4.34 cfs (123 lps) is being gained between the uppermost and lowermost stations. Discharge measurements were taken downstream from springs at the base of Basin A (Spring SPR-2) and Basin B (Spring SPR-3). Combined flow from both springs totals approximately 3.30 cfs (93.45 lps). The remainder of the gain in baseflow in Honey Creek is 1.04 cfs (29.45 lps). Additional discharge from discrete springs or alluvial throughflow may not be easily accounted for. However, the majority of the gain in flow to Honey Creek basin near Honey Creek is coming from the fluvial-level springs.

Figure 18. Graph of stream discharge measurements (main channel of Honey Creek).

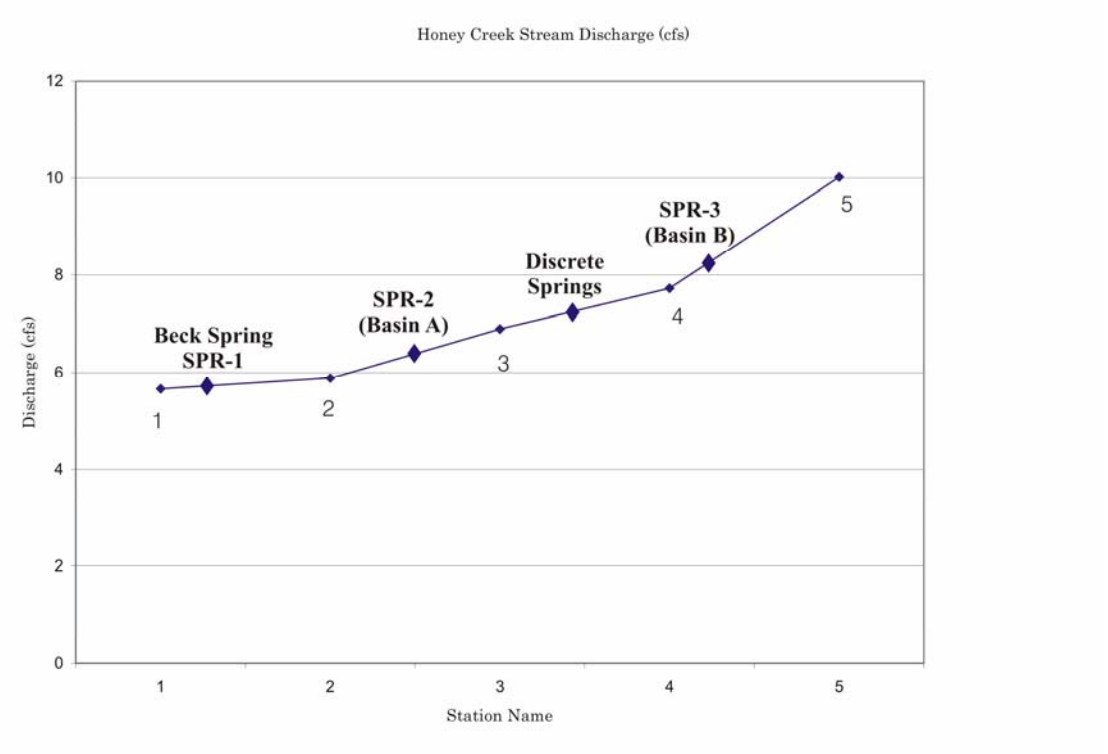

Table 5. Honey Creek stream discharge measurements (taken 1 May 2001).

Station Name	Discharge (cfs)
1	5.66
2	5.885
3	6.9
4	7.73
5	10.02
Spring SPR-2 (Basin A)	1.697
Spring SPR-3 (Basin B)	1.6

Discharge measurements are helpful to characterize the groundwater and surface water interaction near the stream channel. The alluvial material in the bed of Honey Creek may act as a lesser aquifer as groundwater from springs moves toward the creek at a perpendicular angle (influent conditions). Larkin and Sharp (1992) classify stream-aquifers in which the groundwater flux moves toward a river as baseflow-component dominated. Sophocleous (2002) defines *baseflow* as "water that enters a stream from persistent, slowly varying sources and maintains streamflow between water-input events." In this case, we are observing an influx of groundwater toward Honey Creek.

Precipitation vs. Runoff

Rainfall intensity rarely exceeds infiltration capacity in areas of high infiltration rates. On uplands, Horton overland flow does not occur often on much of the land surface (Dunne and Leopold, 1978, p. 263). Figure 19 shows the effect of precipitation on runoff within the intermittent tributary of Basin A (USGS, 2001). These data are provided in Appendix H. Runoff occurs following a period of precipitation that sufficiently saturates the ground surface, causing overland sheetflow to occur. This confirms that infiltration rates are high on the uplands of Honey Creek basin and that flow within the upland tributaries is intermittent.

Figure 19. Graph showing precipitation vs. runoff (15 August to 30 September 2001).

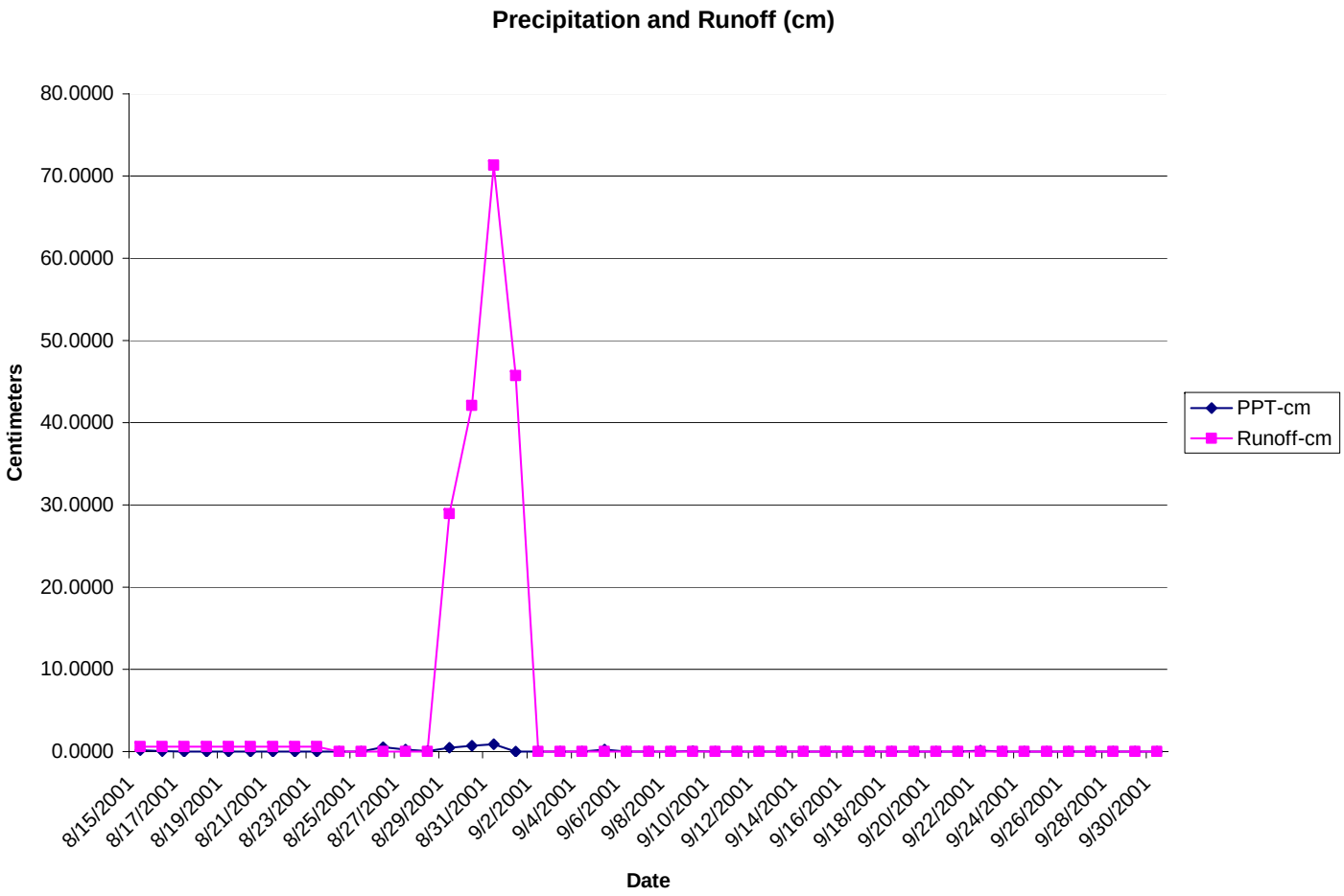

Precipitation vs. Water Levels in Shallow and Deep Water Wells

A continuum in groundwater flow in carbonate aquifers typically ranges between storm flow (quick flow) via solution conduits and solutionally enlarged fractures and slow flow through fine fractures and pores. During storm events, water may enter Honey Creek quickly in response to input events such as direct precipitation and subsurface storm flow or interflow (Sophocleous, 2002). In fractured and karst terrain, surface and groundwater interaction may occur through fracture flow and solution conduits that may provide more rapid influx of water into Honey Creek and its tributaries. Springs, exposed along limestone ledges of Honey Creek and its tributaries respond more rapidly to subsurface storm flow than do springs at the bottom of the basin. Storm flow is different from baseflow because it is not persistent and only contributes streamflow during storm events. Interflow is defined by Beven (1989) as near-surface flow within the soil profile that results in seepage into a stream channel within the period of the storm flow hydrograph. If interflow encounters a seepage face or storm flow encounters a solution conduit leading to a spring orifice, then storm flow or interflow may grade into *return flow* where the subsurface flow contributes runoff or overland flow (Dunne and Black, 1970; Sophocleous, 2002).

Figures 20 show precipitation versus groundwater levels in deep and shallow water wells in Honey Creek Basin. Wells locations are shown on Figure 2 and 9. Depth to groundwater tables are shown from one deep water well (TWDB # 68-13-102) that is 61 m deep and a shallow water well (TWDB # 68-13-101) that is 6 m deep. Figures 21 shows precipitation, runoff, and elevation of water in a deeper well (#68-01-314) at Comfort and a shallow well (#6802609) at Waring, Texas.

Figure 20. Sampling results of A and B) precipitation versus groundwater level fluctuations in shallow and deep water wells (15 August to 30 September 2001) (provisional data from USGS, 2001). C) groundwater level fluctuations in shallow and deep water wells (January to December 2001) (USGS, 2001).

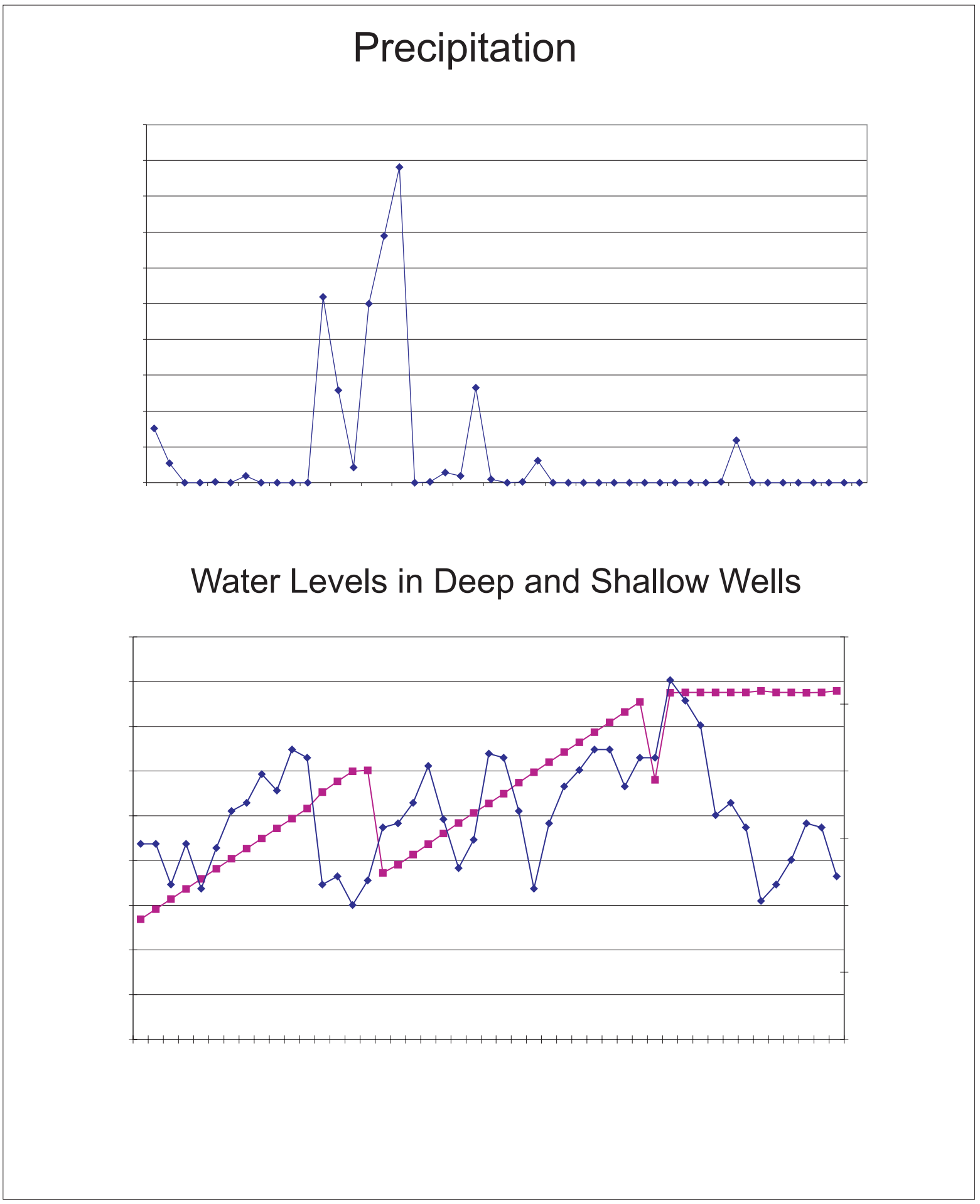

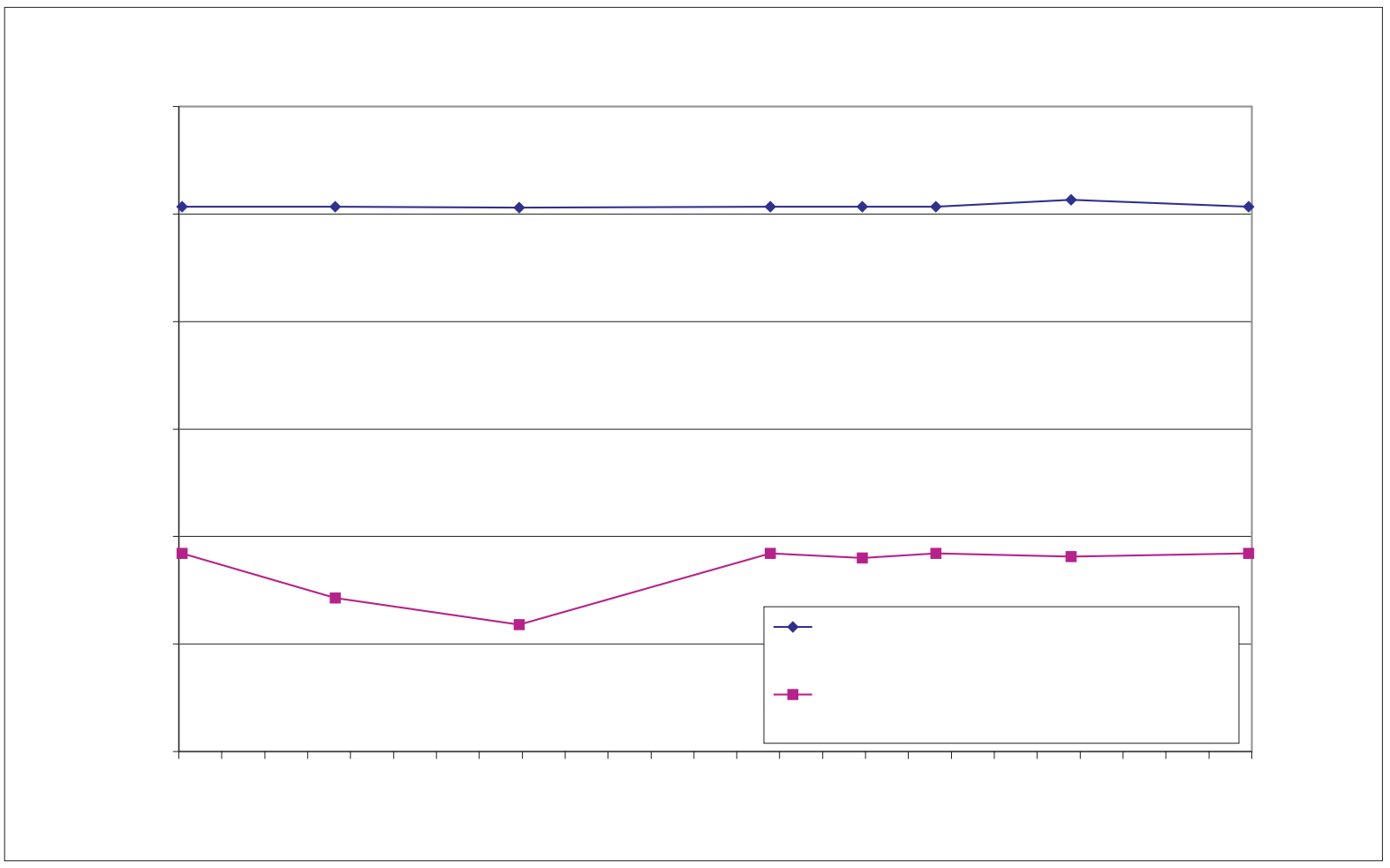

Figure 21. 2001 Charts of A) precipitation data (NOAA Cooperative Weather Station), B) runoff (USGS Guadalupe River at Comfort and Spring Branch, Stations, C) 2001 water levels for Well # 6801314 and W#686802609, and D) 2001 water levels for Well # 6813101 and W#6813102, January 2001 - December 2001.

A

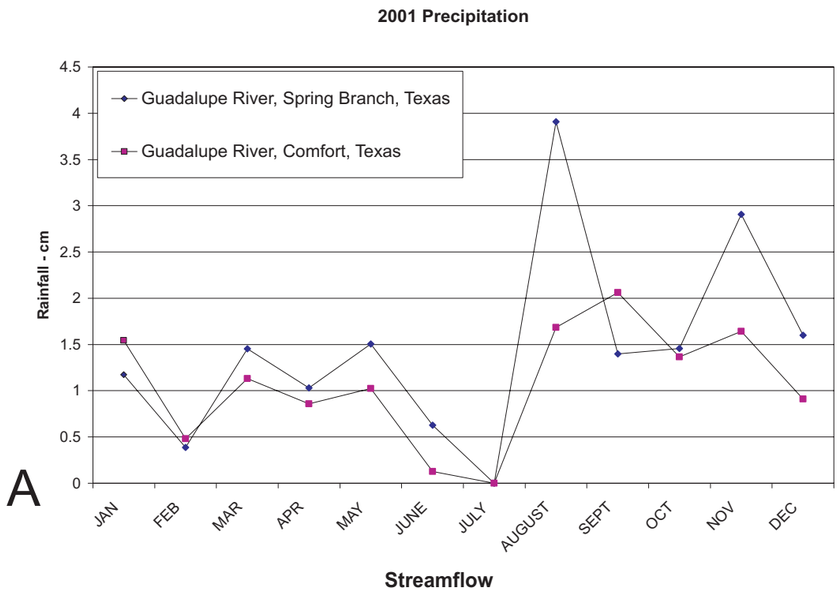

B

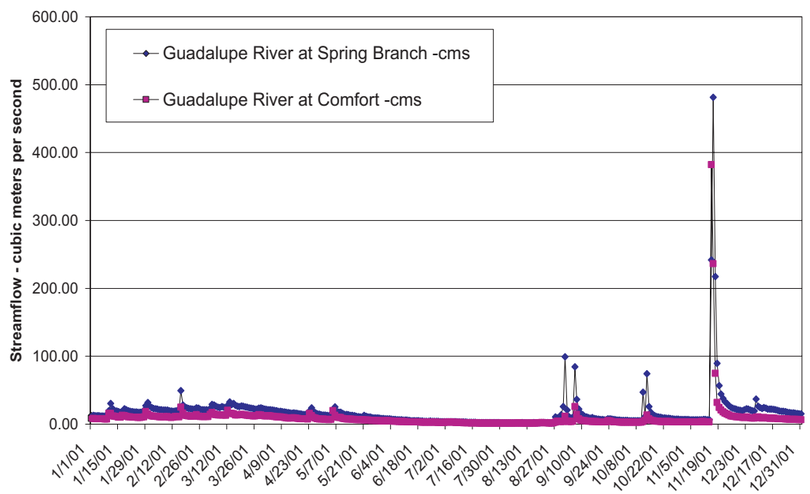

C

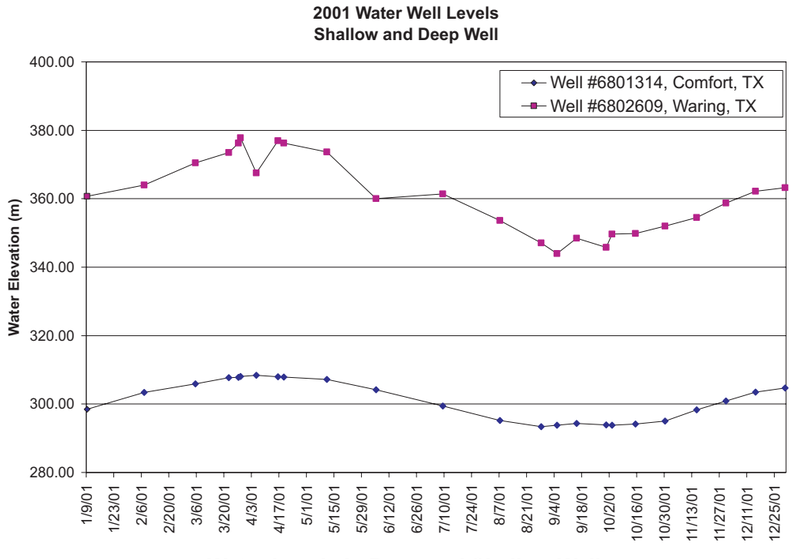

D

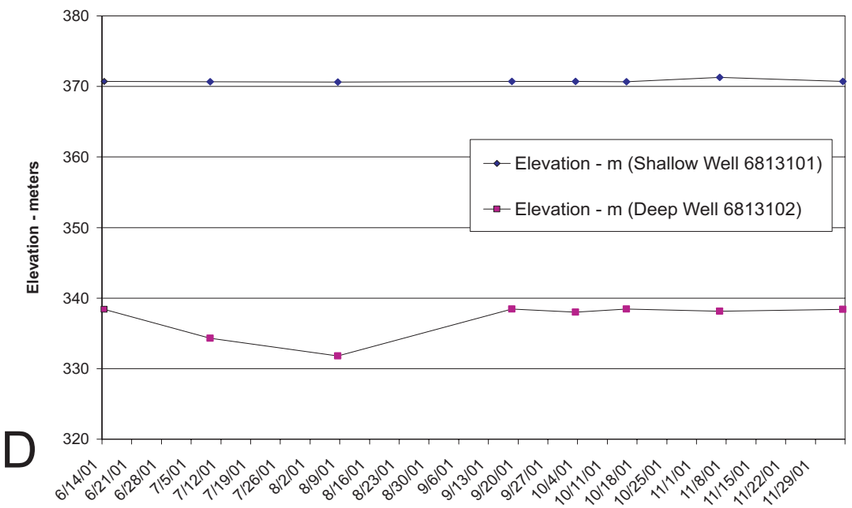

Water depths of deep and shallow water tables at Honey Creek State Natural Area respond differently to precipitation events. Hydrograph measurements of water levels from USGS observation wells (Figure 20) show that the perched water table has a narrower range of fluctuation (measured in cm) than the deeper water levels. This is possibly due to rapid discharge from perched aquifer springs that prevents the perched groundwater table from rising rapidly. The fluctuation of the water in the deeper water wells shows a more persistent response (measured in meters) of the deeper regional aquifer levels to precipitation, recharge, and return flow. This pattern further emphasizes the ability of the perched groundwater table to transmit returnflow via perched aquifer springs and conduits that discharge into the intermittent upland tributaries. Subsequently, springs provide discharge runoff toward recharge features downstream and prevent water from rising quickly in the stratigraphically perched aquifer.

Longitudinal Profile Development

The longitudinal profile of the Basin B tributary of Honey Creek State Natural Area was correlated with springs, lithology, and caves to represent the hydrogeologic characteristics of this fluviokarst drainage network (Figure 13). All knickpoints occur at perpendicular fracture sets and form step-like ledges with detached or missing blocks of limestone. The detached blocks suggest a mechanical erosion process that occurs during floods (Wohl, 1992). Limestone treads form long reaches of the stream channel between knickpoints where corrosion processes form scalloped and fluted limestone surfaces (White, 1988 and Springer et al, 2003). Canyon walls contain solution cavities and seeps formed along vertical fractures or lithologic contacts between limestone and marl or rocks with differential permeabilities. Canyon walls

also form smooth overhangs that may be relict walls of stream caves or spring conduits (Photo 3C). Often a stream swallet is found beneath a spring or seepage face, suggesting a possible hydrologic connection that existed prior to the downcutting of the canyon (Photo 2B). Alluvial gravels and boulders may obscure additional stream swallets.

Identification and Mapping Using Arcview GIS

The potentiometric surface (Figure 9), longitudinal stream profile (Figure 13 and Figure 14), locations of springs, seeps, caves, fractures, and knickpoints were analyzed using Arcview GIS and Spatial Analyst. The results of the potentiometric surface were compared with previous studies by Veni (1994a) and Mace et al. (2000).

Potentiometric Surface

Potentiometric surface maps show that water-table levels are influenced by the location of springs and rivers. A regional potentiometric surface map (created using Spatial Analyst and ArcGIS) illustrates that the groundwater gradient is toward the southeast, except in locations where streams and springs divert local groundwater flow (Figure 9). The regional groundwater gradient is toward the southeast, as is the gradient of the major rivers of Texas (TWC, 1989). The potentiometric surface of a stratigraphically perched aquifer within Honey Creek basin has a steeper gradient toward the incised channels of Honey Creek, the Guadalupe River to the north, and Cibolo Creek to the south (Figure 10 and Figure 11). These results agree with the results of previous potentiometric maps produced by Veni (1994a, Figure 4.36 and 4.37), and Mace (2000, Figure 9).

Within the Honey Creek drainage basin, many water wells obtain water from the Middle Trinity aquifer (Figure 2). The deep (static) potentiometric surface is at an

approximate elevation of 330 meters above sea level (TWDB, 2005, USGS, 2001), which correlate to the presence of springs within Honey Creek and the Guadalupe River (Figure 3, Figure 4, Figure 9, Figure 16, Figure 20, and Figure 21). Springs at the base of Honey Creek are found at slightly lower elevations that the groundwater measured in wells on the uplands. This suggests that the potentiometric surface steepens toward the incised creeks and rivers (Figure 13) and is a subdued reflection of topography (Kuniansky and Holligan, 1994, Mace et al., 2000).

CONCLUSIONS

The geomorphologic coevolution of the surface and subsurface drainage systems has shaped Honey Creek State Natural Area and larger Honey Creek basin. These findings suggest that groundwater sapping and stream piracy processes follow spring conduit and solutionally enlarged fracture orientations. Evidence of groundwater sapping (the erosion and weathering of rock and soil by groundwater) includes seepage erosion along of marl risers hillslopes, headward erosion of springs due to groundwater sapping, and block failure at fractures and knickpoints. Spring sapping erodes a hillslope where a spring emerges. Seepage erosion occurs where a saturated bedding plane forms hillslope seepage along canyon walls.

Surface and subsurface drainage appear to have shaped each other in the following ways at Honey Creek State Natural Area. Block failure forms knickpoints where fractures intersect streams at perpendicular angles, providing avenues for erosion. Spring conduits and streams intersect perched groundwater at or above lithologic contacts. Surface water and groundwater in conduits flow downward along the steepest available gradient toward the entrenched canyon of Honey Creek and its tributaries. Drainage catchment basins are connected by fault-controlled solutionally

enlarged fractures and conduits that allow communication between groundwater from different basins. Preserve Cave and Honey Creek Stream Cave pirate groundwater from adjacent basins to spring orifices within Honey Creek basin.

This research presents multiple methods used to identify evidence of groundwater sapping via the headward erosion of stream conduits and seepage erosion of hillslopes. Karst dissolution is controlled by a concentration of flow (surface and subsurface) along local and regional fracture orientations and by differential erodability and permeabilities of rock substrate. Although groundwater sapping and piracy of surface streams by spring conduits are not necessarily the primary means by which the orientations of surface streams and spring conduits are formed, evidence of these processes may be used to predict the locations of potential pathways for surface water and groundwater interaction.

These data were all combined to add detail to the longitudinal profile that provided a graphical representation of the distribution of features typically associated with groundwater sapping along a tributary to Honey Creek. All knickpoints identified in Basin B were associated with fractures. Observations in other basins at Honey Creek State Natural Area resulted in the discovery of fractures and block failure at all knickpoints. Springs are not associated with knickpoints, although they are usually found downstream along the canyon sidewalls at a similar elevation within the canyon walls. This demonstrates the presence of groundwater at or near the elevation of knickpoints, where seepage may contribute to block and slope failure resulting in the headward erosion of streams at knickpoints. At least 90% spring orifices above fluvial base level showed evidence of spring sapping, including a talus pile, headcuts, and an incised downstream channel. The remaining 10% were formed in the vertical sidewalls of the canyon along fractures that were perpendicular to the

creek bed. Stream discharge measurements demonstrate that Honey Creek basin is a gaining stream fed by fluvial level springs and runoff from the upland tributaries. The comparison of precipitation, runoff, and potentiometric surface provide evidence of a perched groundwater system, repetitive stratigraphic sequence, and potential for upland seepage erosion and spring sapping that extends groundwater-sapping geomorphology in to the uplands. Drainages, cave, and spring conduit segments are dominantly aligned with regional fracture trends.

Although spring sapping and groundwater piracy processes are secondary to structural controls on drainage, they do play a role in the co-evolution of the surface and subsurface drainage patterns. Maps of caves and spring conduits were overlain on topographic maps show that some caves (such as Honey Creek Stream Cave and Preserve Cave) cross surface water drainage divides and may pirate groundwater from one surface drainage basin to another. Alone, these tools do not necessarily provide definitive evidence of groundwater sapping and spring piracy. Nevertheless, they offer a better understanding of the drainage patterns at Honey Creek State Natural Area and the larger Honey Creek basin. These data provide a baseline from which to expand future research regarding the interaction of groundwater and surface water within Honey Creek basin.

To expand this study, erosion plots could be located near seepage faces and lithologic contacts identified in this study, near perched groundwater sources. Erosion pins or other methodologies could be used to quantify spring sapping or knickpoint erosion (often evident in the tributary canyons after individual storm events). Hillslope erosion measurements were initiated as a part of an unrelated study regarding the potential affects on erosion in response to the prescribed trimming of Ashe juniper trees as a part of an on-going study at Honey Creek State Natural Area.

Hillslope erosion measurements provide baseline data for an on-going paired basin study regarding the response of hillslopes to Ashe juniper trimming. The addition of weirs at the bottom of each test plot is needed to better quantify erosion rates in response to storm events or juniper trimming. In Basin B, clearing of Ashe juniper trees began in November 2004 and is ongoing. Future studies of these paired test plots could involve measurement of land surface changes and spring response to the juniper trimming or runoff events.

Several aspects of this research could be further developed, such as measurement of spring sapping where springs emerge in canyons, hillslope seepage erosion, and knickpoint migration. Maps of karst recharge features, caves, springs, faults, and geologic rock outcrops may be helpful in predicting potential groundwater flowpaths for future dye tracing studies. This and future studies are important as they relate to surface and groundwater management practices at Honey Creek State Natural Area and the larger Honey Creek basin.

APPENDICES

Appendix A. Site Feature Map

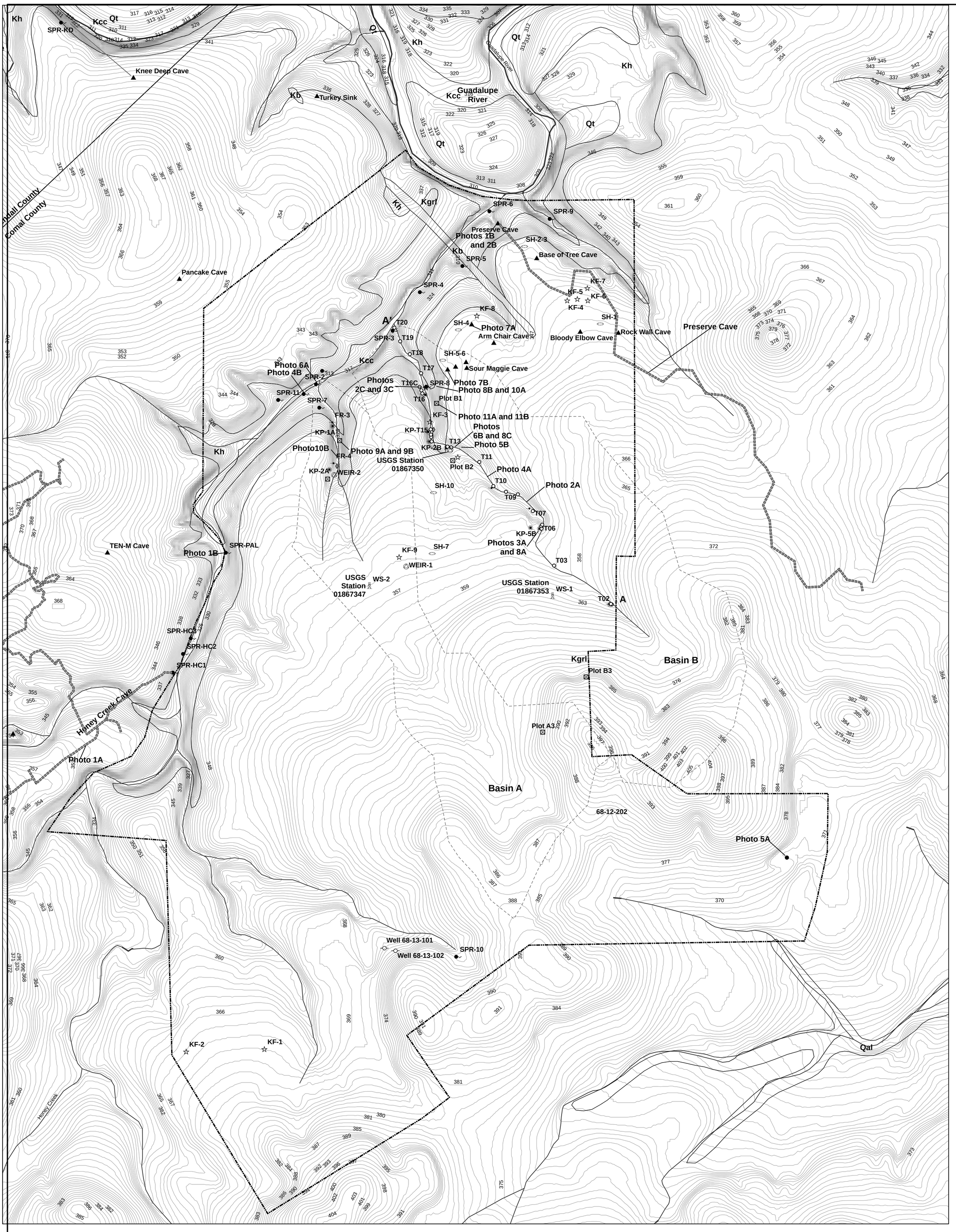

Stream and River Data: National Hydrography Dataset, 2005.
Honey Creek Footprint: Texas Speleological Society, 1994.
Map of Honey Creek Water Cave.
Preserve Cave Footprint: Sumbera, J. and Veni G, 1986,
Trip report #2 and field reconnaissance,
unpublished report to Texas Parks and Wildlife Department, 2 p.

0 445 890 1,780
Feet

0 145 290 580
Meters

N

Legend

- Honey Creek State Natural Area
- Cave
- Erosion Plot
- Fracture
- Geologic Contact
- Karst Feature
- Knickpoint
- Long Profile
- Paleospring
- Sinkhole
- Spring
- USGS Stream Gauge
- Water Well
- Weather Station
- Elevation (meters)

Qal - Alluvium; gravel
Qt - Terrace alluvium
Kb - Basalt, minor occurrences
Kgrl - Lower Glen Rose Formation
Kh - Hensel Formation
Kcc - Cow Creek Formation

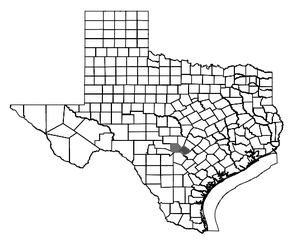

SITE FEATURE MAP
HONEY CREEK
STATE NATURAL AREA
AND SURROUNDING AREA
COMAL AND KENDALL
COUNTIES, TEXAS

Appendix B. USGS Real-Time Stations, Comal and Kendall County, Texas (USGS, 2001)

USGS streamflow and weather measurement stations (USGS, 2001).

USGS Station #	Name	Location	Contributing Drainage Area	Gauge Data NGVD29	Station Type	Data Type	Begin Date	End Date
08167000	Guadalupe River at Comfort, TX	Latitude 29°58'10", Longitude 98°53'33" NAD27	839 square miles (2173 square km)	1,369.83 ft above sea level (417.5242 km above sea level)	Surface Water	Real-time water quality, peak streamflow and daily streamflow	08-30-01	08-30-01
08167347	Unnamed Tributary To Honey Creek Site 1C, near Spring Branch, TX	Latitude 29°51'18.11", Longitude 98°29'03.83" NAD83, Comal County, Texas , Hydrologic Unit 12100201 Basin A	0.35 square miles (0.9square km)	1,100 feet above msl (335.28 km above sea level)	Surface Water	Real -Time and Water Quality	08-30-01	08-30-02
08167350	Unnamed Tributary Honey Creek Site 1T nr Spring Branch, TX	Latitude 29°51'00.87", Longitude 98°28'21.29" NAD27, Comal County, Texas , Hydrologic Unit 12100201 Basin B	0.18 square miles (.47 square km)	1,180 feet above msl (359.66 km above seal level)	Surface Water and Meteorological	Real-Time and Water Quality	08-30-01	08-30-02
08167353	Unnamed Tributary of Honey Creek Site 2T, near Spring Branch, TX	Latitude 29°51'21.35", Longitude 98°28'42.52" NAD83, Comal County, Texas , Hydrologic Unit 12100201 Basin B	0.43 square miles (1.1 square km)	1,118 feet (340.77 km above seal level)	Surface Water	Real-Time and Water Quality	08-30-01	08-30-02
08167500	Guadalupe River, near Spring Branch, TX	Latitude 29°51'37", Longitude 98°23'00" NAD27, Comal County, Texas , Hydrologic Unit 12100201	1,315 square miles (3405.83 square km)	948.10 feet above msl (288.98 meters above sea level)	Surface Water	Real-Time, Water Quality, Peak Streamflow, and Daily Streamflow	08-30-01	08-30-02

Appendix C. Field Test Plot Erosion Pin Data

Plot Code:	Horizontal Position (Column)	Vertical Position (Row)	Slope in degrees	May-01 to Sept-01 (cm)	Sept-01 to Jan-02 (cm)	Jan-02 to Aug-02 (cm)	Mean Change (May-01 to Aug-02) (cm)	Notes
B1	1	A – Top	32.00	-1.90	0.10	-0.10	-0.63	Heavy sheetflow
B1	1	B	32.00	-0.40	-0.10	0.00	-0.17	9-29-01 – pedestal - Rocky slope
B1	1	C	32.00	0.40	-1.30	1.05	0.05	9-29-01 – pedestal
B1	1	D – Mid	32.00	-1.00	0.40	-0.20	-0.27	
B1	1	E	32.00	-0.20	0.00	-0.20	-0.13	9-29-01 - pedestal
B1	1	F	32.00	-1.30	-0.60	-0.10	-0.67	
B1	1	G-Bottom	32.00	1.90	3.90	-1.80	1.33	Heavy sheetflow
B1	2	A – Top	32.00	-0.70	-9.30	0.00	-3.33	1-26-02 Missing Pin
B1	2	B	32.00	-7.00	1.20	-0.10	-1.97	Heavy sheetflow - 9-29-01 (desiccation cracks)
B1	2	C	32.00	-0.20	0.30	-0.40	-0.10	9-29-01 - pedestal
B1	2	D – Mid	32.00	-0.10	0.60	0.30	0.27	9-29-01 – slight pedestal
B1	2	E	32.00	-1.15	0.35	-0.80	-0.53	
B1	2	F	32.00	-1.00	0.50	0.10	-0.13	Heavy sheetflow
B1	2	G-Bottom	32.00	0.40	6.00	-1.20	1.73	
B1	3	A – Top	32.00	-0.10	-0.30	0.10	-0.10	9-29-01 (sed. On top of washer)
B1	3	B	32.00	-0.10	0.70	-0.40	0.07	
B1	3	C	32.00	0.10	0.90	0.10	0.37	
B1	3	D – Mid	32.00	-0.30	0.90	0.20	0.27	
B1	3	E	32.00	0.00	-0.10	-0.20	-0.10	
B1	3	F	32.00	-0.80	3.70	-2.10	0.27	

Plot Code:	Horizontal Position (Column)	Vertical Position (Row)	Slope in degrees	May-01 to Sept-01 (cm)	Sept-01 to Jan-02 (cm)	Jan-02 to Aug-02 (cm)	Mean Change (May-01 to Aug-02) (cm)	Notes
B1	3	G-Bottom	32.00	-0.90	0.80	1.20	0.37	
B1	4	A – Top	32.00	-0.60	1.70	-0.60	0.17	9-29-01 (twig upslope)
B1	4	B	32.00	-0.05	1.65	-1.40	0.07	
B1	4	C	32.00	-0.40	0.20	0.20	0.00	
B1	4	D – Mid	32.00	-0.70	0.10	0.40	-0.07	
B1	4	E	32.00	-0.20	0.00	0.00	-0.07	
B1	4	F	32.00	-0.30	0.70	-0.20	0.07	
B1	4	G - Bottom	32.00	-0.40	-0.20	0.20	-0.13	
B1	5	A – Top	32.00	-0.90	0.20	0.10	-0.20	9-29-01 (desiccation cracks)
B1	5	B	32.00	0.05	-0.05	0.10	0.03	
B1	5	C	32.00	-1.10	3.50	-1.90	0.17	
B1	5	D – Mid	32.00	-0.10	0.30	-0.30	-0.03	
B1	5	E	32.00	-0.40	-0.10	0.05	-0.15	
B1	5	F	32.00	-0.10	0.10	-0.60	-0.20	
B1	5	G-Bottom	32.00	-0.40	-0.10	0.00	-0.17	
B1	6	A – Top	32.00	-3.60	0.20	0.00	-1.13	
B1	6	B	32.00	-0.40	1.00	-0.10	0.17	
B1	6	C	32.00	-0.20	0.80	-0.20	0.13	fire ant mounds 1-26-02
B1	6	D - Mid	32.00	-0.40	1.10	0.40	0.37	
B1	6	E	32.00	-0.30	0.00	0.00	-0.10	
B1	6	F	32.00	-0.60	0.10	-0.20	-0.23	
B1	6	G-Bottom	32.00	-0.40	0.00	0.10	-0.10	
B1	1	A – Top	11.00	-0.55	1.55	-0.30	0.23	9-29-01 (dessic. cracks)
B1	1	B	11.00	-0.15	0.15	0.00	0.00	
B1	1	C-Mid	11.00	-0.10	0.30	-0.20	0.00	
B1	1	D - Mid	11.00	0.10	0.00	0.10	0.07	
B1	1	E	11.00	-0.30	0.20	-0.20	-0.10	
B1	1	F – Bottom	11.00	-0.80	0.30	-0.10	-0.20	
B1	2	A – Top	11.00	0.50	-0.40	-0.20	-0.03	Canopy

Plot Code:	Horizontal Position (Column)	Vertical Position (Row)	Slope in degrees	May-01 to Sept-01 (cm)	Sept-01 to Jan-02 (cm)	Jan-02 to Aug-02 (cm)	Mean Change (May-01 to Aug-02) (cm)	Notes
B1	2	B	11.00	0.35	-0.35	-0.20	-0.07	
B1	2	C- Mid	11.00	-0.20	0.20	-0.20	-0.07	
B1	2	D - Mid	11.00	0.70	-0.20	-1.15	-0.22	
B1	2	E	11.00	0.10	-0.20	-0.20	-0.10	
B1	2	F – Bottom	11.00	-0.30	0.60	0.20	0.17	
B1	3	A – Top	11.00	0.10	0.60	-0.70	0.00	
B1	3	B	11.00	-0.80	0.20	-0.10	-0.23	
B1	3	C- Mid	11.00	-0.30	0.50	-0.10	0.03	
B1	3	D - Mid	11.00	-0.20	0.20	0.40	0.13	
B1	3	E	11.00	-0.70	1.00	-0.30	0.00	
B1	3	F – Bottom	11.00	-0.30	0.30	-0.20	-0.07	
B1	4	A – Top	11.00	-1.80	0.40	0.10	-0.43	washer jammed in rock crevasse
B1	4	B	11.00	-1.40	-0.40	-0.20	-0.67	
B1	4	C-Mid	11.00	-0.20	0.00	-0.20	-0.13	
B1	4	D - Mid	11.00	-0.30	0.20	-0.50	-0.20	
B1	4	E	11.00	0.60	-1.00	0.00	-0.13	
B1	4	F – Bottom	11.00	-0.30	-0.10	-0.10	-0.17	
B1	5	A – Top	11.00	-0.40	0.00	0.10	-0.10	
B1	5	B	11.00	-0.10	-0.15	0.30	0.02	
B1	5	C-Mid	11.00	-0.30	0.20	-0.20	-0.10	
B1	5	D - Mid	11.00	-0.30	0.30	0.90	0.30	
B1	5	E	11.00	-0.30	0.40	-0.10	0.00	
B1	5	F – Bottom	11.00	-0.30	0.40	0.00	0.03	
B1	6	A – Top	11.00	0.20	0.60	0.00	0.27	
B1	6	B	11.00	-0.30	0.30	0.00	0.00	
B1	6	C-Mid	11.00	-0.25	0.25	0.00	0.00	
B1	6	D - Mid	11.00	-0.50	0.70	-0.50	-0.10	
B1	6	E	11.00	-0.20	0.00	0.10	-0.03	
B1	6	F – Bottom	11.00	0.60	0.60	-0.10	0.37	
B3	1	A – Top	20.00	-0.10	-0.90	0.00	-0.33	
B3	1	B	20.00	0.10	-0.10	0.10	0.03	
B3	1	C-Mid	20.00	0.80	0.10	0.00	0.30	heavy sheetflow

Plot Code:	Horizontal Position (Column)	Vertical Position (Row)	Slope in degrees	May-01 to Sept-01 (cm)	Sept-01 to Jan-02 (cm)	Jan-02 to Aug-02 (cm)	Mean Change (May-01 to Aug-02) (cm)	Notes
B3	1	D - Mid	20.00	0.10	-0.10	0.00	0.00	
B3	1	E	20.00	0.00	-0.10	0.10	0.00	
B3	1	F – Bottom	20.00	0.00	-0.10	0.10	0.00	heavy sheetflow
B3	2	A – Top	20.00	0.00	-0.10	0.00	-0.03	
B3	2	B	20.00	0.00	0.00	1.10	0.37	
B3	2	C-Mid	20.00	1.30	-0.60	-0.40	0.10	
B3	2	D - Mid	20.00	1.20	-0.40	0.90	0.57	Gravel
B3	2	E	20.00	0.10	-0.11	0.01	0.00	Ashe Juniper (AJ) canopy
B3	2	F – Bottom	20.00	0.00	0.00	0.00	0.00	AJ canopy
B3	3	A – Top	20.00	0.00	0.40	-0.40	0.00	
B3	3	B	20.00	0.00	-0.10	0.00	-0.03	
B3	3	C-Mid	20.00	0.10	0.00	0.00	0.03	
B3	3	D - Mid	20.00	0.50	0.00	0.00	0.17	
B3	3	E	20.00	0.00	0.80	0.40	0.40	
B3	3	F – Bottom	20.00	-0.10	0.10	0.00	0.00	
B3	4	A – Top	20.00	0.00	0.20	-0.20	0.00	
B3	4	B	20.00	0.10	0.00	0.10	0.07	
B3	4	C-Mid	20.00	0.50	0.00	-0.10	0.13	AJ canopy
B3	4	D - Mid	20.00	-1.50	-0.40	-0.40	-0.77	AJ canopy
B3	4	E	20.00	0.10	-0.10	0.00	0.00	
B3	4	F – Bottom	20.00	0.30	-0.30	0.10	0.03	AJ canopy
B3	5	A – Top	20.00	-1.10	-0.10	0.10	-0.37	
B3	5	B	20.00	-0.10	0.20	-0.10	0.00	
B3	5	C-Mid	20.00	0.00	0.40	0.20	0.20	
B3	5	D - Mid	20.00	-0.50	1.10	0.10	0.23	AJ canopy
B3	5	E	20.00	0.20	-0.20	0.10	0.03	
B3	5	F – Bottom	20.00	0.20	0.00	0.10	0.10	AJ canopy
B3	6	A – Top	20.00	0.00	0.00	0.10	0.03	
B3	6	B	20.00	0.70	-0.50	0.50	0.23	AJ canopy & trunk
B3	6	C-Mid	20.00	-1.30	0.20	0.20	-0.30	
B3	6	D - Mid	20.00	-0.30	-0.30	0.30	-0.10	AJ canopy
B3	6	E	20.00	0.00	-0.20	0.20	0.00	AJ

Plot Code:	Horizontal Position (Column)	Vertical Position (Row)	Slope in degrees	May-01 to Sept-01 (cm)	Sept-01 to Jan-02 (cm)	Jan-02 to Aug-02 (cm)	Mean Change (May-01 to Aug-02) (cm)	Notes
B3	6	F – Bottom	20.00	0.20	-0.20	0.10	0.03	Limestone below marl slope. - forams
A1	1	A – Top	32.00	1.50	-0.90	-0.20	0.13	
A1	1	B	32.00	0.00	-0.40	-0.10	-0.17	
A1	1	C-Mid	32.00	0.90	-1.20	-0.30	-0.20	
A1	1	D - Mid	32.00	-0.40	-0.10	-0.40	-0.30	heavy sheetflow
A1	1	E	32.00	-0.20	-0.30	-0.20	-0.23	
A1	1	F – Bottom	32.00	0.00	0.10	-0.20	-0.03	
A1	2	A – Top	32.00	0.20	-0.30	-0.10	-0.07	
A1	2	B	32.00	0.00	1.60	-0.40	0.40	
A1	2	C-Mid	32.00	0.80	-0.30	-0.30	0.07	
A1	2	D - Mid	32.00	0.00	0.00	-0.20	-0.07	
A1	2	E	32.00	0.00	0.60	0.10	0.23	
A1	2	F – Bottom	32.00	0.40	1.10	-0.20	0.43	
A1	3	A – Top	32.00	0.00	1.50	-1.40	0.03	
A1	3	B	32.00	0.10	1.70	-0.60	0.40	9-29-01 pedestal – sheetflow
A1	3	C-Mid	32.00	0.00	-0.30	0.10	-0.07	
A1	3	D - Mid	32.00	0.00	0.70	0.40	0.37	
A1	3	E	32.00	0.30	-0.90	-0.10	-0.23	
A1	3	F – Bottom	32.00	-0.10	-0.10	4.95	1.58	
A1	4	A – Top	32.00	0.00	0.40	-0.10	0.10	
A1	4	B	32.00	1.30	-0.80	0.00	0.17	Sheetflow
A1	4	C-Mid	32.00	0.00	0.20	0.50	0.23	
A1	4	D - Mid	32.00	0.00	-0.10	-0.30	-0.13	
A1	4	E	32.00	0.00	0.40	-0.30	0.03	
A1	4	F – Bottom	32.00	1.80	0.50	-0.50	0.60	
A1	5	A – Top	32.00	-0.90	-0.20	0.30	-0.27	
A1	5	B	32.00	0.00	-0.60	-0.15	-0.25	
A1	5	C-Mid	32.00	-0.30	0.10	-0.30	-0.17	
A1	5	D - Mid	32.00	0.00	-0.10	-0.20	-0.10	
A1	5	E	32.00	0.10	-0.20	0.50	0.13	

Plot Code:	Horizontal Position (Column)	Vertical Position (Row)	Slope in degrees	May-01 to Sept-01 (cm)	Sept-01 to Jan-02 (cm)	Jan-02 to Aug-02 (cm)	Mean Change (May-01 to Aug-02) (cm)	Notes
A1	5	F – Bottom	32.00	-0.30	0.10	-0.20	-0.13	
A1	6	A – Top	32.00	-0.20	-0.30	0.10	-0.13	
A1	6	B	32.00	0.00	0.60	-0.60	0.00	
A1	6	C-Mid	32.00	0.00	0.70	-0.40	0.10	Sheetflow
A1	6	D - Mid	32.00	0.00	0.70	-0.60	0.03	
A1	6	E	32.00	0.00	0.50	-0.10	0.13	
A1	6	F – Bottom	32.00	-0.20	0.70	0.00	0.17	
A2	1	A – Top	11.00	0.00	0.10	-0.10	0.00	AJ canopy
A2	1	B	11.00	0.00	0.30	0.00	0.10	
A2	1	C-Mid	11.00	0.00	0.00	-0.10	-0.03	
A2	1	D - Mid	11.00	0.00	0.10	-0.10	0.00	
A2	1	E	11.00	0.00	0.10	-0.10	0.00	AJ canopy
A2	1	F – Bottom	11.00	0.00	0.00	-0.10	-0.03	
A2	2	A - Top	11.00	0.00	0.00	0.10	0.03	9-29-01 (pedestal)
A2	2	B	11.00	1.10	0.10	-0.45	0.25	
A2	2	C-Mid	11.00	0.00	0.40	-0.40	0.00	
A2	2	D - Mid	11.00	0.00	0.40	-0.20	0.07	
A2	2	E	11.00	0.00	0.10	0.10	0.07	
A2	2	F – Bottom	11.00	-0.30	1.60	-0.10	0.40	
A2	3	A – Top	11.00	0.00	0.00	0.00	0.00	
A2	3	B	11.00	0.00	-0.30	-0.20	-0.17	
A2	3	C-Mid	11.00	0.00	0.40	-0.40	0.00	
A2	3	D - Mid	11.00	0.00	0.30	-0.10	0.07	
A2	3	E	11.00	0.30	0.20	-0.10	0.13	
A2	3	F – Bottom	11.00	0.00	0.20	-0.20	0.00	
A2	4	A – Top	11.00	0.00	0.50	-0.20	0.10	
A2	4	B	11.00	0.00	0.50	-0.20	0.10	
A2	4	C-Mid	11.00	0.00	0.60	-0.20	0.13	
A2	4	D - Mid	11.00	0.00	0.36	-0.56	-0.07	
A2	4	E	11.00	0.00	0.20	-0.20	0.00	
A2	4	F – Bottom	11.00	0.00	0.80	-0.30	0.17	
A2	5	A – Top	11.00	0.00	0.40	-0.10	0.10	
A2	5	B	11.00	0.00	0.50	-0.10	0.13	

Plot Code:	Horizontal Position (Column)	Vertical Position (Row)	Slope in degrees	May-01 to Sept-01 (cm)	Sept-01 to Jan-02 (cm)	Jan-02 to Aug-02 (cm)	Mean Change (May-01 to Aug-02) (cm)	Notes
A2	5	C-Mid	11.00	0.00	0.20	0.00	0.07	
A2	5	D - Mid	11.00	0.00	0.50	0.00	0.17	
A2	5	E	11.00	0.00	0.40	-0.30	0.03	9-29-01 (pedestal)
A2	5	F – Bottom	11.00	0.00	0.00	-0.30	-0.10	
A2	6	A – Top	11.00	0.00	0.00	0.00	0.00	
A2	6	B	11.00	0.00	1.00	-0.30	0.23	
A2	6	C-Mid	11.00	0.00	0.30	0.00	0.10	
A2	6	D - Mid	11.00	0.00	-0.30	-0.30	-0.20	AJ canopy
A2	6	E	11.00	0.00	0.00	0.20	0.07	
A2	6	F – Bottom	11.00	0.00	0.00	0.10	0.03	
A3	1	A – Top	20.00	0.10	1.00	-0.10	0.33	
A3	1	B	20.00	0.50	0.00	0.20	0.23	
A3	1	C-Mid	20.00	0.20	0.00	-0.10	0.03	AJ canopy
A3	1	D - Mid	20.00	0.20	0.20	1.90	0.77	AJ canopy
A3	1	E	20.00	0.60	-0.40	0.00	0.07	
A3	1	F – Bottom	20.00	-0.20	0.70	-0.60	-0.03	
A3	2	A – Top	20.00	0.50	0.30	0.10	0.30	
A3	2	B	20.00	0.70	-0.40	0.10	0.13	
A3	2	C-Mid	20.00	-0.10	-0.10	-0.10	-0.10	AJ canopy
A3	2	D - Mid	20.00	-0.10	0.00	-0.10	-0.07	
A3	2	E	20.00	0.30	3.00	0.00	1.10	
A3	2	F – Bottom	20.00	0.00	-0.10	0.20	0.03	AJ canopy
A3	3	A – Top	20.00	0.15	-0.40	0.50	0.08	
A3	3	B	20.00	0.40	0.20	0.00	0.20	
A3	3	C-Mid	20.00	0.10	-0.60	0.50	0.00	AJ canopy
A3	3	D - Mid	20.00	-0.10	0.70	-0.70	-0.03	
A3	3	E	20.00	0.10	-0.40	-0.20	-0.17	
A3	3	F – Bottom	20.00	0.30	3.50	-3.80	0.00	AJ canopy
A3	4	A – Top	20.00	-0.10	0.00	0.00	-0.03	
A3	4	B	20.00	-0.60	-0.20	0.10	-0.23	
A3	4	C-Mid	20.00	-0.20	0.50	-0.30	0.00	small heavy sheetflow
A3	4	D - Mid	20.00	-0.10	0.10	0.00	0.00	
A3	4	E	20.00	0.60	-0.60	0.20	0.07	AJ canopy

Plot Code:	Horizontal Position (Column)	Vertical Position (Row)	Slope in degrees	May-01 to Sept-01 (cm)	Sept-01 to Jan-02 (cm)	Jan-02 to Aug-02 (cm)	Mean Change (May-01 to Aug-02) (cm)	Notes
A3	4	F – Bottom	20.00	-0.70	0.10	-0.20	-0.27	
A3	5	A – Top	20.00	0.50	-0.35	0.25	0.13	AJ canopy
A3	5	B	20.00	2.30	-0.85	-0.25	0.40	AJ canopy
A3	5	C-Mid	20.00	0.50	0.50	-0.10	0.30	
A3	5	D - Mid	20.00	-0.10	-0.10	-0.10	-0.10	
A3	5	E	20.00	0.20	0.00	0.00	0.07	
A3	5	F – Bottom	20.00	-0.30	0.10	0.00	-0.07	
A3	6	A – Top	20.00	0.10	-0.60	0.20	-0.10	
A3	6	B	20.00	0.00	-0.40	0.10	-0.10	AJ canopy
A3	6	C-Mid	20.00	0.00	0.40	-0.10	0.10	
A3	6	D - Mid	20.00	0.00	0.10	-0.10	0.00	
A3	6	E	20.00	0.20	0.30	-0.30	0.07	AJ canopy
A3	6	F – Bottom	20.00	-0.20	-0.10	-0.10	-0.13	
				-21.10	47.25	-18.65	2.50	

Appendix D. Soil Sampling Results

ID	Slope Position	Position Along Longitudinal Profile of Tributaries	Elevation (ft)	Lithologic Substrate	Total Carbon %	Calcite %	Dolomite %	$CaCO_3$ EQ %	C from carbonates %	Organic Carbon %
A1 - Top 1	top of slope	lower basin	1090	calcareous marl	7.12	3.2	0.7	4.1	0.45	7.14
A1 - Top 2	top of slope	lower basin	1090	calcareous marl	8.16	2.8	1.4	4.3	0.48	8.25
A1 - Mid 1	mid-slope	lower basin	1090	calcareous marl	6.33	6.7	1.3	8.0	0.90	5.83
A1 - Mid 2	mid-slope	lower basin	1090	calcareous marl	6.59	8.0	1.8	9.9	1.13	5.80
A1 - Bottom 1	base of slope	lower basin	1090	calcareous marl	8.27	16.5	1.0	17.6	2.00	6.64
A1 - Bottom 2	base of slope	lower basin	1090	calcareous marl	8.06	12.8	2.2	15.2	1.71	6.77
A2 - Top 1	top of slope	mid-basin	1110	limestone	3.02	0.0	0.0	0.0	0.00	3.23
A2 - Top 2	top of slope	mid-basin	1110	limestone	2.74	0.0	0.0	0.0	0.00	2.95
A2 - Mid 1	mid-slope	mid-basin	1110	limestone	4.25	4.3	0.9	5.2	0.59	3.91
A2 - Mid 2	mid-slope	mid-basin	1110	limestone	3.95	3.2	0.7	4.0	0.46	3.71
A2 - Bottom 1	base of slope	mid-basin	1110	limestone	4.63	0.0	0.0	0.0	0.00	4.96
A2 - Bottom 2	base of slope	mid-basin	1110	limestone	4.60	0.9	0.5	1.4	0.15	4.79
A3 - Top 1	top of slope	upper basin	1240	caliche	13.60	33.4	2.4	36.0	4.09	10.05
A3 - Top 2	top of slope	upper basin	1240	caliche	13.57	32.3	1.7	34.1	3.87	10.27
A3 - Mid 1	mid-slope	upper basin	1240	caliche	10.85	54.4	1.2	55.8	6.48	4.51

ID	Slope Position	Position Along Longitudinal Profile of Tributaries	Elevation (ft)	Lithologic Substrate	Total Carbon %	Calcite %	Dolomite %	$CaCO_3$ EQ %	C from carbonates %	Organic Carbon %
A3 - Mid 2	mid-slope	upper basin	1240	caliche	11.04	56.6	0.4	57.0	6.65	4.52
A3 - Bottom 1	base of slope	upper basin	1240	caliche	10.21	76.7	1.7	78.5	9.34	0.88
A3 - Bottom 2	base of slope	upper basin	1240	calcareous marl	10.22	74.8	1.3	76.2	9.06	1.17
B1 - Top 1	top of slope	lower basin	1090	calcareous marl	8.11	10.6	1.7	12.4	1.40	7.16
B1 - Top 2	top of slope	lower basin	1090	calcareous marl	8.20	10.5	1.8	12.5	1.39	7.33
B1 - Mid 1	mid-slope	lower basin	1090	calcareous marl	10.21	5.4	1.8	7.4	0.82	10.02
B1 - Mid 2	mid-slope	lower basin	1090	calcareous marl	10.94	7.6	1.7	9.4	1.06	10.54
B1 - Bottom 1	base of slope	lower basin	1090	calcareous marl	8.48	20.1	2.6	23.0	2.70	6.09
B1 - Bottom 2	base of slope	lower basin	1090	calcareous marl	8.08	18.2	2.9	21.2	2.42	5.98
B2 - Top 1	top of slope	mid-basin	1110	limestone	3.62	0.0	0.0	0.0	0.00	3.81
B2 - Top 2	top of slope	mid-basin	1110	limestone	3.01	0.0	0.0	0.0	0.00	3.21
B2 - Mid 1	mid-slope	Mid-basin	1110	limestone	2.92	0.0	0.0	0.0	0.00	3.07
B2 - Mid 2	mid-slope	Mid-basin	1110	limestone	2.49	0.0	0.0	0.0	0.00	2.62
B2 - Bottom 1	base of slope	Mid-basin	1110	limestone	2.60	0.0	0.0	0.0	0.00	2.77
B2 - Bottom 2	base of slope	Mid-basin	1110	limestone	2.53	0.0	0.0	0.0	0.00	2.66

ID	Slope Position	Position Along Longitudinal Profile of Tributaries	Elevation (ft)	Lithologic Substrate	Total Carbon %	Calcite %	Dolomite %	$CaCO_3$ EQ %	C from carbonates %	Organic Carbon %
B3 - Top 1	top of slope	upper basin	1240	caliche	10.29	31.3	3.7	35.4	4.09	6.43
B3 - Top 2	top of slope	upper basin	1240	caliche	10.52	38.7	3.0	41.9	4.87	5.84
B3 - Mid 1	mid-slope	upper basin	1240	caliche	10.28	48.6	3.6	52.5	6.10	4.31
B3 - Mid 2	mid-slope	upper basin	1240	caliche	10.26	49.6	3.2	53.1	6.15	4.25
B3 - Bottom 1	base of slope	upper basin	1240	caliche	10.24	57.1	1.6	58.8	6.89	3.43
B3 - Bottom 2	base of slope	upper basin	1240	caliche	10.38	57.0	3.0	60.2	7.03	3.45

Appendix E. Particle Size Distribution Data

Particle Size Distribution Data

Plot ID – Slope Position	VCSAND	CSAND	MSAND	FSAND	VFSAND	TSAND	FSILT	TSILT	FCLAY	TCLAY	Texture	Coarse Fragments
A1 - Top 1	1.1	1.3	2.1	4.0	2.8	11.3	15.3	23.9	42.2	64.8	C	24
A1 - Top 2	1.2	1.8	2.0	3.4	2.7	11.1	16.7	23.4	0.0	65.5	C	8
A1 - Mid 1	1.5	1.8	2.1	4.4	4.0	13.8	17.1	26.1	34.5	60.1	C	21
A1 - Mid 2	3.1	2.1	1.9	5.5	4.1	16.7	18.5	26.6	31.9	56.7	C	21
A1 - Bottom 1	4.1	2.9	3.3	5.8	4.9	21.0	16.7	25.7	30.7	53.3	C	24
A1 - Bottom 2	3.9	3.2	3.3	5.5	4.7	20.6	17.9	25.3	30.5	54.1	C	35
A2 - Top 1	0.1	0.3	0.5	1.7	6.5	9.1	13.4	19.9	44.6	71.0	C	1
A2 - Top 2	0.0	0.6	1.8	3.7	7.0	13.1	188.4	24.4	29.3	62.5	C	n/a
A2 - Mid 1	1.2	2.6	3.8	3.8	7.3	17.3	26.0	29.9	11.6	52.8	C	2
A2 - Mid 2	0.4	3.0	2.6	5.0	7.6	18.6	25.7	32.2	10.5	49.2	C	4
A2 - Bottom 1	0.2	0.5	0.8	2.0	7.0	10.5	17.8	22.3	40.0	67.2	C	7
A2 - Bottom 2	0.2	0.9	1.1	2.5	7.3	12.0	20.1	22.2	17.8	65.8	C	1
A3 - Top 1	3.2	3.0	2.6	2.4	7.7	18.9	27.7	45.1	11.0	36.0	SiCL	83
A3 - Top 2	4.0	3.3	2.6	2.4	6.9	19.2	30.5	43.8	10.6	37.0	SiCL	72
A3 - Mid 1	2.5	2.7	2.6	4.2	8.7	20.7	32.3	42.7	14.2	36.6	CL	43
A3 - Mid 2	2.9	2.2	2.3	4.0	9.3	20.7	32.4	44.1	13.2	35.2	CL	46
A3 - Bottom 1	1.6	1.1	0.9	1.7	7.5	12.8	50.9	43.4	6.4	23.8	SiL	0
A3 - Bottom 2	0.7	0.8	1.1	2.4	8.8	13.8	48.0	61.3	6.2	24.9	SiL	1
B1 - Top 1	1.2	1.5	2.0	3.0	4.1	11.7	23.4	30.8	33.8	57.5	C	18
B1 - Top 2	1.1	1.6	2.3	3.3	4.2	12.6	23.1	30.0	28.7	57.4	C	17
B1 - Mid 1	1.2	1.6	3.2	4.5	3.9	14.6	22.6	31.7	16.1	53.7	C	13
B1 - Mid 2	1.4	2.1	3.1	4.5	4.3	15.8	20.4	30.5	23.7	53.7	C	17
B1 - Bottom 1	1.8	4.1	4.6	7.3	7.4	27.6	17.9	23.7	32.3	48.7	C	25
B1 - Bottom 2	4.2	3.5	4.3	6.3	7.0	24.6	20.3	28.8	23.9	46.6	C	27
B2 - Top 1	3.5	0.5	1.5	5.5	13.0	20.6	17.8	23.9	42.0	55.5	C	0
B2 - Top 2	0.1	0.4	1.2	4.7	11.7	18.1	16.8	23.1	42.4	58.8	C	1

Plot ID – Slope Position	VCSAND	CSAND	MSAND	FSAND	VFSAND	TSAND	FSILT	TSILT	FCLAY	TCLAY	Texture	Coarse Fragments
B2 - Mid 1	0.1	1.5	2.6	7.4	11.5	23.1	20.3	29.3	15.8	47.6	C	0
B2 - Mid 2	0.0	1.4	2.1	6.0	10.1	19.6	20.1	29.9	19.7	51.5	C	n/a
B2 - Bottom 1	0.0	1.0	1.9	5.1	9.6	17.6	23.1	31.2	15.7	51.2	C	n/a
B2 - Bottom 2	0.1	0.9	2.9	5.2	9.3	17.4	21.7	29.9	16.2	52.7	C	n/a
B3 - Top 1	2.3	2.4	2.5	3.7	7.5	18.4	27.7	42.5	17.0	39.1	SiCL	45
B3 - Top 2	3.1	2.5	2.7	3.1	10.3	21.7	28.9	44.1	15.3	34.2	CL	46
B3 - Mid 1	2.4	2.5	2.5	2.3	8.8	18.5	33.6	44.6	14.4	36.9	SiLCL	38
B3 - Mid 2	2.6	2.4	2.1	2.0	9.0	18.1	33.1	44.8	13.2	37.1	SiLCL	28
B3 - Bottom 1	3.9	3.3	3.6	3.9	9.5	24.2	32.8	45.0	8.6	30.8	CL	60
B3 - Bottom 2	3.4	3.1	3.4	5.1	8.7	23.7	33.4	45.9	10.0	30.4	CL	66

Appendix F. Soil Sample Characterization Worksheets

Test Plot A1 (bottom of Basin A) Soil Sample Classification Worksheet - 8/25/2001

	Top Depth (cm)	Slope (Degrees)	Moisture (wet, moist, dry)	Structure (type)	Primary Color (code from color book)	Second Color (code from color book)	Consistence (loose, friable, firm, extremely firm)	Texture (name)	Rocks (none, few, many)	Roots (none, few many)	Carb-onnate (none, slight, strong)	Terrace/ Basin Position	Profile Position
Top1	10	32	moist	Blocky	7.5R:2/2 very dark brown	7.5R:8/2 very pale brown	friable	silty clay loam	Few	few	none	riser, baseslope colluvium	Backslope
Top2	10	32	moist	Blocky	7.5R:2/2 very dark brown	7.5R:8/2 very pale brown	friable	silty clay loam	Few	few	none	riser, baseslope colluvium	Backslope
Mid1	10	23	moist	Blocky	7.5R:2/2 very dark brown	7.5R:8/2 very pale brown	friable	silty clay loam	Few	few	none	riser, baseslope colluvium	Footslope
Mid2	10	23	moist	Blocky	7.5R:2/2 very dark brown	7.5R:8/2 very pale brown	friable	silty clay loam	Few	few	none	riser, baseslope colluvium	Footslope
Bottom 1	10	21	moist	Blocky	7.5R:2/2 very dark brown	7.5R:8/2 very pale brown	friable	silty clay loam	Few	few	none	riser, baseslope colluvium	Toeslope
Bottom 2	10	21	moist	Blocky	7.5R:2/2 very dark brown	7.5R:8/2 very pale brown	friable	silty clay loam	Few	few	none	riser, baseslope colluvium	Toeslope

Plot A1 Notes: Soil samples were taken along slope. Sample sites were generally less sloping than other areas on the hillslope because flaggy limestone tended to form random slope angles and sediment tends to "pond" between the limestone fragments. Slope shape: convex linear; Geomorphology: baseslope colluvium, bottom of basin; well drained; tree cover: Ashe juniper and Texas oak greater that 60% canopy cover with sparse grass clumps; Sed Clastics: dolomite; Topography: steep wavy.

Test Plot A2 (Basin A – Middle) Soil Sample Classification Worksheet - 8/25/2001

	Top Depth (cm)	**Slope (Degrees)**	**Moisture (wet, moist, dry)**	**Structure (type)**	**Primary Color (code from color book)**	**Second Color (code from color book)**	**Consistence (loose, friable, firm, extremely firm)**	**Texture (name)**	**Rocks (none, few, many)**	**Roots (none, few many)**	**Carb-onnate (none, slight, strong)**	**Terrace/ Basin Position**	**Profile Position**
Top1	10	12	moist	blocky	7.5R:4/4 reddish dark brown	7.5R:2/2 very dark brown	Friable	silty clay	none	few	none	riser sideslope	backslope
Top2	10	12	moist	blocky	7.5R:4/4 reddish dark brown	7.5R:2/2 very dark brown	Friable	silty clay	none	few	none	riser sideslope	backslope
Mid1	10	6	moist	blocky	7.5R:2/2 very dark brown		Friable	silty clay	few	few	none	riser sideslope	Footslope
Mid2	10	6	moist	blocky	7.5R:2/2 very dark brown		Friable	silty clay	few	few	none	riser sideslope	Footslope
Bottom 1	10	14	moist	blocky	7.5R:2/2 very dark brown		Friable	silty clay	few	few	none	riser sideslope	Toeslope
Bottom 2	10	14	moist	Blocky	7.5R:2/2 very dark brown		Friable	silty clay	few	few	none	riser sideslope	Toeslope

Plot A2 Notes: Soil samples were taken along slope. Sample sites were generally less sloping than other areas on the hillslope because flaggy limestone tended to form random slope angles and sediment tends to "pond" between the limestone fragments. Method: Near Surface due to shallow depth to bedrock.

Test Plot A3 (Top of Basin A) Soil Sample Classification Worksheet - 8/25/2001

	Top Depth (cm)	Slope (Degrees)	Moisture (wet, moist, dry)	Structure (type)	Primary Color (code from color book)	Second Color (code from color book)	Consistence (loose, friable, firm, extremely firm)	Texture (name)	Rocks (none, few, many)	Roots (none, few many)	Carb-onnate (none, slight, strong)	Terrace/ Basin Position	Profile Position
Top1	10	22	moist	Blocky	7.5R:2/2 very dark brown	firm	silty clay	fine silty clay	many	slight	few	riser/ headslope	backslope
Top2	10	22	moist	Blocky	7.5R:2/2 very dark brown	firm	silty clay	fine silty clay	many	slight	few	riser/ headslope	backslope
Mid1	10	17	moist	Blocky	7.5R:2/2 very dark brown	firm	silty clay	fine silty clay	many	slight	few	riser/ headslope	footslope
Mid2	10	17	moist	Blocky	7.5R:2/2 very dark brown	firm	silty clay	fine silty clay	many	slight	few	riser/ headslope	footslope
Bottom 1	10	16	moist	Platy	7.5R:6/3 pale brown	friable	silty clay	fine silty clay loam	few	slight	few	riser/ headslope	toeslope
Bottom 2	10	16	moist	Platy	7.5R:6/3 pale brown	friable	silty clay	fine silty clay loam	few	slight	few	riser/ headslope	toeslope

NOTES: Soil samples were taken along slope. Sample sites were generally less sloping than other areas on the hillslope because flaggy limestone tended to form random slope angles and sediment tends to "pond" between the limestone fragments. Foraminifera lens at base of slope marks a marly layer, unlike Plot B3 that has limestone at its base with the foraminifera layer about 5 feet downslope. Slope Shape: convex; Geomorphology: Noseslope - head of basin; Drainage: well drained; Grass clumps are less than 10% and Ashe juniper shrubs ~50%; Sed clastics: LMS, Dolomite, and Marl; Tope: sloping wavy.

Test Plot B1 (bottom of Basin B Soil Sample Classification Worksheet - 8/25/2001

	Top Depth (cm)	Slope (Degrees)	Moisture (wet, moist, dry)	Structure (type)	Primary Color (code from color book)	Second Color (code from color book)	Consistence (loose, friable, firm, extremely firm)	Texture (name)	Rocks (none, few, many)	Roots (none, few many)	Carb-onnate (none, slight, strong)	Terrace/ Basin Position	Profile Position
Top1	10	15	moist	blocky (subangular)	7.5R:2/1 black		friable	silty clay loam	many	few	none	riser baseslope	backslope
Top2	10	15	moist	blocky (subangular)	7.5R:2/1 black		friable	silty clay loam	many	few	none	riser baseslope	backslope
Mid1	10	30	moist	blocky (subangular)	7.5R:2/1 black	7.5R:8/1 very pale brown	friable	silty clay loam	many	few	none	riser baseslope	footslope
Mid2	10	30	moist	blocky (subangular)	7.5R:2/1 black	7.5R:8/1 very pale brown	friable	silty clay loam	many	few	none	riser baseslope	footslope
Bottom 1	10	29	moist	blocky (subangular)	7.5R:2/1 very dark brown	7.5R:8/1 very pale brown	friable	silty clay loam	many	many	none	riser baseslope	toeslope
Bottom 2	10	29	moist	blocky (subangular)	7.5R:2/1 very dark brown	7.5R:8/1 very pale brown	friable	silty clay loam	many	many	none	riser baseslope	toeslope

Plot B1 Notes: Soil samples were taken along slope. Sample sites were generally less sloping than other areas on the hillslope because flaggy limestone tended to form random slope angles and sediment tends to "pond" between the limestone fragments. Slope shape: convex/linear; Geomorphology: baseslope (colluvium) - bottom of basin; Drainage: well drained with flooding rare; tree cover: mature Texas oak and Ashe juniper (60% canopy cover); sparse grass clumps; Sed clastics: LMS, dolomite; Topography: Steep and wavy. Carbonate fragments fizz slightly in acid. Method: Near Surface due to shallow depth to bedrock.

Test Plot B2 (Basin B –Middle) Soil Sample Classification Worksheet - 8/25/2001

	Top Depth (cm)	Slope (Degrees)	Moisture (wet, moist, dry)	Structure (type)	Primary Color (code from color book)	Second Color (code from color book)	Consistence (loose, friable, firm, extremely firm)	Texture (name)	Rocks (none, few, many)	Roots (none, few many)	Carb-onate (none, slight, strong)	Terrace/ Basin Position	Profile Position
Top2	10	8	moist	Blocky	7.5R:2/2 very dark brown		friable	silty clay	few with cobbles	many	none	riser/ sideslope	backslope
Mid1	10	8	moist	Blocky	7.5R:2/2 very dark brown		friable	silty clay	few with cobbles	many	none	riser/ sideslope	footslope
Mid2	10	10	moist	Blocky	7.5R:3/3 dark reddish brown		friable	silty clay	few with cobbles	few to many	none	riser/ sideslope	footslope
Bottom 1	10	10	moist	Blocky	7.5R:3/3 dark reddish brown		friable	silty clay	few with cobbles	few to many	none	riser/ sideslope	toeslope
Bottom 2	10	11	moist	Blocky	7.5R:2/2 very dark brown	7.5R:3/3 dark reddish brown	friable	silty clay	few with cobbles	many	none	riser/ sideslope	toeslope

Plot B2 Notes: Soil samples were taken along slope. Sample sites were generally less sloping than other areas on the hillslope because flaggy limestone tended to form random slope angles and sediment tends to "pond" between the limestone fragments. Slope shape: linear/linear; Geomorphology: sideslope - midbasin; Drainage: well drained with flooding rare; Tree cover: shrub to 15-foot tall Ashe juniper (15% canopy cover); scattered grass clumps; Sed clastics: dolomite Topography: sloping and flaggy. Method: Near Surface due to shallow depth to bedrock. Other Site Characteristics: Hillslope, Mid Basin, near weir, bedrock at ~10 cm.

Test Plot B3 (Basin B –Middle) Soil Sample Classification Worksheet - 8/25/2001

	Top Depth (cm)	Slope (Degrees)	Moisture (wet, moist, dry)	Structure (type)	Primary Color (code from color book)	Second Color (code from color book)	Consistence (loose, friable, firm, extremely firm)	Texture (name)	Rocks (none, few, many)	Roots (none, few many)	Carb-onate (none, slight, strong)	Terrace/ Basin Position	Profile Position
Top2	10	15	slightly moist	blocky (subangular)	7.5R:2/2 very dark brown	7.5R:8/2 very pale brown	friable	silty clay loam	few	few	slight	riser/headslope	backslope
Mid1	10	15	slightly moist	blocky (subangular)	7.5R:2/2 very dark brown	7.5R:8/2 very pale brown	friable	silty clay	few	few	slight	riser/headslope	backslope
Mid2	10	20	slightly moist	blocky (subangular)	7.5R:2/2 very dark brown	7.5R:8/2 very pale brown	friable	silty clay	few	few	slight	riser/headslope	footslope
Bottom 1	10	20	slightly moist	blocky (subangular)	7.5R:2/2 very dark brown	7.5R:8/2 very pale brown	friable	silty clay	few	few	slight	riser/headslope	footslope
Bottom 2	10	28	slightly moist	blocky (subangular)	7.5R:2/2 very dark brown	7.5R:8/2 very pale brown	friable	silty clay	many (fine to sand)	many	slight	riser/headslope	toeslope

Plot B3 Notes: Soil samples were taken along slope. Sample sites were generally less sloping than other areas on the hillslope because flaggy limestone tended to form random slope angles and sediment tends to "pond" between the limestone fragments. Slope shape: convex/concave; Geomorphology: noseslope at head of drainage basin; Drainage: well drained with no flooding; tree cover: shrubs to 15' tall Ashe juniper (35% canopy cover); sparse grass clumps; Sed clastics: Limestone, dolomite, with interbedded marl that is reticulate to platy; Topography: wavy.

Appendix G. Orientations of Scanline Fracture Data (FR-2), Honey Creek Stream Cave Conduits, Other Karst Features and Fractures, and Streams

Table G.1. Scanline Fracture Orientations (FR-2)

Transect Number	Transect Distance (m)	Aperture (cm)	Bearing (Decl. 0)	Azimuth	Fracture Length (m)	Spacing (m)	Asperity (URC) (straight length/ actual length)
1	0.4	6	N-15 E	23.50	3.03	0.50	1.06
2	0.9	0.3	N-65 E	73.50	3.03	0.60	1.06
3	1.5	5.5	N-50 E	58.50	2.42	0.60	1.03
4	2.1	0.3	N-40 E	48.50	3.03	0.40	1.07
5	2.5	0.3	N-15 E	23.50	3.03	0.10	1.03
6	2.6	0.04	N-70 E	78.50	2.42	0.12	1.03
7	2.72	0.04	N-05 E	13.50	0.91	0.11	1.03
8	2.83	0.04	N-40 E	48.50	3.03	0.17	1.03
9	3	0.2	N-05 E	13.50	22.73	2.50	1.03
10	5.5	1.2	N-60 W	308.50	9.09	1.50	1.03
11	7	0.3	N-20 E	28.50	9.09	0.40	1.05
12	7.4	0.2	N-70W	298.50	3.03	0.13	1.03
13	7.53	0.3	N-40 W	328.50	1.52	0.82	1.01
14	8.35	0.04	N-25 E	33.50	2.12	1.45	1.05
15	9.8	0.2	N-32 E	40.50	1.21	0.10	1.02
16	9.9	1.1	N-65 E	73.50	1.52	0.70	1.03
17	10.6	0.3	N-60 E	68.50	4.55	0.77	1.01
18	11.37	0.3	N-25 E	33.50	1.21	0.03	1.03
19	11.4	0.1	N-25 E	33.50	0.30	0.02	1.03
20	11.42	0.2	N-20 E	28.50	0.91	0.09	1.03
21	11.51	0.05	N-65 E	73.50	0.15	0.04	1.03
22	11.55	0.5	N-65 E	73.50	1.21	0.15	1.03
23	11.7	6	N-30 E	38.50	2.12	0.80	1.01
24	12.5	3	E-W	98.50	6.06	1.10	1.03
25	13.6	0.9	N-0E	48.50	45.45	1.10	1.03
26	14.7	4	N-35 E	43.50	1.52	0.65	1.03
27	15.35	3	N-80 E	88.50	0.61	0.15	1.03
28	15.5	0.2	N-S	8.50	0.30	0.10	1.03
29	15.6	1	N-20 E	88.50	6.06	0.10	1.03
30	15.7	0.7	N-55 E	63.50	0.30	1.10	1.03
31	16.8	0.5	N-20 E	28.50	6.06	1.00	1.05

Transect Number	Transect Distance (m)	Aperture (cm)	Bearing (Decl. 0)	Azimuth	Fracture Length (m)	Spacing (m)	Asperity (URC) (straight length/ actual length)
32	17.8	1	N-35 E	43.50	9.09	0.30	1.03
33	18.1	1	N-20 W	348.50	9.09	0.40	1.03
34	18.5	0.3	N-55 W	313.50	1.52	0.10	1.03

Table G.2. Honey Creek Stream Cave Orientation Measurements

Name	Latitude	Longitude	Altitude (ft.)	Depth (ft.)	Width (ft	Corrected (Polar) Azimuth	Azimuth	Length (ft.)	Elevation (ft.
1	29.86154	-98.51033	1146	125.00	6.60	338.00	158	166	1021
2	29.86125	-98.51070	1146	125.00	6.60	42.00	222	48	1021
3	29.86092	-98.51092	1126	100.00	6.60	24.00	204	42	1026
4	29.86052	-98.51085	1126	100.00	6.60	346.00	166	45	1026
5	29.86028	-98.51061	1126	110.00	6.60	313.00	133	35	1016
6	29.85977	-98.51118	1126	110.00	6.60	38.00	218	79	1016
7	29.85491	-98.51551	1102	80.00	6.60	43.00	223	438	1022
8	29.85322	-98.51749	1102	80.00	6.60	39.00	219	268	1022
9	29.85257	-98.51920	1110	90.00	6.60	60.00	240	180	1020
10	29.85230	-98.51883	1110	93.00	6.60	304.00	124	47	1017
11	29.85198	-98.51879	1111	93.00	6.60	348.00	168	36	1018
12	29.85187	-98.51848	1111	93.00	6.60	286.00	106	32	1018
13	29.85149	-98.51830	1111	93.00	6.60	331.00	151	46	1018
14	29.85111	-98.51799	1111	93.00	6.60	318.00	138	52	1018
15	29.85081	-98.51775	1111	93.00	6.60	319.00	139	41	1018
16	29.85047	-98.51752	1112	94.00	6.60	323.00	143	43	1018
17	29.85033	-98.51721	1112	94.00	6.60	291.00	111	34	1018
18	29.85009	-98.51721	1112	94.00	6.60	354.00	174	27	1018
19	29.84998	-98.51696	1112	94.00	6.60	291.00	111	27	1018
20	29.84971	-98.51696	1112	95.00	6.60	354.00	174	30	1017
21	29.84952	-98.51662	1118	104.00	6.60	297.00	117	39	1014
22	29.84936	-98.51628	1112	105.00	6.60	292.00	112	37	1007
23	29.84898	-98.51594	1117	105.00	6.60	316.00	136	54	1012
24	29.84880	-98.51547	1122	105.00	6.60	288.00	108	50	1017
25	29.84828	-98.51482	1147	130.00	6.60	306.00	126	85	1017

Name	Latitude	Longitude	Altitude (ft.)	Depth (ft.)	Width (ft	Corrected (Polar) Azimuth	Azimuth	Length (ft.)	Elevation (ft.
26	29.84659	-98.51705	1147	130.00	6.60	43.00	223	286	1017
27	29.84586	-98.51653	1147	130.00	6.60	43.00	223	489	1017
28	29.84297	-98.52035	1147	130.00	6.60	311.00	131	304	1017
29	29.84497	-98.52249	1147	130.00	6.60	311.00	311	304	1017
30	29.84586	-98.51653	1147	130.00	6.60	43.00	43	489	1017
31	29.84729	-98.51451	1147	130.00	6.60	314.00	134	104	1017
32	29.84801	-98.51519	1147	130.00	6.60	314.00	314	104	1017
33	29.84912	-98.50907	1167	150.00	6.60	49.00	229	315	1017
34	29.84810	-98.51025	1167	150.00	6.60	39.00	219	161	1017
35	29.84691	-98.50783	1127	110.00	6.60	328.00	148	274	1017
36	29.84745	-98.50680	1127	110.00	6.60	321	321	61	1017
37	29.84640	-98.50742	1127	110.00	6.60	48.00	228	114	1017
38	29.86371	-98.47523	1127	110.00	6.60	11	11	120	1017
39	29.86324	-98.47521	1127	110.00	6.60	10	10	39	1017
40	29.86371	-98.47486	1127	110.00	6.60	27	27	62	1017
41	29.86318	-98.47432	1127	99.00	6.60	312.00	132	78	1028
42	29.84537	-98.50779	1127	100.00	6.60	11.00	191	120	1027
43	29.84467	-98.50848	1127	100.00	6.60	34.00	214	103	1027
44	29.84589	-98.50630	1127	110.00	6.60	54.00	234	59	1017
45	29.84551	-98.50612	1127	110.00	6.60	331.00	151	46	1017
46	29.84421	-98.50444	1117	100.00	6.60	325.00	145	196	1017
47	29.84381	-98.50534	1126	109.00	6.60	57.00	237	98	1017
48	29.84322	-98.50503	1117	100.00	6.60	329.00	149	72	1017
49	29.84246	-98.50332	1117	100.00	6.60	324.00	144	140	1017
50	29.84327	-98.50143	1117	100.00	6.60	57	57	204	1017
51	29.84308	-98.50130	1117	100.00	6.60	323.00	143	25	1017
52	29.84680	-98.49411	1042	25.00	6.60	53.00	53	628	1017

Name	Latitude	Longitude	Altitude (ft.)	Depth (ft.)	Width (ft	Corrected (Polar) Azimuth	Azimuth	Length (ft.)	Elevation (ft.
53	29.84572	-98.49737	1097	80.00	6.60	323	323	75	1017
54	29.84556	-98.49774	1097	80.00	6.60	323	323	75	1017
55	29.86398	-98.47709	1020	0.00	6.60	57.00	237	40	1020
56	29.86317	-98.47614	1020	0.00	6.60	306.00	126	119	1020
57	29.86325	-98.47541	1020	0.00	6.60	302.00	122	76	1020
58	29.86290	-98.47532	1020	0.00	6.60	284.00	104	85	1020
59	29.86247	-98.47461	1020	0.00	6.60	320.00	140	65	1020
60	29.86227	-98.47351	1127	110.00	6.60	286.00	106	65	1017
61	29.86306	-98.47397	1127	110.00	6.60	358.00	178	37	1017
62	29.86119	-98.47361	1127	110.00	6.60	0.00	180	62	1017
63	29.86175	-98.47357	1127	110.00	6.60	289.00	109	58	1017
64	29.86083	-98.47272	1135	110.00	6.60	292.00	112	95	1025
65	29.86054	-98.47210	1145	115.00	6.60	48	48	68	1030
66	29.86096	-98.47144	1145	115.00	6.60	319.00	139	79	1030
67	29.86058	-98.47113	1145	120.00	6.60	286.00	106	52	1025
68	29.86034	-98.47044	1145	120.00	6.60	321.00	141	72	1025
69	29.85999	-98.47018	1140	120.00	6.60	271.00	91	47	1020
70	29.85991	-98.46945	1140	120.00	6.60	318.00	138	71	1020
71	29.85956	-98.46916	1140	120.00	6.60	278.00	98	48	1020
72	29.85939	-98.46844	1140	120.00	6.60	337.00	157	72	1020
73	29.85886	-98.46825	1140	120.00	6.60	353.00	173	63	1020
74	29.85824	-98.46824	1170	150.00	6.60	340.00	160	68	1020
75	29.85632	-98.46767	1175	150.00	6.60	340.00	160	60	1025
76	29.85562	-98.46750	1181	155.00	6.60	342.00	162	80	1026
77	29.85517	-98.46678	1181	155.00	6.60	299.00	119	86	1026
78	29.85481	-98.46541	1181	155.00	6.60	23	23	53	1026
79	29.85440	-98.46568	1181	155.00	6.60	84	84	56	1026

Name	Latitude	Longitude	Altitude (ft.)	Depth (ft.)	Width (ft	Corrected (Polar) Azimuth	Azimuth	Length (ft.)	Elevation (ft.
80	29.85492	-98.46500	1181	155.00	6.60	67	67	42	1026
81	29.85463	-98.46466	1181	155.00	6.60	354	354	0	1026
82	29.85463	-98.46423	1181	155.00	6.60	84	84	42	1026
83	29.85785	-98.46783	1181	155.00	6.60	312.00	132	59	1026
84	29.85783	-98.46781	1160	155.00	6.60	309.00	129	3	1005
85	29.85740	-98.46750	1160	155.00	6.60	322.00	142	57	1005
86	29.85684	-98.46781	1160	155.00	6.60	20.00	200	69	1005
87	29.85440	-98.46626	1181	155.00	6.60	323.00	143	58	1026
88	29.85485	-98.46657	1181	155.00	6.60	325.00	145	41	1026
89	29.85429	-98.46417	1181	155.00	6.60	345.00	165	38	1026
90	29.86007	-98.47355	1176	21.00	3.00	300.00	300	20	1155

Table G.3. Orientation of Karst Features and Fractures at Honey Creek basin.

Name		Length (meters)	Feature Azimuth	Fracture Azimuth
C1	Trash Dump Cave	1.82	305	305
C10 (Arm Chair Cave)	Arm Chair Cave	6.97	70	70
C2	Flat Rock Cave	4.55	327	327
C3- 10	Preserve Cave	15.00	45	
C3- 11		70.00	350	
C3- 12		15.00	310	
C3- 13		25.00	330	
C3- 14		65.00	45	
C3- 15		8.00	330	
C3- 16		8.00	310	
C3- 2		15.00	9	
C3- 3		185.00	330	
C3- 4		65.00	9	
C3- 5		170.00	310	
C3- 6		65.00	65	
C3- 7		15.00	330	
C3- 8		45.00	310	
C3- 9		135.00	330	
C3-1		185.00	330	300
C4	Base of Tree Cave	1.52	330	330
C6-1	Double Cross Cave	16.06	300	300
C6-2		12.42	65	65
C7	Sour Maggie	8.18	280	280

Name		Length (meters)	Feature Azimuth	Fracture Azimuth
C8	Black Heart Cave	5.76	295	295
C9	Bone Head Cave	4.55	287	287
FR-1		2.30		300
KF-1		1.82	305	
KF-2		18.18	315	
KF-3		0.30	345	345
KF-4		0.45	32	32
KF-5		1.00	305	290
KF-6		0.40	40	40
KF-7		7.58		
KF-8		3.00		
KF-9		1.82	285	285
SH-1		22.73		
SH-2		2.27	296	296
SH-3		0.40	55	282
SH-4		6.06	338	338
SH-5		18.18	315	315
SH-6		3.03	80	80
SH-7		1.52	285	285
SH-8		6.06		
SH-9		6	285	285
SH-10		10		
C2	Rockwall Cave	3.03	62	
Saddle Sinks		6.36	332	
Ten-Meter Sink		4.00	285	
Two Hole Pit - 1		3.03		310
Two Hole Pit - 2				320

Table G.4. Orientation of Stream Segments of Honey Creek and its tributaries.

Segment Name	Leg Length (m)	Azimuth (in degrees)
C1	303	350
C2	303	70
C3	303	6
FR-2	606	310
FR-2	121	50
FR-2	606	320
FR-2	182	290
FR-2	455	350
FR-2	212	320
P	606	330
SP1	606	315
SP2	303	355
SP3	606	310
1	606	305
2	212	305
3	121	310
4	121	315
5	121	315
6	1818	50
7	606	330
8	606	25
9	606	45
10	152	25
11	606	45
12	1212	325
13	1818	50
14	606	320
15	909	50
16	909	320
17	909	320

Appendix H. Runoff, Precipitation, and Water Levels in Shallow and Deep Water Wells (USGS, 2001)

Day (#)	Deep Well Surface Elevation m	Shallow Well Surface Elevation - m	Deep Well Potent-iometric Surface Elevation - m	Shallow Well Potent-iometric Surface Elevation - m	Precip-itation - cm	Runoff-cm
15-Aug-01	370	369	329.69	365.95	0.15	0.61
16-Aug-01	370	369	329.92	365.95	0.05	0.61
17-Aug-01	370	369	330.14	365.92	0.00	0.61
18-Aug-01	370	369	330.36	365.95	0.00	0.61
19-Aug-01	370	369	330.59	365.91	0.00	0.61
20-Aug-01	370	369	330.81	365.94	0.00	0.61
21-Aug-01	370	369	331.04	365.97	0.02	0.61
22-Aug-01	370	369	331.27	365.98	0.00	0.61
23-Aug-01	370	369	331.49	366.00	0.00	0.61
24-Aug-01	370	369	331.72	365.99	0.00	0.00
25-Aug-01	370	369	331.94	366.02	0.00	0.00
26-Aug-01	370	369	332.16	366.01	0.52	0.00
27-Aug-01	370	369	332.53	365.92	0.26	0.00
28-Aug-01	370	369	332.77	365.92	0.04	0.00
29-Aug-01	370	369	332.99	365.90	0.50	28.96
30-Aug-01	370	369	333.02	365.92	0.69	42.06
31-Aug-01	370	369	330.73	365.96	0.88	71.32
1-Sep-01	370	369	330.91	365.96	0.00	45.72
2-Sep-01	370	369	331.13	365.98	0.00	0.00
3-Sep-01	370	369	331.37	366.00	0.03	0.00
4-Sep-01	370	369	331.60	365.96	0.02	0.00
5-Sep-01	370	369	331.84	365.93	0.27	0.00
6-Sep-01	370	369	332.07	365.95	0.01	0.00
7-Sep-01	370	369	332.27	366.01	0.00	0.00
8-Sep-01	370	369	332.49	366.01	0.00	0.00
9-Sep-01	370	369	332.74	365.97	0.06	0.00
10-Sep-01	370	369	332.98	365.91	0.00	0.00
11-Sep-01	370	369	333.20	365.96	0.00	0.00
12-Sep-01	370	369	333.42	365.99	0.00	0.00
13-Sep-01	370	369	333.64	366.00	0.00	0.00
14-Sep-01	370	369	333.87	366.02	0.00	0.00
15-Sep-01	370	369	334.09	366.02	0.00	0.00
16-Sep-01	370	369	334.32	365.99	0.00	0.00
17-Sep-01	370	369	334.55	366.01	0.00	0.00
18-Sep-01	370	369	332.80	366.01	0.00	0.00
19-Sep-01	370	369	334.75	366.07	0.00	0.00

Day (#)	Deep Well Surface Elevation m	Shallow Well Surface Elevation - m	Deep Well Potent-iometric Surface Elevation - m	Shallow Well Potent-iometric Surface Elevation - m	Precip-itation - cm	Runoff-cm
20-Sep-01	370	369	334.76	366.05	0.00	0.00
21-Sep-01	370	369	334.76	366.03	0.00	0.00
22-Sep-01	370	369	334.76	365.97	0.12	0.00
23-Sep-01	370	369	334.76	365.98	0.00	0.00
24-Sep-01	370	369	334.76	365.96	0.00	0.00
25-Sep-01	370	369	334.79	365.90	0.00	0.00
26-Sep-01	370	369	334.76	365.92	0.00	0.00
27-Sep-01	370	369	334.76	365.93	0.00	0.00
28-Sep-01	370	369	334.75	365.96	0.00	0.00
29-Sep-01	370	369	334.76	365.96	0.00	0.00
30-Sep-01	370	369	334.80	365.92	0.00	0.00

BIBLIOGRAPHY

Abbott, P.L., 1975, On the hydrology of the Edwards Limestone, south-central Texas: Journal of Hydrology, v. 24, no. 3/4, p. 251–269.

Abbott, P.L., 1979, Drainage-basin evolution and aquifer development in a karstic limestone terrain, south-central Texas, USA: Earth Surface Processes, v. 4.

Ashworth, J.B., 1983, Ground-water availability of the Lower Cretaceous Formations in the Hill Country of south-central Texas: Texas Department of Water Resources Report 273, 173 p.

Asquith, W.H. and Rousell, M.C., 2003 Atlas of Interoccurence Intervals for Selected Thresholds of Daily Precipitation in Texas, USGS, Water Resource Investigation Report 03-4281, US Dept. of Interior in cooperation with the Texas Department of Transportation.

Baker, V.R., with case studies by Kochel, R.C., Baker, V.R., Laity, J.E., and Howard, A.D., 1990, Spring sapping and valley network development, *in* Higgins, C.G. and Coates, D.R., Groundwater Geomorphology, The role of Subsurface Water in Earth Surface Processes and Landforms, Geological Society of America Special Paper 252, p. 235–265.

Barker, R.A. and Ardis, A.F., 1992, Configuration of the base of the Edwards-Trinity aquifer system and hydrogeology of the underlying pre-Cretaceous rocks, west central Texas: U.S. Geological Survey Water Resources Investigation Report 91–4071, 25 p.

Barker, R.A., and Ardis, A.F., 1996, Hydrogeologic framework of the Edwards-Trinity aquifer system, west-central Texas: U.S. Geological Survey Professional Paper 1421–B, 61 p. with plates.

Barker, R.A., Bush P.W., Baker, E.T., Jr. 1994, Geologic history and hydrogeologic setting of the Edwards-Trinity aquifer System, West-Central, Texas. U.S, Geological Survey, Water-Resources Investigations Report 94–4039.

Barnes, V.E., 1974, Revised 1983, Geologic atlas of Texas, San Antonio Sheet, Robert Hamilton Cuyler memorial edition: University of Texas-Austin, Bureau of Economic Geology, 1 sheet, scale 1:250,000.

Batte, C.D., 1984, *Soil survey of Comal and Hays Counties*, Texas. US Department of Agriculture, Soil Conservation Service, in cooperation with the Texas Agricultural Experiment Station.

Beven, K.J., 1989, Interflow in Morel-Seytoux H.J (ed.) Unsaturated flow in hydrologic modeling: theory and practice, Kluwer, Dordrecht, pp 191-219.

Boix-Fayos, C., Calvo-Cases, A., Imeson, A.C., and Soriano-Soto, M.D., 2001, Influence of soil properties on the aggregation of some Mediterranean soils and the use of aggregate size and stability as land degradation indicators, Catena Supplement, v. 44, issue 1, p. 47–67.

Brune, G., 1981, Springs of Texas, Volume 1: Branch-Smith Inc., Fort Worth, Texas, 566 p.

Carr, J.T., Jr., 1967, The climate and physiography of Texas; Texas Water Development Board Report 53, 27 p.

Collins, E.D., and Hovorka, S.D., 1997, Structure Map of the San Antonio Segment of the Edwards aquifer and Balcones Fault Zone, South-Central Texas: Structural Framework of a Major Limestone aquifer: Kinney, Uvalde, Medina, Bexar, Comal, and Hays Counties. Austin: University of Texas Bureau of Economic Geology, Miscellaneous Map No. 38.

Collins, E.D., 2000, Geologic Map of the New Braunfels, Texas 30 x 60 Minute Quadrangle, University of Texas Bureau of Economic Geology.

Compton, R.R., 1985, Geology in the field, John Wiley and Sons, New York.

Cooper, J.D., 1964, Geology of Spring Branch area, Comal and Kendall Counties, Texas: The University of Texas, Austin, Master's thesis, 183 p.

Dremanis, A., 1962, Quantitative gasometric determination of calcite and dolomite by using the Chittick apparatus, Journal of Sedimentary Petrology, v. 32, p. 520–529.

Dugas, W.A., Hicks, R.A. and Wright, P., 1998, Effect of removal of *Juniperus ashei* on evapotranspiration and runoff in the Seco Creek Watershed. Water Resources Research, v. 34, no 6, p. 1499–1506.

Dunne, T., 1977, Evaluation of erosion conditions and trends; in Kunkle, S.H., ed., Guidelines for watershed management, FAO Conservation Guide I, United Nations Food and Agriculture Organization, Rome, Italy, p. 53–83.

Dunne, T., 1990, Hydrology, mechanics, and geomorphic implications of erosion by subsurface flow, *in* Higgins, C.G. and Coates, D.R., Groundwater Geomorphology, The role of Subsurface Water in Earth Surface Processes and Landforms, Geological Society of America Special Paper 252, p. 1–28.

Dunne T. and Black, R., 1970, An experimental investigation of runoff production in permeable soils, Water Resources Res., v. 6, p. 478–490.

Dunne, T. and Leopold, L.B., 1978, Water in Environmental Planning, W.H. Freeman and Company, New York, 818 p.

Elliott, W.R., 1991, Texas Speleological Survey Report on the 60 longest and deepest caves, The Texas Caver, v. 36, no. 6, p. 122.

Ford, A.L., and Van Auken, O.W., 1982, The distribution of woody species in the Guadalupe River floodplain forest in the Edwards Plateau of Texas: *Southwestern Naturalist*, v. 27, p. 383–392.

Fabel, D., Henricksen, D. Finlayson, B.L., and Webb, J.A., 1998, Knickpoint recession in karst terrains: an example from the Buchan karst, southeaster Australia, Earth Processes and Landforms, v. 21, issue 5.

Fenneman, N.M. 1931, Physiography of western United States, New York, McGraw-hill, 534 pp.

Ferrill, D.A., Morris, A.P., 2003, Dilational normal faults: Journal of Structural Geology, vol. 25/2 p. 183-196.

Freeze, A.R., 1987, Modeling interrelationships between climate, hydrology, and hydrogeology and the development of slopes, *in* Anderson M.G., and Richards, K.S., eds., Slope Stability: New York, John Wiley & sons, p. 381–403.

Fyodorova, A. and Sasowsky, I. 1999, Silica dissolution and the development of sandstone caves: Geological Society of America Abstracts with Programs, v.31, no. 7, p. A51.

George, W.O., 1952, Geology and ground-water resources of Comal County, Texas: US Geological Survey Water-Supply Paper 1138, 126 p.

Gillieson, D., 1996, Caves: Processes, Development, Management, Blackwall Publishers, p. 143 – 165.

Gould, F.W., 1975, Texas Plants - A Checklist and Ecological Summary. College Station: Texas A&M University.

Gustavson, T. C., and Simpkins, W. W., 1989, Geomorphic processes and rates of retreat affecting the Caprock Escarpment, Texas Panhandle: The University of Texas at Austin, Bureau of Economic Geology Report of Investigations No. 180, 49 p.

Guyton, W. F. and Associates, 1993, Northern Bexar County water resources study for the Edwards Underground Water District- Volume 1: Ground water: final report to the Edwards Underground Water District, San Antonio, Texas, 66 p.

Hack, J.T., 1960, Interpretation of erosional topography in humid temperate regions, Amer. J. Sci., 258-A, 80-97.

Hack, J.T., 1965, Geology of the Shenandoah Valley and origin of the residual ore deposits, Geological Survey Professional Paper 484, Department of the Interior, United States Printing Office, Washington, D.C. p.1-84.

Hammond, W. W., 1984, Hydrogeology of the Lower Glen Rose aquifer, South-Central Texas: Ph.D. dissertation, The University of Texas at Austin. 243 p.

Harding, K.A. and Ford, D.C., 1993, Impacts of primary deforestation upon limestone hillslopes in northern Vancouver Island, British Columbia. Environmental Geology, v. 21, p. 137-143.

Higgins, C., 1984, Piping and sapping: Development of landforms by groundwater outflow, *in* LaFleur, R.G., ed., Groundwater as a geomorphic agent: The Binghamton Symposia in Geomorphology, International Series 13: Boston, Massachusetts, Allen and Unwin, p 18-58.

Horton, R.E., 1945, Erosional development of streams and their drainage basins: a hydrophysical approach to quantitative morphology. Bulletin of the Geological Society of America 56, 275-370

Howard, A., 1988, Groundwater sapping on Mars and Earth, i*n* Howard, **et al**., eds., Sapping features of the Colorado Plateau: A comparative planetary geology field guide: Washington, D.C., National Aeronautics and Space Administration, p 71-83.

Imeson, A.C., Lavee, H. and Calvo, A., Cerdá, A., 1998, The erosional response of calcareous soils along a climatological gradient in Southeast Spain, Geomorphology, v. 24, p. 3-16.

Johnsson, M. 1999, Speleogenesis, stream capture, and geomorphic development as recorded in cave sediments: Preliminary observations from the Swago Creek area, West Virginia, Geological Society of America Abstracts with Programs, v. 31, no. 7, p. A155.

Kastning, E.H., 1983, Geomorphology and hydrogeology of the Edwards Plateau karst, central Texas, a thesis in geology for Doctor of Philosophy, University of Texas at Austin, 656 p.

Kilmer, V.H. and Alexander, L.Z., 1949, Methods for making mechanical analyses of soil. Soil Science, v. 68, p. 15-24.

Kuniansky, E. L., and Holligan, K.Q., 1994, Simulations of flow in the Edwards–Trinity aquifer system and contiguous hydraulically connected units, west-central Texas: U. S. Geological Survey Water-Resources Investigations Report 93-4039, 40 p.

LaFleur, R.G., 1999, Geomorphic aspects of groundwater flow, Hydrogeology Journal, v. 7 p. 78-93.

Lane, L.J., Diskin, M.H., Wallace, D. E., and Dixon, R.M., 1978, Partial area response on small semiarid watersheds: Water Resources Bulletin, v. 14, no. 5, p. 1143-1158.

LaPointe, P., and Hudson, J., 1985, Characterisation and interpretation of rock mass joint patterns, Spec. Paper, Geological Society of America, v. 199, p. 37.

Larkin, T.J. and Bomar, G.W., 1983, Climatic Atlas of Texas, Texas Department of Water Resources, LP-192, p. 18.

Larkin, R.G., Sharp, J.M., Jr., 1992, On the relationship between river-basin geomorphology, aquifer hydraulics, and ground-water flow direction in alluvial aquifers, Geological Society of America Bulletin, v. 104, p. 1608-1620.

Lavee, H., Imeson, A.C., Pariente, S., and Benyamini, Y., 1991, The response of soils to simulated rainfall along a climatological gradient in an arid and semiarid region, Catena Supplement, v. 19, p. 19-37.

Leopold, L, Emmet, W.W., and Myrick, R.M., 1966, Channel and hillslope processes in semi-arid area, New Mexico; United States Geological Survey Professional Paper 352-G.

Leopold, L., Wolman M., and Miller, J., 1964, Fluvial Processes in Geomorphology, 522 p., W. H. Freeman, San Francisco.

Lonsdale, J.T., 1927, Igneous rocks of the Balcones Fault Region of Texas: University of Texas Bulletin No. 2744, p. 12-13.

Mace, R., Chowdhury, A., Anaya, R., and Way, S., 2000, Groundwater Availability of the Trinity aquifer, Hill Country Area, Texas: Numerical Simulations through 2050, Texas Water Development Board, Austin, Texas.

McMahon, C.A., R.G. Frye, and K.L. Brown, 1984, The Vegetation Types of Texas, Including Cropland, Texas Parks and Wildlife Department., 40 p.

Nash, D., 1996, Groundwater sapping and valley development in the northern Hackness Hills, North Yorkshire, England, Earth Surface Processes and Landforms No. 21,: p. 781-795.

NHD (National Hydrography Dataset), 2005, Streams and Rivers of Upper Guadalupe River Basin (Digital Data), Comal, Kendall, Bexar, Hays, and Blanco Counties.

Nelson, D.W. and Sommers, L.E., 1982, Total carbon, organic carbon and organic matter, In Page, A.L., Method of Soil Analysis, Part II (2nd ed.), Agronomy, v. 9, p. 539-580.

Oberholser, H.C., 1974, The bird life of Texas. University of Texas Press, Austin, Texas.

Palmer, A.N. 1990, Groundwater processes in karst terranes, *in* Higgins, C.G. and Coates, D.R., Groundwater Geomorphology, The role of Subsurface Water in Earth Surface Processes and Landforms, Geological Society of America Special Paper 252, p. 177-210.

Palmer, E.J., 1920, The Canyon Flora of Edwards Plateau, Journal of the Arnold Arboretum, v. 1: p. 233-239

Palmer, E.C., Neck, R.W., and Carran, S.C., 1984, Remote sensing and the Texas Hill Country environment, San Antonio and vicinity: American Society of Photogrammetry Fall Convention.

Pederson, D.T., 2001, Stream piracy revisited: A groundwater sapping solution, GSA Today, Volume 11, No. 9, p. 4 –10.

Pulich, W. 1976. The Golden-cheeked Warbler; A Bioecological Study. Texas Parks and Wildlife Department, Austin, Texas. 172 pp.

Rapp, A., Murray-Rust, D.H., Christiansson, C, and Berry, L., 1972, Soil erosion and sedimentation in four catchments near Dodoma, Tanzania; Geographfiska Annaler, v. 54A, p. 255-318.

Rasco, H.P., 1998, Multiple data set integration and GIS techniques used to investigate linear structural controls in the southern Powder River basin, Wyoming, Thesis submitted to the Eberly College of Arts and Sciences, West Virginia University in partial fulfillment of the requirement for the degree of Master of Science in Geology. 118 pp.

Reeves, R.D. 1967, Ground Water Resources of Kendall County, Texas. Report 60. Austin: Texas Water Development Board.

Riggio, R.F. Bomar, G. W., and Larkin, T.J., 1987, Texas drought - Its recent history (1931-1985): Texas Water Commission, LP-87-04, 74 p.

Rose, P.R., 1972, Edwards Group, surface and subsurface, Central Texas: The University of Texas at Austin, Bureau of Economic Geology Report of Investigations 74, 198 p.

Schoenenberger, P.J. Wysocki, D.A., Benham, E.C., and Broderson, W.D., 1998, Field book for describing and sampling soils, National Resources Conservation Service, USDA, National Soil Survey center, Lincoln, NE.

Schumm, S.A., 1965, Quaternary paleohydrology, in Wright, H.E., Jr. and Frey, D.G., Eds., The Quaternary of the United States, Princeton, Princeton University Press, p. 783 to 794.

Schumm, S.A., Harvey, M.D. and Watson, C.C., 1984, Incised Channels: Morphology, Dynamics and Control, Water Resources Publications, Littleton, Colorado, USA. 200 p.

Soil Survey Staff, 1972, Soil survey laboratory methods and procedures for collecting soil samples, Soil Survey Investigation Report No. 1, USDA, SCS, US Government Printing Office, Washington, D.C.

Seele, H., 1885, A short sketch of Comal County, Texas. A description of its topography, resources, history and statistics, New Braunfels, Center for American History TXC-ZZ Collection.

Sirvent, J., Desir, G., Guttierrez, C., Sancho, C., Benito, G., 1997, Erosion rates in badland areas recorded by collectors erosion pins and profilometer techniques (Ebro Basin, NE-Spain), Geomorphology, v. 18, issue 2, p. 61–75.

Slaughter, Jack D., Jr., 1997, Throughfall, Stemflow, and Infiltration Rates for *Juniperus Ashei* on the Edwards Plateau, Texas, a thesis in geography for Master of Arts, The University of Texas, p. 104-109..

Smith, R.M. and Stamey, W.L., 1965, Determining the range of tolerable erosion, Soil Sciences, col. 100, no. 6, pp. 101–103

Sophocleous, M., 2002, Interactions between groundwater and surface water: The state of the science, Journal of Hydrogeology, v. 10, p 52–67.

Springer, G.S., Wohl, E.E., Foster, J.A., and Boyer, D.G., 2003, Testing for reach-scale adjustments of hydraulic variables to soluble and insoluble strata:

Buckeye Creek and Greenbrier River, West Virginia, Geomorphology, v. 56, p. 201-127.

Steele, J.G. and Bradfield, R., 1934, The significance of size distribution in the clay fraction, Report of the 14th annual meeting, American Soil Science Association, Bulletin 15, p. 88-93.

Steffens, T. and Wright, P, 1996, Seco Creek Water-Quality Demonstration Project annual project report fiscal year 1996: Project Administrators, McFarland, M. (Texas Agricultural Extension Service), Colwick, A. (Natural Resources Conservation Service), and Orange, S. (Farm Service Agency), 338 p.

Stricklin, F.L., Jr. Smith, C.I., and Lozo, F.E., 1971, Stratigraphy of Lower Cretaceous Trinity deposits of central Texas: Austin, University of Texas, Bureau of Economic Geology Report of Investigations, 71, 63 p.

Sumbera, J. and Veni G, 1986, Trip report #2 and field reconnaissance, unpublished report to Texas Parks and Wildlife Department, 2 p.

Terzaghi, R.D., 1965, Sources of error in joint surveys, Geotechnique, v. 15, p. 287–304.

TCEQ (Texas Commission on Environmental Quality), 1996, Edwards aquifer Recharge Zone Boundary Maps.

TPWD (Texas Parks and Wildlife Department), 1999, Watershed Cedar Removal Studies Set At State Natural Areas, Texas Parks and Wildlife Newsstand Report.

TPWD (Texas Parks and Wildlife Department), 2001, Karst Feature Data for Honey Creek State Natural Area.

TSS (Texas Speleological Society), 1994, *Texas Wild Caves, The Caves and Karst of Texas*, A guidebook for the 1994 convention of the National Speleological Society with Emphasis on the Southwestern Edwards Plateau, W.R. Elliott and G. Veni, Eds, pp. 18, 219.

TWC (now Texas Commission on Environmental Quality), 1989, Ground Water Quality of Texas - An overview of natural and man-affected conditions, prepared by ground water protection unit staff of the Texas Water Commission, Report 89-01, Austin, Texas.

TWDB (Texas Water Development Board), 2005, Water Well Data.

Thurow, T.L., W.H. Blackburn, and C.A. Taylor, Jr. 1987, Rainfall interception by midgrass, shortgrass, and live oak mottes, Journal of Range Management, vol. 40, p. 455-460.

USGS (United States Geological Survey), 2001, Water Resources of the United States, Real-Time Water Data and Provision Data.

USGS (United States Geological Survey), 1995, Digital Orthophotograph, Anhalt Quadrangle.

USFWS (U.S. Fish and Wildlife Service), 1992, Golden-cheeked Warbler Recovery Plan, USFWS, Endangered Species Office, Albuquerque, NM. 88 pp.

Veni, G. 1994a, Geomorphology, hydrogeology, geochemistry, and evolution of the karstic Lower Glen Rose aquifer, south-central Texas, a thesis in geology for Doctor of Philosophy, Pennsylvania State University, p. 386-413.

Veni, G. 1994b, Hydrogeology and evolution of caves and karst in southwestern Edwards Plateau, Texas, Caves and Karst of Texas, Texas Speleological Society, convention guidebook, William R. Elliott and George Veni, eds., Brackettville, Texas, p. 13-29.

Wahl, R., Diamond, D.D., and Shaw, D., 1990, The Golden-Cheeked Warbler: A Status Review, U.S. Fish and Wildlife Service, Ecological Services Office, Austin, Texas.

Weissell, J. and Seidl, M. 1997, Influence of rock strength properties on escarpment retreat across passive continental margins: Geologic Society of America Bulletin, v. 25, p. 631-634.

Wermund, E.G, Cepeda, J.C., and Luttrell, P.E., 1978, Regional distribution of fractures in the southern Edwards Plateau and their relationship to tectonics and caves, Bureau of Economic Geology, The university of Texas at Austin.

White, W.B., 1988, Geomorphology and Hydrology of Karst Terrains, Oxford University Press, New York, 464 pp.

Whitney, M.I., 1952, Some zone marker fossils of the Glen Rose Formation of Central Texas, Journal of Paleontology, v. 26, p. 65–73.

Wilding, L.P., Woodruff, C.M., Jr., Owens, P.R., 2001, Caliche Soils as a Filter Medium for Treatment and Disposal of Wastewater, for Texas Natural Resource Conservation Commission (now TCEQ), Texas On-Site Wastewater Treatment Research Council, MC-178. .

Wilding, L.E. and Woodruff, C.M. Jr., (Consulting Geologist), 1994, Soils And Landforms Of The Central Texas Hill Country: Implications For Wastewater Application, Texas On- Site Wastewater Treatment and Research Council. (Available from Chris Guzman or Terri Chapman, City of Austin 322-3656).

Wilson, W.F., 1986, Glen Rose Formation – central Texas slope expansion features, Contributions to the geology of south Texas, W. L. Stapp, editor, South Texas Geological Society, San Antonio, Texas, p 439.

Wischmeier, W.H. and Smith, D.D., 1978, Predicting Rainfall Erosion Losses, US Department of Agriculture, Agricultural Research Service Handbook 537, 58 pp.

Wohl, E.E., 1992, Bedrock benches and boulder bars: floods in the Burdekin Gorge of Australia, Geologic Society of America, Bulletin 104, p. 770-778.

Woodruff, C. M., Jr., 1974, Evidence for stream piracy along the Balcones Escarpment, central Texas: Geological Society of America, Abstracts with Programs, v. 6, no. 7, p. 1010.

Woodruff, C. M., Jr., 1977, Stream piracy near the Balcones fault zone, central Texas: Journal of Geology, v. 85, no. 4, p. 483-490.

Woodruff, C.M., Jr., and Abbott, P.L., 1979, Drainage-basin evolution and aquifer development in a karstic limestone terrain, south-central Texas: Earth Surface Processes, v. 4, no. 4, p. 319-334.

Woodruff, C.M., Jr., and Abbott, P.L., 1986, Stream piracy and evolution of the Edwards aquifer a long the Balcones Escarpment, central Texas, in Abbot, P.L. and Woodruff, C.M., eds., The Balcones Escarpment, central Texas: Geological Society of America, p 77-90

Woodruff, C.M., Jr., and Marsh, W.M., 1992, Soils, landforms, hydrologic processes, and land-use issues-Glen Rose Formation terrains, Society of Independent Professional Earth Scientists, Central Texas Chapter Field Report and Guidebook.

The vita has been removed from the reformatted version of this document.